

**Development of Test Protocols for Analysis of Low Back Exertions in Standing  
Position**

by

Varun Vinod Soman

A thesis submitted to the Graduate Faculty of  
Auburn University  
in partial fulfillment of the  
Requirements for the Degree of  
Master of Science

Auburn, Alabama  
August 4, 2012

Keywords: Stability, Variability, Range of Motion, Approximate Entropy, Correlation  
Dimension

Copyright 2012 by Varun Soman

Approved by

P. K. Raju, Thomas Walter Distinguished Professor of Mechanical Engineering  
M. Ram Gudavalli, Associate Professor, Palmer College of Chiropractic, IA  
Jeffrey Suhling, Quina Distinguished Professor of Mechanical Engineering  
Dan Marghitu, Professor of Mechanical Engineering

## ABSTRACT

More than 80 percent of people suffer from low back pain at some point in their lifetime costing losses of up to \$9 billion because of treatment and loss of work hours in the US alone. Kinematics and kinetics of body movements can be affected by low back pain and may result in spinal instability.

The aim of this study was to develop testing procedure to quantify stability of the spine during low back motion using both traditional and non-linear methods in standing position. The objective was to quantify movements that are performed repetitively in flexion - extension (FE), lateral bending (LB), and rotation (ROT) of the trunk using traditional and non-linear methods. The study was approved by Institutional Review Boards (IRB) of Auburn University, AL as well as Palmer College of Chiropractic, IA. Nine healthy test subjects were recruited for the study using word of mouth and screened for eligibility by licensed clinicians. Participants were asked to perform 10 cycles of flexion - extension, lateral bending and rotation motion against no resistance, 5 lb, 10 lb and 15 lb resistance. Motion data was recorded at a frequency of 120 Hz for each exertion and for each resistance. Range of Motion (ROM) and non-linear techniques (Correlation Dimension (CoD), Approximate Entropy (ApEn)) were employed to analyze the motion data. EMG data was recorded at a frequency of 1200 Hz from six muscle groups: Erector Spinae, Multifidus, Latissimus Dorsi, Internal Obliques, External

Obliques and Rectus Abdominis. Mean and median frequency of the recorded signals were analyzed to see the effect of increasing load on muscle fatigue.

The ROM values varied from 7.5 – 40.2 Deg. For FE, 9.06 – 44.6 Deg. for LB and 6.68 – 21.3 Deg. for ROT, the ApEn values ranged from 0.133 – 0.40 while the CoD values ranged from 1.79 – 2.47. The overall results indicated that variability did not change significantly with increasing loads. The EMG results indicated that fatigue was not induced in participant's muscles which might have helped them provide required neuromuscular response to increasing loads. However it is important to keep in mind that the main objective of the thesis was development of test protocol for analysis of low back motion. The test protocol developed herein needs to be further fine tuned before it can be applied for larger studies. Testing method for data recording during rotations needs improvement as there might be inaccuracy involved due to skin motion altering the position of sensors. Also, once the protocol is perfected, further testing needs to be carried out on a larger sample size so that the results can be generalized. Future studies need to consider the following recommendations for obtaining more meaningful data based on healthy subjects. 1) Increase the resistance to motion so that higher fatigue is induced in the participant. 2) Ask the participant to perform the exertions at two different fixed speeds. 3) To minimize the effect of skin stretching during rotation, a plastic plate can be attached to the skin before motion sensors are attached. Once the data base on healthy subjects is obtained, studies on low back pain subjects can be undertaken.

## ACKNOWLEDGEMENT

I would like to express my deep gratitude to my academic advisor, Dr. P. K. Raju, for providing me with the opportunity to work under him on this project. I would also like to thank Dr. M. Ram Gudavalli for being a co-advisor and great mentor and guide during my work at Palmer Center for Chiropractic Research, IA. Also, a special thank you to Dr. Jeffrey Suhling and Dr. Dan Marghitu for all the help they have provided to me during my study period at Auburn University. I would also like to specially mention Dr. Xia Ting who provided valuable technical help during my work at Palmer Center for Chiropractic Research, IA. I also appreciate the help provided by Ms. Kristen Billy in editing the draft of the thesis.

I would like to thank my parents, Mr. Vinod P. Soman and Mrs. Vrunda V. Soman, as well as my younger brother Vikram Soman, for having faith in me and providing endearing love, encouragement and moral support. I would also like to thank all my friends and colleagues for their priceless friendship and support.

Special thanks to Auburn University, National Institutes of Health (NIH) (Grant numbers - 1U19AT004137-01) and National Center for Research Resources (Grant Number - C06 RR15433-01) for providing financial support for the study.

## Table of Contents

Abstract.....	i
Acknowledgement.....	iii
List of Tables.....	vii
List of Figures .....	viii
List of Abbreviations .....	xi
1 Introduction.....	1
1.1 Low Back Pain (LBP) – .....	1
1.2 Stability of Spine .....	3
1.3 Variability.....	4
1.4 Quantification of Variability .....	4
1.5 Nonlinear Methods to Quantify Variability .....	7
1.6 Objectives of the Study .....	10
2 Anatomy of Human Spine.....	14
2.1 The Vertebral Column .....	14
2.1.1 Thoracic Vertebrae.....	16
2.1.2 Lumbar Vertebrae .....	17
2.2 Low Back Musculature .....	18

2.2.1 Erector Spinae .....	19
2.2.2 Multifidus .....	19
2.2.3 Latissimus Dorsi .....	19
2.2.4 Internal Obliques .....	20
2.2.5 External Obliques.....	21
2.2.6 Rectus Abdominis .....	21
3 Methods and Techniques Used .....	23
3.1 Experimental Protocol.....	23
3.2 Sample Size .....	25
3.3 Data Acquisition .....	26
3.4 Motion Data Analysis .....	29
3.4.1 Time series.....	29
3.4.2 Range of Motion (ROM) .....	30
3.4.3 Classification of time series as periodic or chaotic .....	32
3.4.4 Approximate Entropy (ApEn) .....	33
3.4.5 Calculation of ApEn.....	35
3.4.6 Correlation Dimension (CoD) .....	36
3.4.7 Phase Plane Plots .....	37
3.4.8 Standard Phase Space.....	38
3.4.9 Pseudo Phase Space .....	39

3.4.10 Time Lag.....	40
3.4.11 Embedding Dimension .....	41
3.4.12 Measuring Correlation Dimension .....	42
3.5 EMG Data Analysis .....	50
3.5.1 Identifying muscle activation.....	50
3.5.2 Mean and Median Frequency of SEMG signals .....	51
4 Results.....	52
4.1 ROM Results .....	52
4.2 Phase Plane Plots .....	54
4.3 Fast Fourier Transformation (FFT).....	56
4.4 Approximate Entropy (ApEn) Results .....	58
4.5 Correlation Dimension (CoD) Results.....	60
4.6 EMG Frequency Analysis Results.....	63
4.6.1 Mean and Median Frequency during Flexion – Extension motion.....	64
4.6.2 Mean and Median Frequency during Lateral Bending motion.....	68
4.6.3 Mean and Median Frequency during Rotation motion .....	70
5 Discussion .....	73
6 Conclusion.....	80
References.....	81
Appendix.....	87

## List of Tables

Table 1 Demographics.....	25
Table 2 EMG sensor placement .....	28
Table 3 One factor ANOVA test on ApEn results for FE .....	54
Table 4 p-values for ROM results .....	54
Table 5 One factor ANOVA test on ApEn results for FE .....	60
Table 6 p-values for ApEn results .....	60
Table 7 One factor ANOVA test on CoD results for FE.....	62
Table 8 p-values for CoD results.....	62
Table 9 Muscle recruitment during FE, LB and ROT by number of participants. ....	63
Table 10 Mean values of Mean Frequencies with increasing loads during FE .....	67
Table 11 Mean values of Median Frequencies with increasing loads during FE .....	67
Table 12 Mean values for Mean Frequencies with increasing loads during LB.....	69
Table 13 Mean values for Median Frequencies with increasing loads during LB.....	69
Table 14 Mean values of Mean Frequencies with increasing loads during ROT .....	72
Table 15 Mean values of Median Frequencies with increasing loads during ROT ...	72



## List of Figures

Figure 1 The Human Spine (Uwe Gille, Wikipedia.com) .....	15
Figure 2 Thoracic Vertebra (Anatomist90, Wikipedia.com) .....	17
Figure 3 Lumbar Vertebra (Anatomist90, Wikipedia.com) .....	18
Figure 4 Abdominal Muscles (SEER Training Module).....	20
Figure 5 SEMG and motion sensors attached to back muscles and vertebrae respectively .....	26
Figure 6 SEMG sensors attached to abdominal muscles.....	27
Figure 7 Sine Curve .....	30
Figure 8 Time series for flexion-extension against 5 lb resistance .....	30
Figure 9 FFT of a periodic sine curve.....	32
Figure 10 FFT of experimental motion data.....	32
Figure 11 Example of standard phase space.....	39
Figure 12 Pseudo phase space plot of experimental data .....	40
Figure 13 Identifying qualifying neighbors from (a) point 1 and (b) point 2 .....	43
Figure 14 Plot of Correlation Sum vs. Radius .....	47
Figure 15 Sketch showing geometric increase in number of points within circle of radius $\epsilon$ for uniformly spaced points (after Bergé et al. 1984: Fig. VL. 36). (a) One-dimensional attractor (line). (b) Two-dimensional attractor (plane) .....	48
Figure 16 Idealized plot of Correlation Sum vs. Radius for increasing Embedding Dimension ...	49
Figure 17 Muscle Recruitment for ES Left muscle during FE under 5 lb resistance.....	50
Figure 18 ROM results for FE.....	52
Figure 19 ROM results for LB .....	53

Figure 20 ROM results for ROT.....	53
Figure 21 Phase Plane plots for FE data against 0 lb, 5 lb, 10 lb and 15 lb respectively for participant 1 (left to right; top to bottom).....	55
Figure 22 Phase Plane plot of a perfectly periodic (sine wave) time series data.....	56
Figure 23 FFT for FE data against 0 lb, 5 lb, 10 lb and 15 lb respectively for participant 1 (left to right; top to bottom).....	57
Figure 24 FFT of sine wave.....	58
Figure 25 ApEn results for FE.....	58
Figure 26 ApEn results for LB.....	59
Figure 27 ApEn results for ROT.....	59
Figure 28 CoD results for FE.....	61
Figure 29 CoD results for LB.....	61
Figure 30 CoD results for ROT.....	61
Figure 31 ES Left – Mean and Median Frequencies (Left and Right).....	64
Figure 32 ES Right - Mean and Median Frequencies (Left and Right).....	65
Figure 33 LD Left - Mean and Median Frequencies (Left and Right).....	65
Figure 34 LD Right - Mean and Median Frequencies (Left and Right).....	65
Figure 35 MF Left - Mean and Median Frequencies (Left and Right).....	66
Figure 36 MF Right - Mean and Median Frequencies (Left and Right).....	66
Figure 37 ES Right - Mean and Median Frequencies (Left and Right).....	68
Figure 38 EO Right - Mean and Median Frequencies (Left and Right).....	68
Figure 39 LD Right - Mean and Median Frequencies (Left and Right).....	68
Figure 40 MF Right - Mean and Median Frequencies (Left and Right).....	69
Figure 41 ES Left - Mean and Median Frequencies (Left and Right).....	70
Figure 42 ES Right - Mean and Median Frequencies (Left and Right).....	70
Figure 43 LD Left - Mean and Median Frequencies (Left and Right).....	70

Figure 44 LD Right - Mean and Median Frequencies (Left and Right).....	71
Figure 45 MF Left - Mean and Median Frequencies (Left and Right) .....	71
Figure 46 MF Right - Mean and Median Frequencies (Left and Right) .....	71
Figure 47 ROM, ApEn and CoD results for participant 1 during LB .....	75
Figure 48 Mean and Median Frequency results for ES Left muscle for participant 3 during ROT .....	76
Figure 49 Mean and Median Frequency results for ES Right muscle for participant 3 during ROT .....	77
Figure 50 User Report Options.....	94
Figure 51 Orthopedic Angle Selection.....	94
Figure 52 Forceplate Data .....	95
Figure 53 EMG Data 1.....	95
Figure 54 EMG Data 2.....	96
Figure 55 EMG Data 3.....	96

## List of Abbreviations

ROM	–	Range of Motion
ApEn	–	Approximate Entropy
CoD	–	Correlation Dimension
SEMG	–	Surface Electromyography
FE	–	Flexion Extension
LB	–	Lateral Bending
ROT	–	Rotation
ES	–	Erector Spinae
MF	–	Multifidus
LD	–	Latissimus Dorsi
IO	–	Internal Obliques
EO	–	External Obliques
RA	–	Rectus Abdominis

## CHAPTER 1

### INTRODUCTION

#### **1.1 Low Back Pain (LBP) –**

LBP is the second most common cause of disability in US adults (Centers for Disease Control and Prevention) and a common reason for lost work days (Stewart W.F., 2003). When persons of all ages are considered, back pain was the second leading cause for absenteeism in the United States, accounting for approximately 25 percent of all lost workdays in 2009 (Devereaux M., 2009). The condition is also costly, with total costs estimated to be between \$100 and \$200 billion annually in 2006, two-thirds of which are because of decreased wages and productivity (Katz J. N., 2006). More than 80 percent of the population will experience an episode of LBP at some time during their lives (Rubin D. I., 2007). For most, the clinical course is benign, with 95 percent of those afflicted recovering within a few months of onset (Carey T. S. et. al, 1995). Some however, will not recover and will develop chronic LBP (i.e., pain that lasts for 3 months or longer). Recurrences of LBP are also common, with the percentage of subsequent LBP episodes ranging from 20 percent to 44 percent within 1 year for working populations to lifetime

recurrences of up to 85 percent (van Tulder M., 2002). The use of health care services for chronic LBP has increased substantially over the past two decades. Multiple studies using national and insurance claims data have identified greater use of spinal injections (Weiner D. K., 2006). Surgery (Deyo R. A., 2005) and opioid medications (Luo X, 2004) — treatments most likely to be used by individuals with chronic LBP. Studies have also documented increases in medication prescription and visits to physicians, physical therapists, and chiropractors (Feuerstein M, 2004). Because individuals with chronic LBP are more likely to seek care (IJzelenberg W, 2004) and to use more health care services (Carey T. S. et. al., 1995), relative to individuals with acute LBP, increases in health care use are likely driven more by chronic than by acute cases. Increased health care use for chronic LBP could be a function of (1) increased prevalence of chronic LBP; (2) increased proportion of those with chronic LBP who seek care; (3) increased use by those who seek care, or (4) some combination of these factors (Thorpe K. E. et. al., 2004). The documented increase in use of services is often assumed to be because of increased health care seeking or use by those who seek care.

A large number of studies have focused on chronic LBP, but they have not revealed a complete understanding of this condition (Bergman, S. 2007). In order to apprehend this condition, researchers are now focusing on the effect of LBP on trunk movements. Kinematic and kinetic quantities are assumed to be periodic or pseudo periodic based on body characteristics and personal ability to control the lumbar spine. With neuromuscular and musculoskeletal pathologies or injuries, these movements may not be periodic and may result in increased instability of the lumbar spine (Papadakis, N.C. et. al., 2009).

## **1.2 Stability of Spine -**

Local dynamic stability of the spine is defined as the sensitivity of the system to small perturbations, such as the natural stride to stride variations present during locomotion. A study done by Manohar Panjabi explains the factors responsible for stability and normal functioning of the spine. The vertebrae, discs, and ligaments constitute the passive subsystem. All muscles and tendons surrounding the spinal column that can apply forces to the spinal column constitute the active subsystem. The nerves and central nervous system comprise the neural subsystem, which determines the requirements for spinal stability by monitoring the various transducer signals, and directs the active subsystem to provide the needed stability. A dysfunction of a component of any one of the subsystems may lead to one or more of the following three possibilities: (a) an immediate response from other subsystems to successfully compensate, (b) a long-term adaptation response of one or more subsystems, and (c) an injury to one or more components of any subsystem. It is conceptualized that the first response results in normal function, the second results in normal function (but with an altered spinal stabilizing system) and the third leads to overall system dysfunction, producing, for example, low back pain (LBP). In situations where additional loads or complex postures are anticipated, the neural control unit may alter the muscle recruitment strategy, with the temporary goal of enhancing the spine stability beyond the normal requirements (Panjabi M. M.).

### **1.3 Variability –**

Variation, as mentioned in the definition of stability, is inherent within all biological systems and can be characterized as the normal changes that occur in motor performance across multiple repetitions of tasks. For example, a man performs similar repetitive movement while rowing a boat. But, his hands do not follow exactly the same trajectory each and every time. For various reasons, there is some change in trajectory every time. This change in trajectory is known as variation. Until recently, variability was interpreted as the result of random processes (Leon Glass, *'From Clocks to Chaos: The Rhythms of Life'*). However, recent literature from a number of scientific domains has shown that many phenomena previously described as noisy are actually the result of non linear interactions and have a deterministic origin (Gleick, J. 1987. *Chaos: Making a new Science*, Amato, I. 1992. Chaos breaks out at NIH, but order may come of it). Thus, one can get important information regarding the system's behavior by examining the 'noisy' component of the measured signal.

### **1.4 Quantification of Variability –**

In the past years a lot of effort has gone into correctly quantifying the variability in various biological systems. The magnitude of the variability is the measure of stability of that biological system. There are numerous methods and quantities for representing variability. The variability in kinematic, kinetic, and temporal variables can be computed using both traditional and non-traditional approaches. Traditional methods originate from descriptive statistics, while non-traditional methods are those that use techniques from the



study of non-linear dynamical systems to isolate chaotically deterministic variability from other variability components contained within the movement process.

The traditional methods include range, variance, standard deviation (SD), etc. These methods are known as discrete methods. Range is simply the difference between the greatest and the least values and is computed by subtracting the least value from the greatest value. Variance is a measure of variability that uses the sum of the squared deviations between the individual values and the sample mean divided by the approximate degrees of freedom for the sample, while SD is merely square root of variance. Although variance and SD are computed similarly, variance is used less often in variability studies because units of variance are squared, making the interpretation of variability somewhat harder than that of SD ( Fitzgerald, G.K. et. al., 1983).

Collectively, the discrete methods provide a thorough description of the variability of the discrete variables across multiple performance trials. A literature survey shows that hundreds of studies have been conducted where these discrete methods have been applied in the analysis of various human physiological phenomena, such as human gait and heart rate analysis. Let us take a look at some of the recent studies done related to human lumbar spine motion and gait analysis. In 2008, Hsu et. al. measured the range of motion (ROM) of the spine in healthy individuals by using an electromagnetic tracking device to evaluate the functional performance of the spine. The authors used the Flock of Birds electromagnetic tracking device with four receiver units attached to C-7, T-12, S-1, and the mid-thigh region. Forward/backward bending, bilateral side bending, and axial rotation of the trunk were performed in 18 healthy individuals. The average ROM was calculated after three consecutive measurements. The results showed that the thoracic

spine generated the greatest angle in axial rotation and smallest angle in backward bending. The lumbar spine generated the greatest angle in forward bending and smallest angle in axial rotation. The hip joints generated the greatest angle in forward bending and smallest angle in backward bending. Additionally, 40 percent of forward-bending motion occurred in the lumbar spine and 40 percent occurred in the hip joints. Approximately 60 percent of backward bending occurred in the lumbar spine; 60 percent of axial rotation occurred in the thoracic spine; and 45 percent of side bending occurred in the thoracic spine (Chien-Jen Hsu et. al., 2008)

In 2010, Shrawan Kumar studied the muscle activation in combined rotation and flexion of the torso in varying degree of asymmetries of the trunk. Nineteen normal young subjects (seven males and 12 females) were stabilized on a posture-stabilizing platform and instructed to assume a flexed and right rotated posture. A combination 20 degrees, 40 degrees and 60 degrees of rotation, and 20 degrees, 40 degrees and 60 degrees of flexion resulted in nine postures. These postures were assumed in a random order. The subjects were asked to exert their maximal voluntary isometric contraction (MVC) in the plane of rotation of the posture assumed for a period of five seconds. The surface EMG from the external and internal obliques, rectus abdominis, latissimus dorsi and erector spinae at the 10th thoracic and third lumbar vertebral levels was recorded. The abdominal muscles had the least response, at 40 degrees of flexion; the dorsal muscles had the highest magnitude.

With increasing right rotation, the left external oblique continued to decrease its activity. The ANOVA revealed that rotation and muscles had a significant main effect on normalized peak EMG ( $p < 0.02$ ) in both genders. There was a significant interaction

between rotation and flexion in both genders ( $p < 0.02$ ) and rotation and muscle in females. The erector spinae activity was highest at 40 degrees flexion, because of greater mechanical disadvantage and having not reached the state of flexion–relaxation. The abdominal muscle activity declined with increasing asymmetry, because of the decreasing initial muscle length. The EMG activity was significantly more affected by rotation than by flexion ( $p < 0.02$ ) (Shrawan Kumar, 2010).

In 2010, Desai et. al. conducted a study in which they applied discrete methods to analyze variability in trunk muscle activation and other physiological parameters for subjects with and without LBP. The group with LBP and the control group each had 10 participants. Bilateral trunk muscle activity was measured using surface electromyography (EMG); whole body balance was measured by quantifying the dispersion of the centre of pressure (CoP); lumbar range of motion (LROM) was measured with single-axis inclinometers. Individuals with LBP had adaptive recruitment patterns during the side-bridge and modified push-up exercises. CoP dispersion and LROM were not different between the groups for any exercise. The labile surface did not change the difference between groups, and only increased muscle activity during the side-bridge ( $p < 0.05$ ). The labile surface increased LROM ( $p = 0.35$ ) and CoP dispersion ( $p < 0.001$ ) during the quadruped, decreased LROM during squats ( $p = 0.05$ ), and increased CoP dispersion during push-ups ( $p = 0.04$ ) (Imtiaz Desai, 2010).

### **1.5 Nonlinear Methods to Quantify Variability –**

Traditionally, physicians in the medical field use linear models for prediction and problem solving. However, biological systems, including those of humans, are complex

adaptive systems, characterized by multiple interconnected and interdependent parts (Harbourne, R.T. et. al., 2009). These are highly non-linear systems with inherent variability in all healthy organisms. There is growing understanding that linear models are limited in many cases and are certainly not the best models for understanding the nonlinear human system (Stergiou, N. 2004). Professionals in different medical fields, such as biomechanics, epidemiology, etc., are now turning to nonlinear tools for solving such complex systems. Some of these nonlinear methods are Lyapunov Exponents, Approximate Entropy, and Correlation Dimension. Lyapunov Exponent calculates the rate at which adjacent trajectories converge or diverge in reconstructed state space. Approximate Entropy calculates the predictability of a given time series. Correlation dimension is used to quantify chaos in a given time series. Detailed explanation of these non-linear methods has been provided in Chapter 3.

In 2006, Granata and England used non-linear tools to estimate control of dynamic stability during repetitive flexion and extension movements of the lumbar spine. There were 20 healthy subjects who performed repetitive trunk flexion and extension movements at 20 and 40 cycles per minute. Maximum Lyapunov exponents describing the expansion of the kinematic state-space were calculated from the measured trunk kinematics to estimate stability of the dynamic system.

Repeated trajectories from fast paced movements diverged more quickly than slower movement, indicating that local dynamic stability is limited in fast movements. Movements in the mid-sagittal plane showed higher multi-dimensional kinematic divergence than asymmetric movements. Non-linear dynamic systems analyses were successfully applied to empirically measured data (Kevin P. Granata et. al., 2006).

The local dynamic stability of trunk movements was assessed by Graham et. al. in 2011 during repetitive lifting using non-linear Lyapunov analysis. The goal was to assess how varying the load-in-hands affects the neuromuscular control of lumbar spinal stability. Thirty healthy participants (15M, 15F) performed repetitive lifting at 10 cycles per minute for three minutes under two load conditions: zero load and 10 percent of each participant's maximum back strength. Short and long-term maximum finite-time Lyapunov exponents, describing responses to infinitesimally small perturbations, were calculated from the measured trunk kinematics to estimate the local dynamic stability of the system.

The findings indicated improved dynamic spinal stability when lifting the heavier load, meaning that as muscular and moment demands increased, so too did participants' abilities to respond to local perturbations. These results support the notion of greater spinal instability during movement with low loads because of decreased muscular demand and trunk stiffness, and should aid in understanding how lifting various loads contributes to occupational low back pain (Ryan B. Graham et. al., 2011).

In 2009, Kavanagh studied lower trunk motion and speed dependence during walking. He used another nonlinear tool, Approximate Entropy, to do so. The primary purpose of this study was to examine how gait speed influences a healthy individual's lower trunk motion during over-ground walking. Thirteen healthy subjects ( $23 \pm 3$  years) performed five straight-line walking trials at self-selected slow, preferred, and fast walking speeds. Accelerations of the lower trunk were measured in the anterior-posterior (AP), vertical (VT), and mediolateral (ML) directions using a triaxial accelerometer.

The results showed that the value of Approximate Entropy decreased as the walking velocity increased. The main finding of this study was that walking at speeds slower than preferred primarily alters lower trunk accelerations in the frontal plane. Despite greater amplitudes of trunk acceleration at fast speeds, the lack of regularity and repeatability differences between preferred and fast speeds suggested that features of trunk motion are preserved between the same conditions (Justin J. Kavanagh, 2009).

Correlation Dimension is another non-linear parameter that can be used to study the stability of a physiological system. In 2003, Buzzi et. al. investigated the nature of variability present in a time series generated from gait parameters of two different age groups via a non-linear analysis. Twenty females, 10 younger (20–37 years old) and 10 older (71–79 years old) walked on a treadmill for 30 consecutive gait cycles. Time series from selected kinematic parameters of the right lower extremity were analyzed using nonlinear dynamics. The largest Lyapunov exponent and the correlation dimension of all the time series were calculated.

The elderly exhibited significantly larger Lyapunov exponents and correlation dimensions for all parameters evaluated, indicating local instability. The non-linear analysis revealed that fluctuations in the time series of certain gait parameters are not random, but display a deterministic behavior (Ugo H. Buzzi, 2003).

## **1.6 Objectives of the Study –**

From the above illustration described in the previous section, we understand that bio-mechanists and scientists are increasingly starting to employ non-linear analysis methods to study dynamic behavior of various biological systems. But, despite the

advantages that non-linear tools offer, it also has certain limitations. Some of them are mentioned below –

1. Non-linear measurement techniques require mathematical equations and software to evaluate time series data; as a result they must be carried out in a research environment.

2. There is a lack of understanding of variability and complexity in most medical fields.

3. Translation of non-linear measures to clinical problems requires concurrent use of linear tools to make associations and determine clinical meaning.

4. Most of these measures require multiple repetitions or cycles of a movement (Harbourne, R.T et. al., 2009).

Thus, even now the best option remains to study the biological systems using both linear and non-linear methods given the advantages and disadvantages of both. Also, in spite of all the work that has been done previously, plenty of scope for future research remains to better understand the characteristics of biological systems.

In 2008, Lee et. al. studied the effects of trunk exertion force and direction on postural control of the trunk during unstable sitting. Seat movements were recorded while subjects maintained a seated posture on a wobbly chair against different exertion forces (0N, 40N, and 80N) and exertion directions (trunk flexion and extension). Postural control of the trunk was assessed from kinematic variability and non-linear stability analyses (stability diffusion exponent and maximum finite-time Lyapunov exponent).

Kinematic variability and non-linear stability estimates increased as exertion force increased. The study showed that trunk exertion force and exertion direction affect postural control of the trunk (Hyun Wook Lee et. al. 2008).

In one of the previously mentioned studies, Hsu et. al. measured the range of motion (ROM) of the spine in healthy individuals by using an electromagnetic tracking device to evaluate the functional performance of the spine (Chien-Jen Hsu et. al., 2008). Also, Granata and England used non-linear tools to estimate control of dynamic stability during repetitive flexion and extension movements of lumbar spine (Kevin P. Granata et. al., 2006). In 2005, Lamoth et. al. studied the effects of chronic low back pain on trunk coordination and back muscle activity during walking. The study included 19 individuals with non-specific LBP and 14 healthy controls. Gait kinematics and Erector Spinae (ES) activity were recorded during treadmill walking at (1) a self-selected (comfortable) velocity, and (2) sequentially increased velocities from 1.4 up to maximally 7.0 km/h. The angular movements of the thorax, lumbar and pelvis were recorded in three dimensions. ES activity was recorded with pairs of surface electrodes.

Rotational amplitudes were not significantly different between the LBP and control participants. In the LBP participants, the pattern of ES activity was affected in terms of increased (residual) variability, timing deficits, amplitude modifications and frequency changes. The gait of the LBP participants was characterized by a more rigid and less variable kinematic coordination in the transverse plane, and less tight and more variable coordination in the frontal plane, accompanied by poorly coordinated activity of the lumbar ES (Claudine J. C. Lamoth et. al., 2006).



During this literature survey, it was noticed that more research can be done in low back motion and muscle recruitment pattern during the standing position. The effect of increasing load resistance on various trunk motions such as flexion extension, lateral bending and rotation has not yet been investigated. These types of motions are a common occurrence in places such as gymnasiums or warehouses where heavy lifting is required. We may get some valuable insight in characteristics of motion lumbar vertebrae and recruitment of related muscles during these motions.

We have attempted to do this in this particular exercise. The objectives of this study are –

1. Develop a test procedure to measure and record data for lumbar motion and trunk muscle recruitment.
2. Identify particular muscle groups recruited for specific types of low back motions.
3. Analysis of variability of motion and strength generation of low back muscles using traditional discrete and non-linear techniques.
4. Try and suggest the most suitable method to analyze and study these motions.

## CHAPTER 2

### ANATOMY OF HUMAN SPINE

#### **2.1 The Vertebral Column –**

The human spine is composed of 26 individual bony masses, 24 of those are bones called vertebrae. The vertebrae are stacked one on top of the other and form the main part of the spine running from the base of the skull to the pelvis. At the base of the spine, there is a bony plate called the sacrum which is made of five fused vertebrae. The sacrum forms the back part of the pelvis. At the bottom of the sacrum is a small set of four partly fused vertebrae, the coccyx or tailbone. Adding the fused and partly fused bones of the sacrum and coccyx to the 24 vertebrae, the spine has 33 bones all together.

The spine is labeled in three sections: the cervical spine, the thoracic spine and the lumbar spine. Starting from the top, there are seven cervical vertebrae, 12 thoracic vertebrae, and five lumbar vertebrae.

The spinal vertebrae are separated from each other by intervertebral discs. These discs are made of collagen fibers and cartilage. They provide padding and shock absorption for the vertebrae. Each pair of vertebrae creates a movable unit.

The spinal cord runs within the vertebral canal formed by the back parts of the vertebrae. Thirty-one pairs of nerves branch out from the spinal cord through the vertebrae, carrying messages between the brain and every part of the body.

Aging, diseases, accidents and muscular imbalances can cause compression and thinning of the intervertebral discs. This results in pressure on the spinal nerves and wear on the bony vertebrae, and these conditions are common sources of back pain.

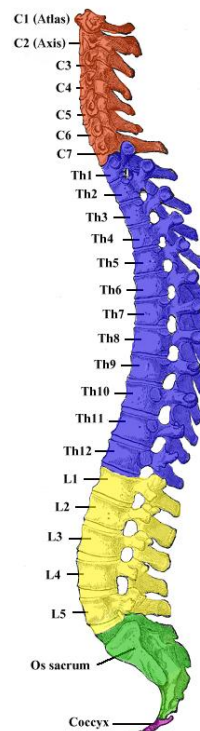


**Figure 1 The Human Spine (Uwe Gille, Wikipedia.com)**

There are four natural curves in the spine. We usually speak in terms of the three that comprise the cervical, thoracic, and lumbar portions of the spine; but, as you can see, the sacrum and coccyx form a curved section as well.

The spinal curves provide architectural strength and support of the spine. They distribute the vertical pressure on the spine, and balance the weight of the body. If the spine were absolutely straight, it would be more likely to buckle under the pressure of the weight of the body.

When all the natural curves of the spine are present, the spine is in a neutral position. This is its strongest position and usually the safest to exercise in. When we have perfect posture the curves of the spine are helping us balance. We are meant to walk and stand in the neutral spine position (Marguerite Ogle, About.com).

### **2.1.1 Thoracic Vertebrae –**

In vertebrates, thoracic vertebrae compose the middle segment of the vertebral column, between the cervical vertebrae and the lumbar vertebrae. In humans, they are intermediate in size between those of the cervical and lumbar regions; they increase in size as one proceeds down the spine, the upper vertebrae being much smaller than those in the lower part of the region. They are distinguished by the presence of facets on the sides of the bodies for articulation with the heads of the ribs, and facets on the transverse processes of all, except the 11th and 12th, for articulation with the tubercles of the ribs. The cervical vertebrae run into the cranium.

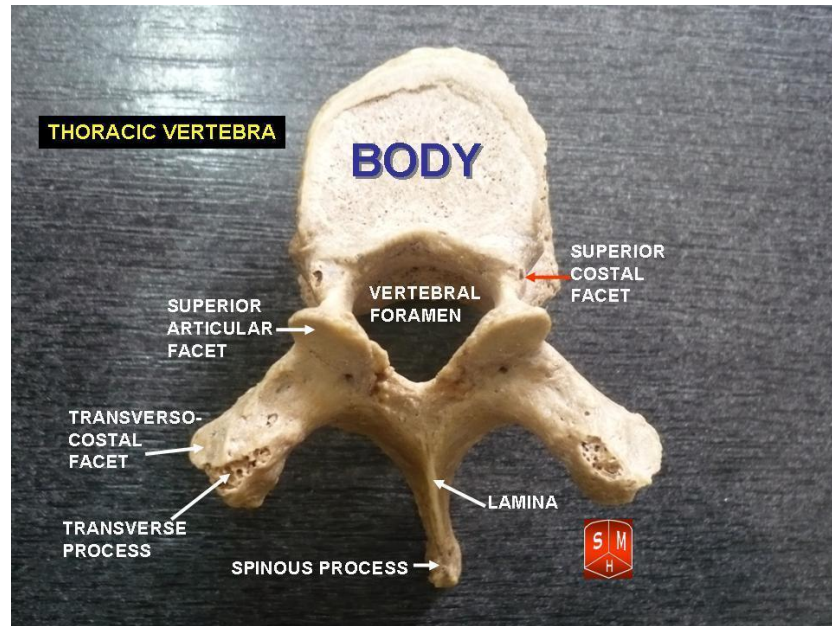


Figure 2 Thoracic Vertebra (Anatomist90, Wikipedia.com)

### First thoracic vertebra –

The first thoracic vertebra has, on either side of the body, an entire articular facet for the head of the first rib, and a demi-facet for the upper half of the head of the second rib. The body is like that of a cervical vertebra, being broad, concave, and lipped on either side. The superior articular surfaces are directed upward and backward; the spinous process is thick, long, and almost horizontal. The transverse processes are long, and the upper vertebral notches are deeper than those of the other thoracic vertebrae. The thoracic spinal nerve 1 (T1) passes out underneath it (Anatomist90, Wikipedia.com).

### 2.1.2 Lumbar Vertebrae –

The lumbar vertebrae are the largest segments of the movable part of the vertebral column, and are characterized by the absence of the foramen transversarium within the

transverse process, and by the absence of facets on the sides of the body. They are designated L1 to L5, starting at the top.

Each lumbar vertebra consists of a vertebral body and a vertebral arch. The vertebral arch, consisting of a pair of pedicles and a pair of laminae, encloses the vertebral foramen (opening) and supports seven processes (Wikipedia.com).

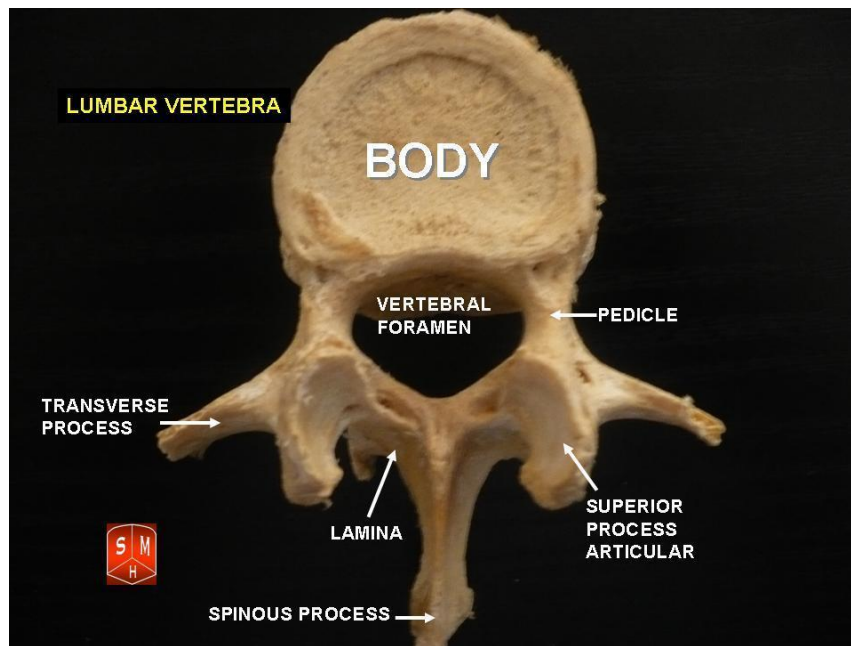


Figure 3 Lumbar Vertebra (Anatomist90, Wikipedia.com)

## 2.2 Low Back Musculature –

In this study, six muscle groups have been used to collect Electromyography (EMG) data. Let us take a look at the muscle groups and their location in the human body.

### **2.2.1 Erector Spinae –**

A deep muscle of the back; it arises from a tendon attached to the crest along the centre of the sacrum (the part of the backbone at the level of the pelvis, formed of five vertebrae fused together). When it reaches the level of the small of the back, the erector divides into three columns, each of which has three parts. The muscle system extends the length of the back and functions to straighten the back and to rotate it to one side or the other (Britannica.com)

### **2.2.2 Multifidus –**

The multifidus muscle consists of a number of fleshy and tendinous fasciculi, which fill up the groove on either side of the spinous processes of the vertebrae, from the sacrum to the axis. The multifidus is a very thin muscle. Deep in the spine, it spans three joint segments, and works to stabilize the joints at each segmental level. The stiffness and stability makes each vertebra work more effectively, and reduces the degeneration of the joint structures (Wikipedia.com).

### **2.2.3 Latissimus Dorsi –**

The latissimus dorsi, meaning 'broadest muscle of the back' (Latin *latus* meaning 'broad', *latissimus* meaning 'broadest' and *dorsum* meaning the back), is the larger, flat, dorso-lateral muscle on the trunk, posterior to the arm, and partly covered by the trapezius on its median dorsal region.

The latissimus dorsi is responsible for extension, adduction, transverse extension (also known as horizontal abduction), flexion (from an extended position), and (medial) internal rotation of the shoulder joint. It also has a synergistic role in extension and lateral flexion of the lumbar spine (Wikipedia.com).

#### **2.2.4 Internal Obliques –**

The internal oblique muscle (of the abdomen) is the intermediate muscle of the abdomen, lying just underneath the external oblique and just above (superficial to) the transverse abdominal muscle.

Its fibers run perpendicular to the external oblique muscle, beginning in the thoracolumbar fascia of the lower back, the anterior two-thirds of the iliac crest (upper part of hip bone) and the lateral half of the inguinal ligament. The muscle fibers run from these points superiomedially (up and towards midline) to the muscle's insertions on the inferior borders of the 10th through the 12th ribs and the linea alba (abdominal midline seam).

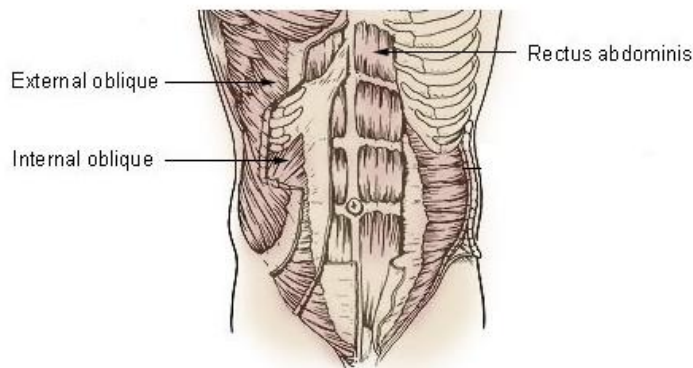


**Figure 4 Abdominal Muscles (SEER Training Module)**



### **2.2.5 External Obliques –**

The external oblique muscle (of the abdomen) (also external abdominal oblique muscle) is the largest and the most superficial (outermost) of the three flat muscles of the lateral anterior abdomen. The external oblique is situated on the lateral and anterior parts of the abdomen. It is broad, thin, and irregularly quadrilateral, its muscular portion occupying the side, its aponeurosis the anterior wall of the abdomen. In most humans (especially females), the oblique is not visible, due to subcutaneous fat deposits and the small size of the muscle.

The external oblique functions to pull the chest downwards and compress the abdominal cavity, which increases the intra-abdominal pressure as in a valsalva maneuver. It also has limited actions in both flexion and rotation of the vertebral column. One side of the obliques contracting can create lateral flexion. It also contributes to compression of abdomen.

### **2.2.6 Rectus Abdominis –**

The rectus abdominis muscle, also known as the "six pack" is a paired muscle running vertically on each side of the anterior wall of the human abdomen (and in some other animals). There are two parallel muscles, separated by a midline band of connective tissue called the linea alba (white line). It extends from the pubic symphysis/pubic crest inferiorly to the xiphisternum/xiphoid process and lower costal cartilages (5–7) superiorly.

The rectus abdominis is an important postural muscle. It is responsible for flexing the lumbar spine, as when doing a "crunch" The rib cage is brought up to where the pelvis is when the pelvis is fixed, or the pelvis can be brought towards the rib cage (posterior pelvic tilt) when the rib cage is fixed, such as in a leg-hip raise. The two can also be brought together simultaneously when neither is fixed in space.

In 2010, Shin et. al. used the lumbar erector spinae muscles to record data during EMG activity analysis of low back extensor muscles during cyclic flexion-extension (Shin et. al., 2010). The same muscle group was used by Mathieu et. al. in their study of EMG and kinematic analysis of trunk flexion-extension in free space (Mathieu et. al. 2000). Dickstein et. al. studied EMG activity of lumbar erector spinae (ES), latissimus dorsi (LD), rectus abdominis (RA), and external oblique (EO) muscles in their study of trunk flexion-extension of post-stroke hemiparetic subjects (Dickstein et. al., 2004).

Ten channels of EMG data were collected from bipolar surface electrodes over the right and left sides of the erector spinae, rectus abdomini, latissimus dorsi, external abdominal obliques, and internal abdominal oblique muscles by Marras and Granata in their study of spine loading during trunk lateral bending motion (Marras et. al., 1997).

Similarly, for trunk rotation Joseph K.-F Ng et. al. collected data from rectus abdominis, external oblique, internal oblique, latissimus dorsi, iliocostalis lumborum and multifidus muscles in their study of EMG activity of trunk muscles and torque output during isometric axial rotation exertion (Joseph K.-F Ng, 2002).

In this study of ours, we are trying to see if meaningful data can be obtained from the six muscle groups that we are studying under the given laboratory conditions.

## CHAPTER 3

### METHODS AND TECHNIQUES USED

#### **3.1 Experimental Protocol –**

During the literature review it was noticed that there was still scope for analysis of low back exertions in the standing position. Flexion-extension, lateral bending, and rotation motions were selected because these are the motions that are repeated plenty of times in day to day routines and hence can affect daily activities to a larger extent.

It was decided that data will be collected for the three motion types against no load and resistances of 5 lbs., 10 lbs. and 15 lbs. to study the effect of increasing loads on stability of low back spine. The participant performed flexion-extension, lateral bending and rotation at no load at first. After the first set of data acquisition, the participant repeated the same exercises against resistances of 5 lbs., 10 lbs. and 15 lbs. The weights for resistance were attached to a rope which was passed over a pulley away from the body of the participant. The participants performed 10 repetitions of each exercise with the rope held close to their chest.

Approvals were obtained from Institutional Review Boards (IRB) of both Auburn University (Protocol Number – 09-344 M41001) and Palmer College of Chiropractic, IA (IRB Assurance Number - 2008G116). Following the IRB approvals, the participants were recruited through word of mouth. The following were the inclusion and exclusion criteria for the participants:

Inclusion Criteria –

1. Participant must be an adult (over 18 years old) and capable of reading and understanding English language.
2. Participant should not have any musculoskeletal injury related to spine, hands or legs in the past 12 months.
3. Participant should not have a pacemaker or any non-removable metal object on them.
4. Participant should not experience any pain in the range of motion while performing the motions mentioned in the testing protocol.

Exclusion Criteria –

The participants were additionally screened for neurological or dermatitis-related symptoms by certified clinicians before they performed the biomechanical tests. The screening was based on questionnaires, physical tests and visual observation. If the participants exhibited those symptoms they were excluded.

### 3.2 Sample Size –

A biomedical study, to be successful, has to have a well-defined problem, an appropriate population, and a reliable procedure and instruments, among other resources. In addition to these, an adequate sample size is one of the most critical parameters to be considered. It must be big enough that it does not waste resources on an inconclusive study, and short enough that it can yield useful results in a timely manner. Sample size is of the utmost importance in experiments involving human or animal subjects for ethical issues. In an over-populated experiment, an unnecessary number of participants are exposed to potentially hazardous tests, while under-populated studies expose subjects to potentially hazardous tests without advancing the research knowledge (Lenth, R.V. 2001).

Finally, the study must be of adequate size, which would be relative to the goal of the study. The present study is a preliminary study, and time and cost are the main constraints. Keeping this in mind, a sample size of ten subjects was considered adequate for this study. 10 males subjects were recruited through word of mouth, though data was only recorded from 9 participants as sensors could not be attached properly to one of the participants. The demographics of the participants were as follows:

Age (yrs)		Height (cm)		Weight (kg)	
Mean	43.22222	Mean	176.4444	Mean	76.68889
SD	17.41248	SD	11.04662	SD	10.1228

**Table 1 Demographics**

### 3.3 Data Acquisition –

Two types of motion data were obtained for this study, motion data and EMG data. The motion data was obtained using the Liberty 24/8 (Polhemus, Vermont, USA) system. Motion data was recorded at 120 samples per second using motion sensors attached to T1, L3, L5 and S1 vertebrae. A fourth order butterworth filter with low pass frequency of 20 Hz was used to filter the motion data. The EMG data was recorded at 1200 samples per second using DELSYS Bagnoli - 12 Channel EMG System. The EMG signals were amplified 1000 times and band passed between 20 Hz and 500 HZ (Lee et. al., 2007; Okubo et. al, 2010). Frequencies less than 20 Hz eliminate noise due to wire sway, whereas frequencies over 500 Hz eliminate noise due to surface contact between the electrodes and the skin (M. B. I. Raez et. al., 2006). Motion Monitor 7.0 software (Innovative Sports Training, Inc.) was used to collect both Motion and EMG data.

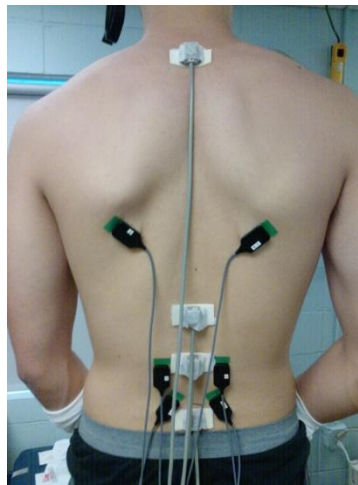


**Figure 5 SEMG and motion sensors attached to back muscles and vertebrae respectively**

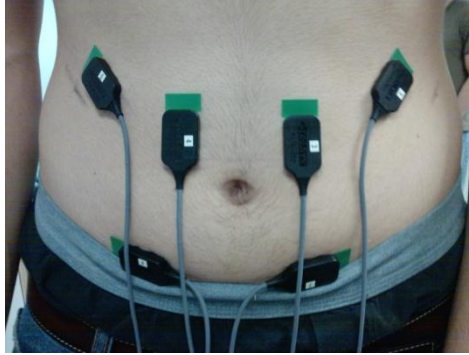


**Figure 6 sEMG sensors attached to abdominal muscles**

sEMG sensor positions were initially marked using body markers. The skin was then prepared using alcohol prep pads and skin abrasive. The skin was initially cleaned using alcohol prep pads to remove any oil present on the surface of the skin. The skin was then gently abraded using skin abrasive to remove any dead cells, which may affect EMG signals, from the surface of the skin. The skin was cleaned again using alcohol prep pads to remove any dead cell debris from the skin. The sEMG sensors were also cleaned using alcohol prep pads to remove any dirt from their surfaces. The sensors were then attached to the skin using double sided tape. As mentioned in the table above, EMG data was obtained from 6 muscles, namely Multifidus, Erector Spinae, Latissimus Dorsi, Internal Obliques, External Obliques and Rectus Abdominis. The locations for the placement of sEMG sensors were determined based on previous studies. (Sridhar Poosapadi Arjunan et. al., 2009; Rafael F Escamilla et. al., 2006).

The motion sensors were attached at T1, L3, L5 and S1 vertebrae. The locations of these vertebrae were found using a palpation technique. The skin was cleaned using alcohol prep pads to remove any oil present on the surface of the skin. The motion sensors were attached to the skin using double-sided tape.

Muscle	Side	Amplifier Ch. No. (Sensor No.)	A/D Board	Channel No.	Location
Erector Spinae	Left	1	0	6	Over the largest muscle mass found by palpation and 4 cm from midline of the spine at the third lumbar vertebrae.
	Right	2	0	7	
Rectus Abdominus	Left	3	0	8	3 cm from the midline of the abdomen and 2 cm above the umbilicus.
	Right	4	0	9	
External Oblique	Left	5	0	10	10 cm from the midline of the abdomen and 4 cm above the ilium at an angle of 45°.
	Right	6	0	11	
Internal Oblique	Left	7	0	12	4 cm above the ilium in the lumbar triangle at an angle of 45°.
	Right	8	0	13	
Multifidus	Left	11	1	0	Bilaterally at the level of L5 and aligned parallel between the line of the posterior-superior iliac spine (PSIS) and the interspinous space of L1 and L2.
	Right	12	1	1	
Latissimus Dorsi	Left	9	0	14	Positioned obliquely (approximately 25° from horizontal in the inferomedial direction) 4 cm below the inferior angle of the scapula.
	Right	10	0	15	

**Table 2 EMG sensor placement**

Once the sensors were attached the participant was asked to wear a harness and anti-vibration gloves for safety. The participant was asked to hold the rope to which the weight was attached close to the chest and then stand in an upright position with his feet in a comfortable position. The chosen position of the feet was marked and was kept constant throughout the data acquisition process. Once the data acquisition started, the participants were asked to hold the neutral position for 2 seconds, then asked to perform 10 repetitions of the three exertions as described above, and then asked to hold the neutral position for 2 seconds again before the data acquisition ended. The data was then



exported from motion monitors using the preference file created (Appendix). The data was exported twice, once for motion data and then for EMG data.

### **3.4 Motion Data Analysis –**

After exporting the data, the data was separated from Excel files to form individual data files for FE, LB and ROT data for 0 lb, 5 lb, 10 lb and 15 lb respectively. Data for the first and the last two seconds when the participant was stationary was eliminated. Data analysis was carried out on these data files.

#### **3.4.1 Time series –**

The motion data obtained is nothing but a time series. A time series is a collection of observations made sequentially through time. Examples occur in a variety of fields ranging from engineering to economics. Examples include daily stock market prices or pressure readings from pressure gauges at some factories (Chatfield Chris, ‘The Analysis of Time Series: An Introduction’). The best way to see how a physical quantity changes with time is to plot a graph.

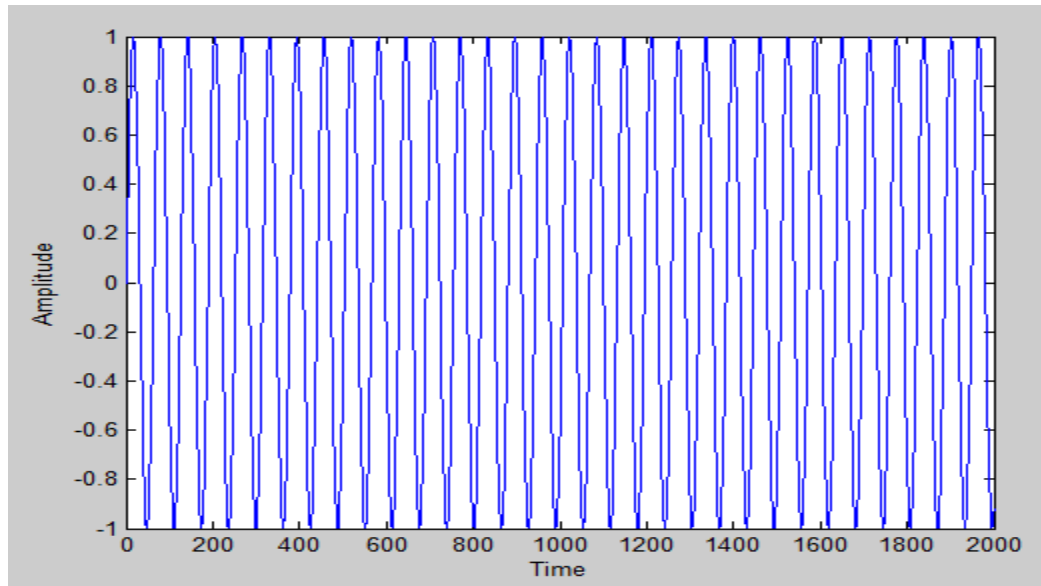


Figure 7 Sine Curve

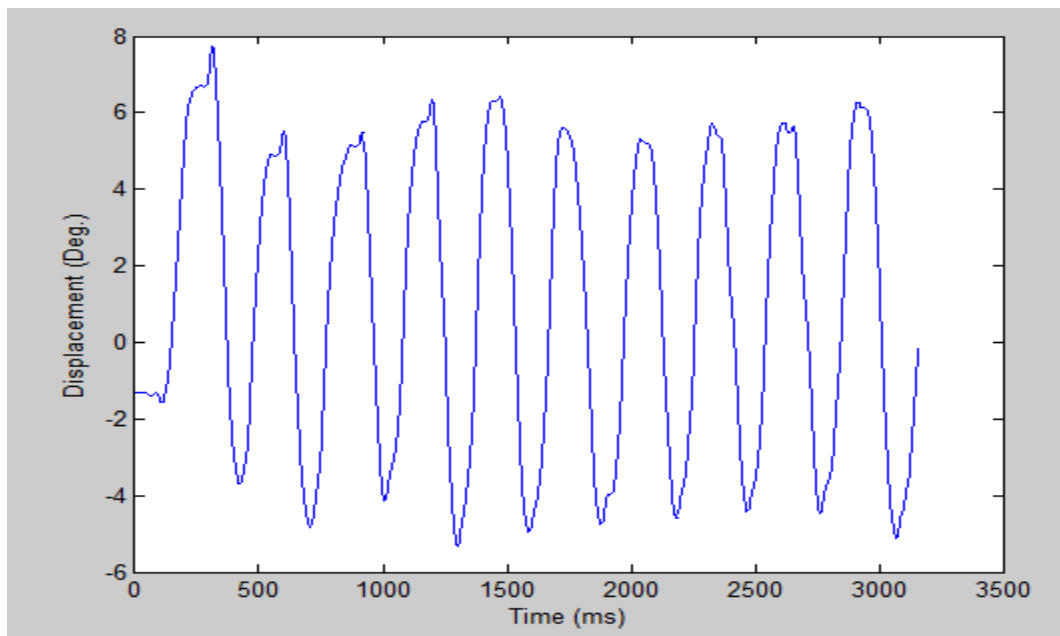


Figure 8 Time series for flexion-extension against 5 lb resistance

### 3.4.2 Range of Motion (ROM) –

ROM tells us the limits between which a person can carry out a particular type of exercise. The flexibility of the spine represents the functional performance of the trunk

mobility. For most spinal surgeries, spinal flexibility is regarded as an important part of preoperative evaluation and postoperative functional outcome assessment (McGregor A. H. et. al. 2004, Nissan M. et. al. 1999). Analysis of spinal ROM may improve our understanding the severity of some spinal disorders, such as progression of ankylosing spondylitis and the surgical effect of multiple-level discectomy or laminectomy. The information derived from changes in spinal ROM is also useful in investigating the development of adjacent-segment instability after fusion procedures (Chou WY et. al. 2002, Lu WW et. al. 1999).

In our study the ROM was studied for flexion-extension, lateral bending and rotation motions. As mentioned before, the participants were asked to perform these three exercises against no load and resistances of 5 lbs, 10 lbs and 15 lbs. The participants were asked to move in their comfortable range of motion without exerting too much force on their lower back muscles. The data was obtained as described previously and analyzed for changes in ROM. A customized MATLAB program was used to study the ROM. The time series data obtained after repetitive trunk FE, LB and ROT was plotted first. The peaks and valleys of the plot were identified and the highest and lowest points were selected. The difference between a successive highest and lowest point was ROM for that particular movement cycle. The average of ROM of a particular time series data was the average of all the ROM values of individual movement cycles.

### 3.4.3 Classification of time series as periodic or chaotic –

The non-linear methods that we are going to apply calculate the chaos in a dynamic system. Before we do this, we have to make sure that the system that we have is indeed chaotic. This can be done using Fast Fourier Transformation (FFT) and Phase Plane plots (L. F. P. Franca et. al. 2001). As is well known, the FFT of a chaotic signal presents continuous spectra over a limited range and the energy is spread over a wider bandwidth. On the other hand, FFT of a periodic signal presents discrete spectra, where a finite number of frequencies contribute for the response (Mullin T. 1993, Moon F. C. 1992).

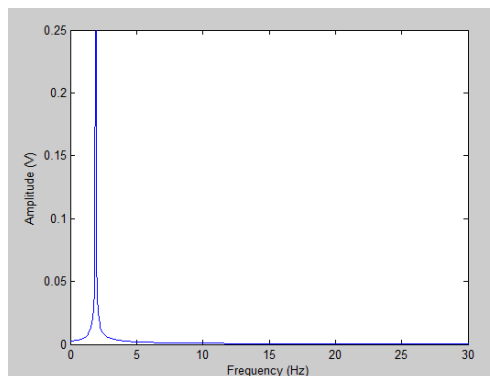


**Figure 9** FFT of a periodic sine curve

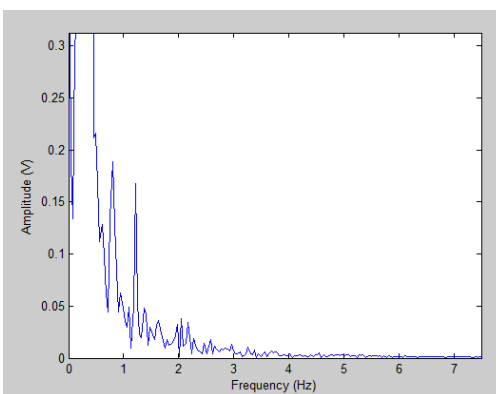


**Figure 10** FFT of experimental motion data

From the above FFT plots we can see that the experimental data contains continuous spectra over a limited range, as opposed to FFT of the sine wave which returns a single frequency. This is an indication that our data might be chaotic.

#### 3.4.4 Approximate Entropy (ApEn) –

Entropy is a statistical concept, which was first introduced by Shanon and Weaver in 1963 as a measure of uncertainty or variability. Similarly, ApEn is a specific method to determine complexity that can quantify the regularity or predictability of a time series (Pincus, 1994). Predictability and regularity are inversely proportional to complexity. The more predictable and regular the time series, the less would be the complexity, and vice versa. Approximate Entropy measures the logarithmic probability that a series of data points a certain distance apart will exhibit similar relative characteristics on the next incremental comparison within the state space (Pincus, 1994). Data points that exhibit greater possibilities of remaining the same distance apart upon comparison will result in lower ApEn values, while those with large differences in distance between them will result in higher ApEn values.

In order to mathematically define ApEn, we need to form a time series of data  $u$  (1),  $u$  (2) ..... $u$  ( $N$ ). These are  $N$  raw data values from measurements taken at equally spaced points in time. We then fix  $m$ , an integer, and  $r$ , a positive real number. The input parameter  $m$  is the length of compared runs, and  $r$  is the tolerance that specifies a filtering level. The first step is to form a sequence of vectors  $x(1), x(2), \dots, x(N - m + 1)$  in  $R^m$ , real  $m$ -dimensional space, defined by  $x(i) = [u(i), \dots, u(i + m - 1)]$ . The second step is to use the sequence  $x(1), x(2), \dots, x(N - m + 1)$  to construct for each  $I, 1 \leq i \leq N - m + 1$ ,  $C_i^m(r) = (\text{number of } x(j) \text{ such that } d[x(i), x(j)] \leq r) / (N - m + 1)$ . We must define  $d[x(i),$

$x(j)$ ] for vectors  $x(i)$  and  $x(j)$ . We follow the Takens modification of formula by defining  $d[x, x^*] = \max |u(a) - u^*(a)|$ , where the  $u(a)$  are the  $m$  scalar components of  $x$ .  $d$  represents the distance between the vectors  $x(i)$  and  $x(j)$ , given by the maximum difference in their respective scalar components. Next we define  $\Phi^m(r) = (N - m + 1)^{-1} \sum_{i=1}^{N-m+1} \ln C_i^m(r)$ , where  $\ln$  is natural logarithm. Lastly we define Approximate Entropy as:

$$\text{ApEn}(m, r, N) = \Phi^m(r) - \Phi^{m+1}(r)$$

As seen above, calculation of ApEn requires selection of two parameters:  $m$ , the number of observation windows to be compared, and  $r$ , the tolerance factor. In order to compare the results, these parameters, along with the data length, must be kept the same for all calculations (Pincus and Goldberger, 1994).

Typically  $m = 2$  or  $3$ ;  $r$  depends greatly on the application (Pincus et. al, 1991). This choice of  $m$  is made to ensure that the conditional probabilities, defined in the equation below for fixed  $m$  and  $r$ , are reasonably estimated from the  $N$  input data points. Theoretical calculations indicate that reasonable estimates of these probabilities, for fixed  $m$  and  $r$  chosen as discussed below, are achieved with between  $10^m$  and  $30^m$  points, analogous to findings of Wolf et al. (Pincus et. al, 1991).

The number of input points for ApEn computations ranges typically from 50 to 5,000 points (Stergiou, 2003; Pincus, 1994; Pincus et. al, 1991). Using fewer than 50 data points yields less meaningful results, especially for  $m = 2$  or  $3$ , while using more than 5,000 points will result in unacceptably long computational time (Pincus et. al, 1991). For noiseless, theoretically described systems, such as Henon maps and logistic maps, it has been shown that if  $\text{entropy}(A) \leq \text{entropy}(B)$ , then  $\text{ApEn}(m, r)(A) \leq \text{ApEn}(m, r)(B)$  and

vice versa. Moreover, for both theoretical and experimental systems, if  $\text{ApEn}(m_1, r_1)(A) \leq \text{ApEn}(m_1, r_1)(B)$ , then  $\text{ApEn}(m_2, r_2)(A) \leq \text{ApEn}(m_2, r_2)(B)$  and vice versa. This ability of ApEn to preserve the order is a relative property and is an important utility of ApEn (Pincus et al, 1991). Considering this, one should not conclude that for the same systems,  $\text{ApEn}(m_1, r_1)(A) \leq \text{ApEn}(m_2, r_2)(B)$ , as ApEn values differ with different  $m$  and  $r$  values. The strength of ApEn is its ability to compare systems.

As explained above there are two critical parameters ( $m$  and  $r$ ) that need to be set in order to achieve reasonable results while using ApEn. Different  $m$  and  $r$  values would result in different results.  $\text{ApEn}(2, 0.1)$  may be different from  $\text{ApEn}(3, 0.01)$  values. This leads to the question of which one should be chosen. ' $r$ ' is effectively a filter level and in order to eliminate the effect of noise in the ApEn calculation, ' $r$ ' must be chosen such that its value is above most of the noise. In order to achieve reasonable results the magnitude of noise should rarely reach ' $r$ '.

Another key factor in choosing the value of  $r$  is that it should be large enough to achieve numerically stable conditional probability estimates in equation (A) above (Pincus et. al, 1991). If the ' $r$ ' value is small, one gets unstable conditional probability estimates, while larger ' $r$ ' values result in detailed system information being lost due to filter coarseness. In the current study a value of 2 was used for  $m$  and  $r$  was 0.2 (Pincus 1990; Pincus 1994; Stergiou, 2004).

### 3.4.5 Calculation of ApEn –

Consider a time series  $SN$ , consisting of  $N$  number of sample size. To compute ApEn we must choose two input parameters,  $m$  and  $r$ . We denote a pattern of  $m$  time series, beginning at measurement  $i$  within  $SN$ , by the vector  $p_m(i)$ . Two patterns,  $p_m(i)$  and

$p_m(j)$ , are said to be similar if the difference between any pair of corresponding measurements in the patterns is less than  $r$  — i.e, if

$$|N(i+k)-N(j+k)| < r, \text{ for } k=0 \text{ to } m$$

Now consider the set  $P_m$  of all patterns of length  $m$  (i.e.,  $p_m(1), p_m(2), \dots, p_m(N-m+1)$ ), within SN. So we may define  $C_{im}(r) = n_{im}(r) / (N-m+1)$  where  $n_{im}(r)$  is the number of patterns in  $P_m$  that are similar to  $p_m(i)$  (provided similarity criterion ' $r$ '). The quantity  $C_m(r)$  is the fraction of length  $m$  that is identical to the pattern of the same length that begins at interval  $i$ . We can calculate  $C_{im}(r)$  for each pattern in  $P_m$ , and we define  $C_m(r)$  as the mean of these  $C_{im}(r)$  values. The quantity  $C_m(r)$  expresses the prevalence of repetitive patterns of length  $m$  in SN. Finally, we define approximate entropy of SN, for patterns of length  $m$  and similarity criterion  $r$ , as

$$\text{ApEn}(m, r) = \ln[C_m(r) / C_{m+1}(r)]$$

Thus, if we find similar patterns in a time series, ApEn estimates the logarithmic likelihood that the next intervals after each of the patterns will differ.

### 3.4.6 Correlation Dimension (CoD) –

The correlation dimension presently is the most popular measure of dimension. It's much like the information dimension but is slightly more complex. The information dimension usually is based on spreading a grid of uniformly sized compartments over the trajectory like a quilt. That's like moving the measuring device over the object by equal, incremental lengths. Analysis for the correlation dimension could also be done with that approach. Instead, however, the usual technique is to center a compartment on each successive datum point in turn, regardless of how many points a region has and how far apart the points may be.



Many types of exponent dimension are essentially impossible to compute in practice, either because they apply to some unattainable limit (such as  $\varepsilon \rightarrow 0$ ) or they are computationally very inefficient. The correlation dimension avoids those problems. Also, for a given dataset, it probes the attractor to a much finer scale than, say, the box-counting dimension. Two data points that plot close together in phase space are highly correlated spatially. (One value is a close estimate of the other.) However, depending on the trajectory's route between them, those same two points can be totally unrelated with regard to time. (The time associated with one point may be vastly and unpredictably different from the time of the other.) The correlation dimension only tests points for their spatial interrelations; it ignores time. (That's also true of the information dimension, but for other reasons it acquired a different name) (Garnett P. Williams, 1997).

Before we go to the measuring procedure for the CoD, we need to understand some basic concepts, namely Phase Space Plots, Time Delay and Embedding Dimension.

### **3.4.7 Phase Plane Plots –**

We'll begin by setting up the arena or playing field. One of the best ways to understand a dynamical system is to make those dynamics visual. A good way to do that is to draw a graph. Two popular kinds of graph show a system's dynamics. One is the ordinary time-series graph that we've already discussed (Fig. 1.1). Usually, that's just a two-dimensional plot of some variable (on the vertical axis, or ordinate) versus time (on the horizontal axis, or abscissa).

Right now we're going to look at the other type of graph. It doesn't plot time directly. The axis that normally represents time therefore can be used for some other variable. In other words, the new graph involves more than one variable (besides time). A

point plotted on this alternate graph reflects the state or phase of the system at a particular time (such as the phase of the Moon). The space on the new graph has a special name: phase space or state space.

The phase space includes all the instantaneous states the system can have. As a complement to the common time-series plot, a phase space plot provides a different view of the evolution. Also, whereas some time series can be very long and therefore difficult to show on a single graph, a phase space plot condenses all the data into a manageable space on a graph.

Chaos theory deals with two types of phase space: standard phase space (my term) and pseudo phase space. The two types differ in the number of independent physical features they portray (e.g. temperature, wind velocity, humidity, etc.) and in whether a plotted point represents values measured at the same time or at successive times (Garnett P. Williams, 1997).

#### **3.4.8 Standard Phase Space –**

Standard phase space (hereafter just called phase space) is the phase space defined above: an abstract space in which coordinates represent the variables needed to specify the state of a dynamical system at a particular time. On a graph, a plotted point neatly and compactly defines the system's condition for some measuring occasion, as indicated by the point's coordinates (values of the variables). For example, we might plot a baby's height against its weight. Any plotted point represents the state of the baby (a dynamical system!) at a particular time, in terms of height and weight. The next plotted point is the same baby's height and weight at one time interval later, and so on. Thus, the succession

of plotted points shows how the baby grew over time. That is, comparing successive points shows how height has changed relative to weight, over time,  $t$ .

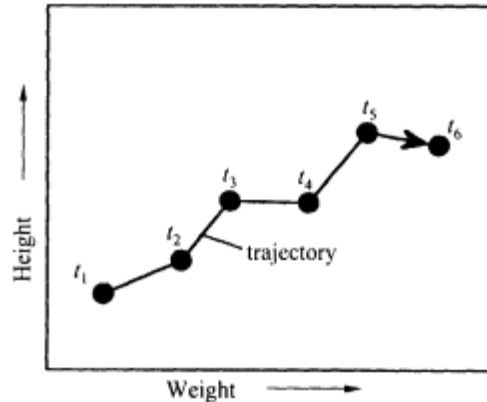


Figure 11 Example of standard phase space

### 3.4.9 Pseudo Phase Space –

Each axis on a standard phase space graph represents a different variable (e.g. Fig. 12). In contrast, our graph of the one-dimensional map plots two successive measurements ( $x_{t+1}$  versus  $x_t$ ) of one measured feature,  $x$ . Because  $x_t$  and  $x_{t+1}$  each have a separate axis on the graph, chaosologists (those who study chaos) think of  $x_t$  and  $x_{t+1}$  as separate variables ("time-shifted variables") and of their associated plot as a type of phase space. However, it's not a real phase space because the axes all represent the same feature (e.g., stock price) rather than different features. Also, each plotted point represents sequential measurements rather than a concurrent measurement. Hence, the graphical space for a one-dimensional map is really a pseudo phase space. Pseudo phase space is an imaginary graphical space in which the axes represent values of just one physical feature, taken at different times (Garnett P. Williams, 1997).

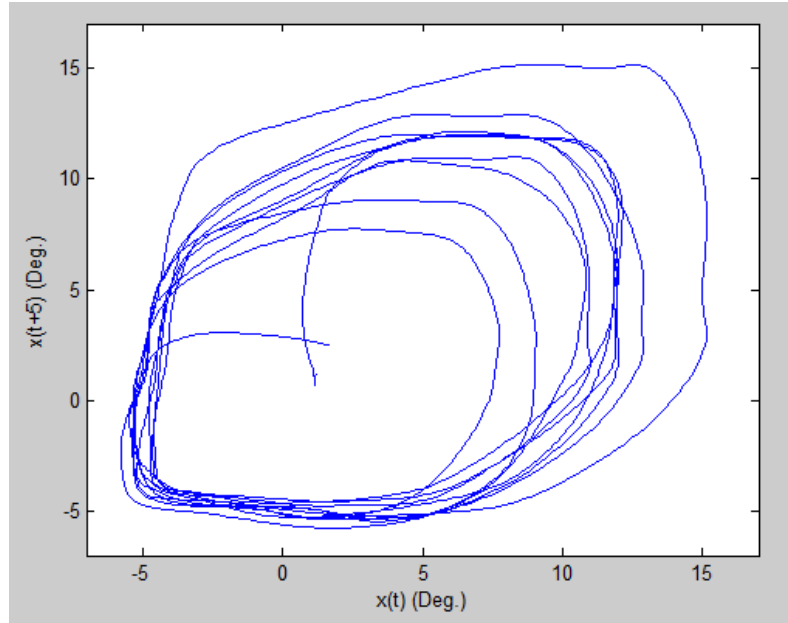


Figure 12 Pseudo phase space plot of experimental data

### 3.4.10 Time Lag –

To properly reconstruct a state space, it is essential to quantify an appropriate time delay and embedding dimension for the investigated time series. Investigation of the characteristics of the state space is a powerful tool for examining a dynamic system because it provides information that is not apparent by just observing the time series (Abarbanel, 1996; Baker and Gollub, 1996). To reconstruct the state space, a state vector was created from the time series. This vector was composed of mutually exclusive information about the dynamics of the system (Eq. (1)).

$$y(t) = [x(t), x(t-T_1), x(t-T_2)\dots\dots\dots] \quad (1)$$

where  $y(t)$  was the reconstructed state vector,  $x(t)$  was the original data, and  $x(t - T_i)$  was time delay copies of  $x(t)$ . The time delay ( $T_i$ ) for creating the state vector was determined by estimating when information about the state of the dynamic system at  $x(t)$  was different from the information contained in its time-delayed copy. If the time delay was

too small then no additional information about the dynamics of the system would be contained in the state vector. Conversely, if the time delay was too large then information about the dynamics of the system may be lost, and this can result in random information (Abarbanel, 1996; Baker and Gollub, 1996). Selection of the appropriate time delay was performed by using an average mutual information algorithm (Eq. (2); Abarbanel, 1996).

$$I_{x(t), x(t+T)} = \sum P(x(t), x(t+T)) \log_2 \frac{P(x(t), x(t+T))}{P(x(t))P(x(t+T))} \quad (2)$$

where  $T$  was the time delay,  $x(t)$  was the original data,  $x(t + T)$  was the time delay data,  $P(x(t), x(t + T))$  was the joint probability for measurement of  $x(t)$  and  $x(t + T)$ ,  $P(x(t))$  was the probability for measurement of  $x(t)$ , and  $P(x(t + T))$  was the probability for measurement of  $x(t + T)$ . The probabilities were constructed from the frequency of  $x(t)$  occurring in the time series. Average mutual information was iteratively calculated for various time delays and the selected time delay was at the first local minimum of the iterative process (Abarbanel, 1996; Stergiou et al., 2004). This selection was based on previous investigations that have determined that the time delay at the first local minimum contains sufficient information about the dynamics of the system to reconstruct the state vector (Abarbanel, 1996).

### **3.4.11 Embedding Dimension –**

Embedding dimension is the number of variables required to define a given dynamic system. The minimum embedding dimension in the reconstruction producer was estimated using an algorithm proposed by Kennel et al. (1992). The algorithm is based on the idea that in the passage from dimension  $d$  to  $d + 1$ , one can differentiate between points on the orbit that are true neighbors and those that are false. A false neighbor is a point in the data set that is identified as a neighbor solely because of viewing the attractor

in an embedding space that is too small. When the point in the data has achieved a large enough embedding space, all neighbors of every attractor point in the multivariate phase space will be true neighbors.

#### **3.4.12 Measuring Correlation Dimension –**

The procedure for getting the correlation dimension involves not only lag but also the embedding dimension—the number of pseudo phase space axes. For any given practical problem, there is no way to determine the correct embedding dimension in advance. It depends on the attractor's true dimension in regular phase space, and that value is what we're trying to find. The correct embedding dimension emerges only after the analysis.

Once the lag is specified, the procedure usually begins with an embedding dimension of two (two-dimensional pseudo phase space). First, situate the measuring cell such that its center is a datum point in the pseudo phase space. Next, count the number of data points in the cell. After that, center the cell on the reconstructed trajectory's next point (in the ideal approach) and make a new count. Keep repeating that same procedure, systematically moving the cell's center to each successive point on the trajectory. (Some people choose center points at random to get a representative sample of the attractor, instead of going to every point on the trajectory.) Let's look at an example with just five data points (Garnett P. Williams, 1997).

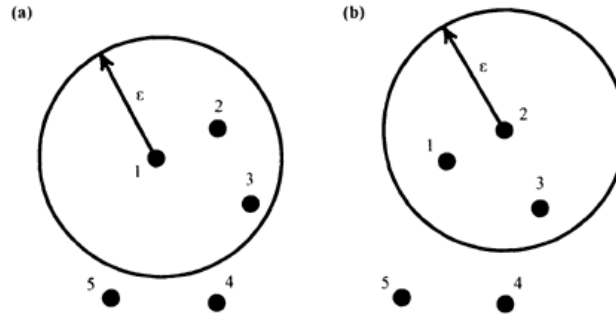


Figure 13 Identifying qualifying neighbors from (a) point 1 and (b) point 2

Next we center our circle on point 2, keeping the same radius as before (Fig. 14). Within the circle at its new location, points 1 and 3 now qualify. (As before, the reference point doesn't count.) Keeping that same radius and systematically centering the circle on each point, in turn, we count the qualifying points within each circle. Once through the entire dataset with the *same* radius, we add up the total number of qualifying points for that radius. For example, Figure 14 has a total of eight points for the radius indicated. (We get two points when the circle is centered at point 1, two more when it is on point 2, two again at point 3, and one point each for centering on points 4 and 5.) Having obtained the total for the radius chosen, we now work only with that total rather than with the numbers pertaining to any particular point. I'll refer to that total (eight in this example) in a general way as the "total number of points within radius  $\epsilon$ " or the "total number of qualifying points."

The total number of points defining the trajectory (i.e., the size of the basic-dataset) obviously influences the total count for a given radius. For instance, the count of qualifying points for a given radius is much smaller for a trajectory made up of ten points than for a trajectory of 10,000 points. For comparison purposes, therefore, we normalize each count of qualifying points, to account for the total available on the trajectory. That

means dividing each total of qualifying points by some maximum reference constant. That constant here is the maximum number of total points obtainable by applying the circling-and-counting procedure to each point throughout the dataset, for a given radius. The normalized result is the **correlation integral or correlation sum**,  $C_\epsilon$ , for the particular radius:

$$C_\epsilon = \frac{\text{Total number of points within radius } \epsilon}{\text{Largest number of mathematically possible points}}$$

$$= \frac{\text{Total number of points within radius } \epsilon}{N(N-1)} \quad (3)$$

in which  $N$  is the total number of points in the dataset (i.e., on the trajectory).

A special version of the ratio that defines the correlation sum (3) comes from considering the limit as  $N$  becomes large. When  $N$  is very large, the 1 in  $N-1$  becomes negligible. For all practical purposes,  $N-1$  then becomes simply  $N$ . The quantity  $N(N-1)$  (the denominator in the definition of correlation sum) therefore becomes  $N(N)$  or  $N^2$ . Thus, in the limit of infinitely large  $N$  we can define the correlation sum (3) as:

$$C_\epsilon = \lim_{n \rightarrow \infty} \frac{\text{Total number of points within radius } \epsilon}{N.N} \quad (4)$$

In the technical literature, Equation 24.2 often appears in an imposing symbol form, as follows:

$$C_\epsilon = \lim_{n \rightarrow \infty} \frac{1}{N.N} \sum_{i=1}^N \sum_{j=1}^N G(\epsilon - |x_i - x_j|) \quad (5)$$

The  $x_i$  in Equation 5 stands for a point on which we center our measuring device (e.g., our circle).  $x_j$  is each other point on the trajectory (each point to which we'll measure the distance from the circle's center point  $x_i$ ). For each center point, the absolute distance between  $x_i$  and  $x_j$  is  $|x_i - x_j|$ . The distance formula gives that absolute distance.



The next thing Equation 5 says to do is to subtract that distance from radius  $\epsilon$ . In symbols, that means computing  $\epsilon - |x_i - x_j|$ . If the answer is negative, then the measured distance  $|x_i - x_j|$  is greater than  $\epsilon$ . That means point  $x_j$  is beyond the circle of radius  $\epsilon$  and therefore doesn't qualify for our count. On the other hand, if  $\epsilon - |x_i - x_j|$  is positive, then  $|x_i - x_j|$  is smaller than  $\epsilon$ , and the point  $x_j$  is within the circle.

We now have to devise a way to earmark the qualifying points (the points within the circle). (In the highly unlikely event that the distance to a point *equals* the radius, we can count it or not, as long as we're consistent throughout the analysis.) Equation 5's next ingredient (to the left of the distance symbols) is  $G$ .  $G$  is an efficient way to label each qualifying point — that is, each point for which  $\epsilon - |x_i - x_j|$  is positive ( $>0$ ). In another sense,  $G$  acts as a sort of gatekeeper or admissions director. (The technical literature gives it the imposing name of the **Heaviside function**.) It lets all *qualifying* points into the ballgame for further action and nullifies all others. If  $\epsilon - |x_i - x_j|$  is positive, the point  $x_j$  has to be counted, as just explained. For all those cases the computer program assigns a value of 1 to the entire expression  $G(\epsilon - |x_i - x_j|)$ . If, instead,  $\epsilon - |x_i - x_j|$  is negative, the point  $x_j$  is beyond the radius of the measuring device. For those cases, the computer program assigns a value of 0 to  $G(\epsilon - |x_i - x_j|)$ .

Normalization is the equation's final job. As explained above, that's done by dividing the total number of qualifying points by the total number of available points. Strictly, the total number of available points is  $N(N-1)$ . Hence, we'd multiply the counted total by  $1/[N(N-1)]$ . Equation 5 uses the approximation (per Eq. 4) and so multiplies by  $1/N^2$ , with  $N^2$  being the total number of available points or pairs on the trajectory in the abstract limit where  $N$  becomes infinitely large. And that's all there is to Equation 5.

Having determined the correlation sum for our first radius, we next increase the radius and go through the entire dataset with the new radius. The larger radius catches more points than the smaller radius did. That is, the new radius yields a larger total number of qualifying points (numerator in Eq. 3). The normalization constant  $N^2$  depends only on the size of the basic dataset and so is constant regardless of the radius  $\epsilon$ . Hence, the larger  $\epsilon$  yields a larger correlation sum.

The idea is to keep repeating the entire procedure, using larger and larger radii. Each new radius produces a larger and larger total of qualifying points and a larger correlation sum. We end up with a dataset of successively larger radii and their associated correlation sums. Those radii and correlation sums apply *only* to the two-dimensional pseudo phase space in which we've been working. We now have to go to a three-dimensional pseudo phase space (an embedding dimension of three) and compute a similar dataset (or, rather, tell our computer to do it). All computed distances with the distance formula now involve three coordinates instead of two. Once the radii and associated correlation sums for three-dimensional pseudo phase space are assembled, we move on to four embedding dimensions, then five, and so on. A typical analysis involves computing a dataset for embedding dimensions of up to about ten. You might get by with fewer, or you might need more, depending on what a plot of the data shows. That plot is the next step.

For each embedding dimension, the correlation sum is plotted against the radius. Except for tail regions at the ends of the distribution, data for a given embedding dimension tend to plot as a straight line (a power law) on log paper (Fig. 14) (Garnett P. Williams, 1997).

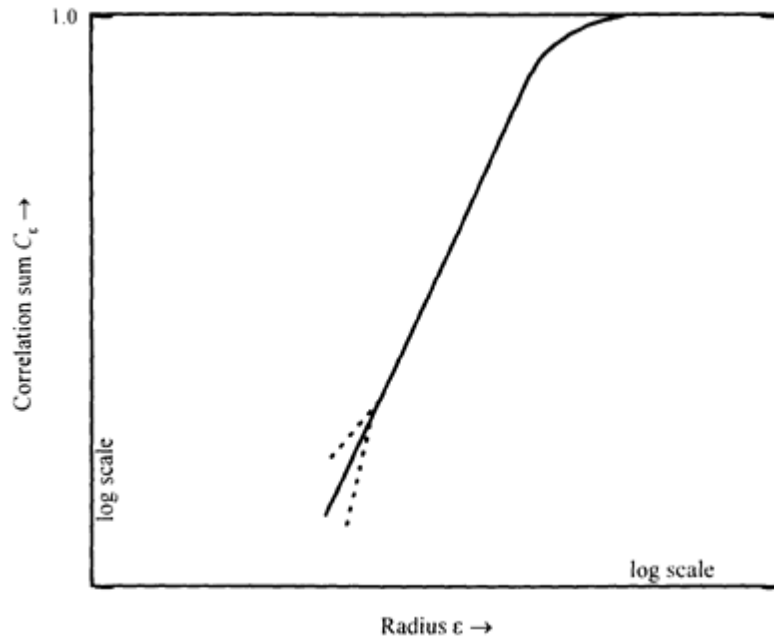


**Figure 14 Plot of Correlation Sum vs. Radius**

Figure 15, involving the special case of *uniformly distributed* phase space points, shows the reason for the power law. One center point is enough to demonstrate the power-law relation. For a given embedding dimension and center point, we choose a radius and count the number of qualifying points ( $N_\epsilon$ ). Using the same center point, we then repeat for larger and larger radii. A plot of such data (not included here) shows that  $N_\epsilon \propto \epsilon^{\text{dimension}}$ , which is a power law. For instance, data for the one dimensional case (Fig. 16 (a)) follow the relation  $N_\epsilon \propto \epsilon^1$ . In the two-dimensional case (Fig. 16 (b)), the data adhere to the rule  $N_\epsilon \propto \epsilon^2$ , and so on. Also, that proportionality doesn't change if we deal with a correlation sum rather than just  $N_\epsilon$ . The numerator in the correlation sum just increases by a constant multiplier that equals the number of center points; the denominator, based on the size of the dataset, is also a constant.

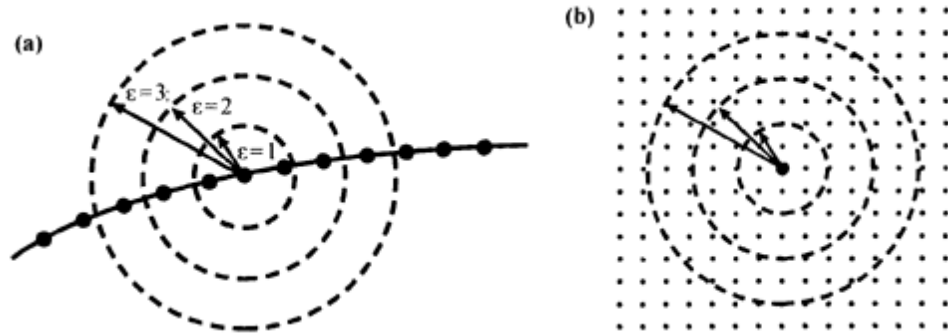


Figure 15 Sketch showing geometric increase in number of points within circle of radius  $\epsilon$  for uniformly spaced points (after Bergé et al. 1984: Fig. VL. 36). (a) One-dimensional attractor (line). (b) Two-dimensional attractor (plane)

Why does Figure 14 have tail regions where the power law no longer holds? The general idea is the same as we discussed for the information dimension. As we increase our measuring radius  $\epsilon$ , it eventually becomes so large that it starts to catch nearly all the available points. That is, it catches fewer and fewer new points. The numerator in Equation 4 (total number of points within radius  $\epsilon$ ) then increases at a lesser rate than at smaller radii. The plotted data then depart from a power law, and the relation becomes flatter (upper end of curve in Fig. 14). The radius finally becomes so large that it catches all possible points, no matter where it's centered. Thereafter, the total number of points remains constant at the maximum available in the data. The numerator and denominator in Equation 4 then are equal, and the correlation sum becomes 1 (its maximum possible value).

A tail region also occurs at small radii. The reason is that, in practice, data include noise and aren't uniformly distributed. Some small radius marks the beginning of a zone where measuring errors (noise) are of the same magnitude as true values. We can then no longer distinguish between the two. Furthermore, qualifying points become very scarce at small radii. In fact, even with noiseless data, our radius is eventually so small that it

doesn't catch any points. All of these features lead to unreliable statistics. The result is that the plotted relation at the smallest radii might curve away from the straight line, in either direction (Fig. 15).

We have, then, a scaling region (middle segment of plotted line), just as we found on a related plot when deriving the information dimension.

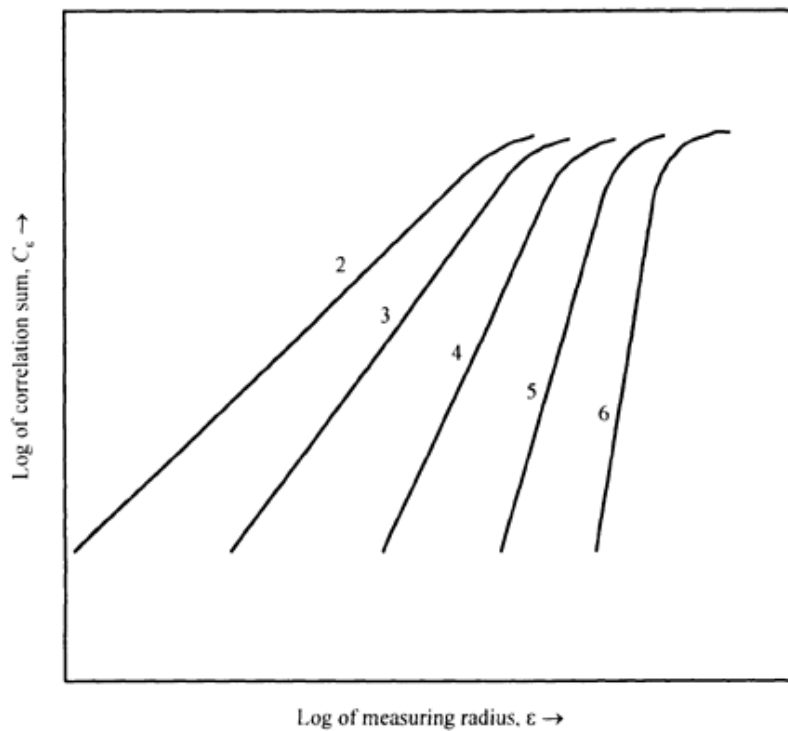


**Figure 16 Idealized plot of Correlation Sum vs. Radius for increasing Embedding Dimension**

The slope of the scaling region gives us the value of the CoD for that particular embedding dimension. Fig. 16 shows us the plots of correlation sum vs. measuring radius for successive embedding dimensions. As we can see from Fig. 16, the slope of the scaling region for the successive embedding dimensions tends to saturate to one particular value. This value of the slope is our CoD for the given time series (Garnett P. Williams, 1997).

### 3.5 EMG Data Analysis –

#### 3.5.1 Identifying muscle activation –

EMG data was acquired from 6 muscle groups using 12 channels of DELSYS sEMG sensors. The first step was to identify the muscles recruited for each type of low back exertion. This was done by plotting the EMG signals as a time series and then observing the nature of the graph. Below you can see the nature of the raw and RMS value graphs for ES Left muscle under 5 lb resistance during FE. It can be observed that there is a spike in muscle activity during FE motion and decrease in muscle activity when the participant is in neutral position.

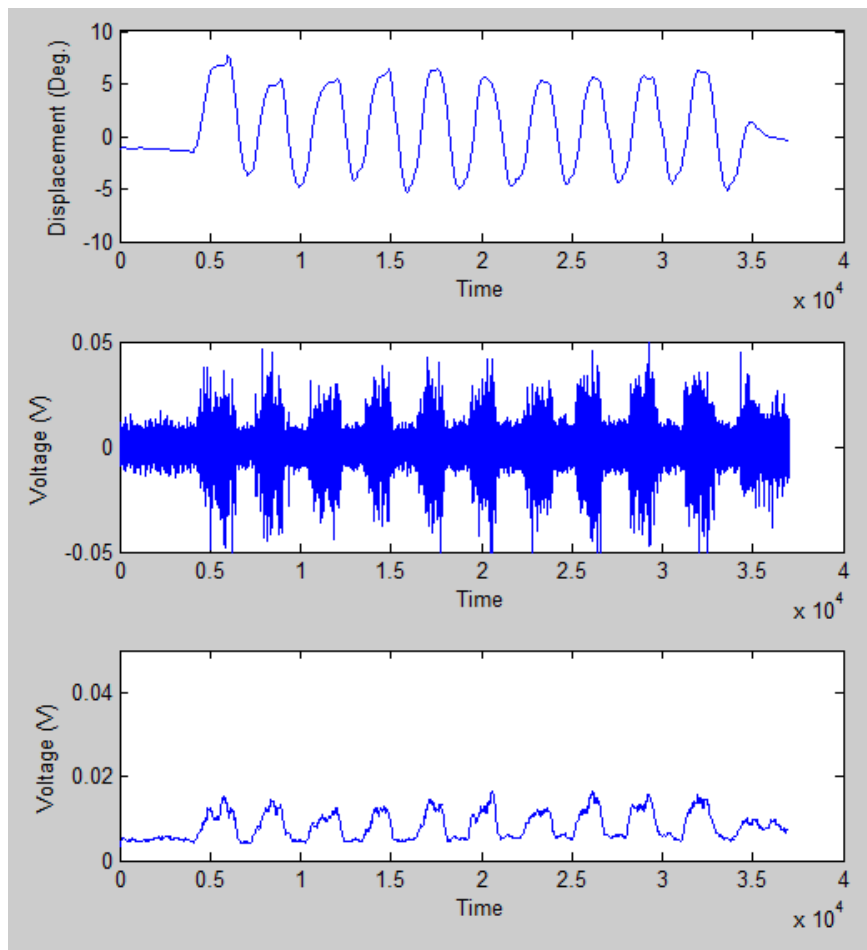


Figure 17 Muscle Recruitment for ES Left muscle during FE under 5 lb resistance

If a muscle is not recruited, then the spike in muscle activity is absent throughout the motion indicating that the muscle is not getting exerted under motion.

### **3.5.2 Mean and Median Frequency of SEMG signals –**

The next step was to calculate the mean and median frequencies of the recorded sEMG signals. The median frequency is the frequency at which 50% of the total power within the epoch is reached. Mean frequency is the frequency at which the average power within the epoch is reached (BIOPAC Systems Inc., Application notes). Previous research has shown that the mean and median frequencies decrease with fatigue induced in muscles (Bilodeau et. al., 2003; Mannion et. al., 1997). It would be interesting to see how the mean and median frequencies in the muscles under consideration vary with increase in resistance to motion. The mean and median frequencies were calculated using customized MATLAB programs in the Biomechanics et. al. Toolbox (BEAT) created by Ian Kremenec and Ali Sheikhzadeh from the Nicholas Institute of Sports Medicine and Athletic Trauma. The mean was calculated as the ratio of sum of product of signal amplitude and frequency to sum of amplitudes, whereas the median frequency was calculated as the frequency which divides the area under the amplitude vs frequency graph in two equal parts.

## CHAPTER 4

### RESULTS

Traditional (ROM) and non-traditional (ApEn and Cod) methods were used to study low back motion during FE, LB and ROT under resistance of 0 lb, 5 lb, 10 lb and 15 lb. Muscle activation under the same exertions was studied using mean and median frequency analysis.

#### 4.1 ROM Results –

The ROM results for all nine participants for flexion-extension, lateral bending, and rotation for exercises against no load and against resistances of 5 lb, 10 lb and 15 lb have been plotted in graphs 1(a), 1(b), and 1(c) respectively.

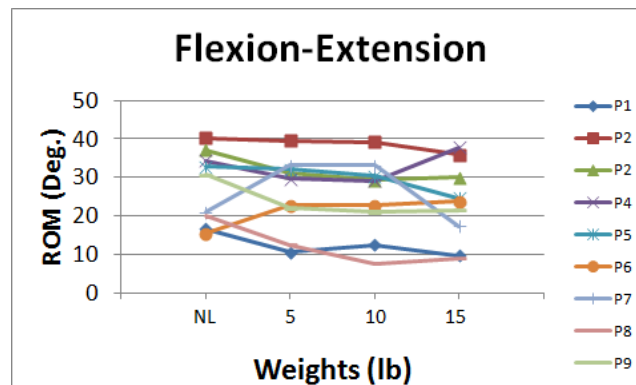


Figure 18 ROM results for FE



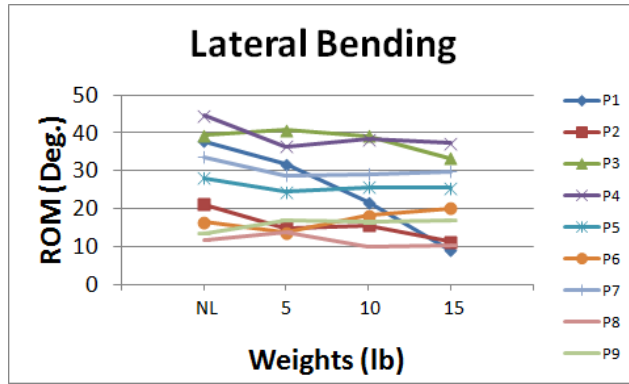


Figure 19 ROM results for LB

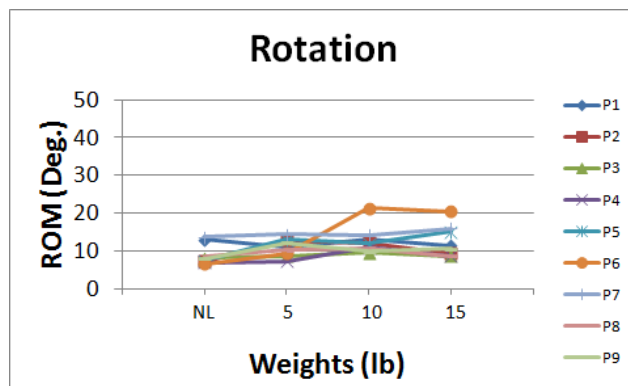


Figure 20 ROM results for ROT

One factor ANOVA test revealed that the ROM did not change significantly ( $p > 0.05$ ) as the resistance increased from zero to 15 lb during all three types of exercise.

SUMMARY						
<i>Groups</i>	<i>Count</i>	<i>Sum</i>	<i>Average</i>	<i>Variance</i>		
Column 1	9	248.2337	27.58152	87.75713		
Column 2	9	233.7492	25.97214	94.77536		
Column 3	9	225.004	25.00045	101.5264		
Column 4	9	209.7471	23.30524	105.3682		
ANOVA						
<i>Source of Variation</i>	<i>SS</i>	<i>df</i>	<i>MS</i>	<i>F</i>	<i>P-value</i>	<i>F crit</i>
Between Groups	86.55527	3	28.85176	0.296351	0.827739	2.90112
Within Groups	3115.417	32	97.35677			
Total	3201.972	35				

**Table 3 One factor ANOVA test on ApEn results for FE**

<b>Exercise</b>	<b>p-value</b>
Flexion - Extension	0.8277
Lateral Bending	0.716
Rotation	0.0907

**Table 4 p-values for ROM results**

#### **4.2 Phase Plane Plots –**

Phase Plane Plots were plotted to give a general idea of the dynamics of the system. The original time series was plotted against a lagged time series using time delay calculated by first minimum of average mutual information method. Below are the phase plane plots plotted for Participant 1 during FE, LB and ROT motion against 0 lb, 5 lb, 10 lb and 15 lb resistance.

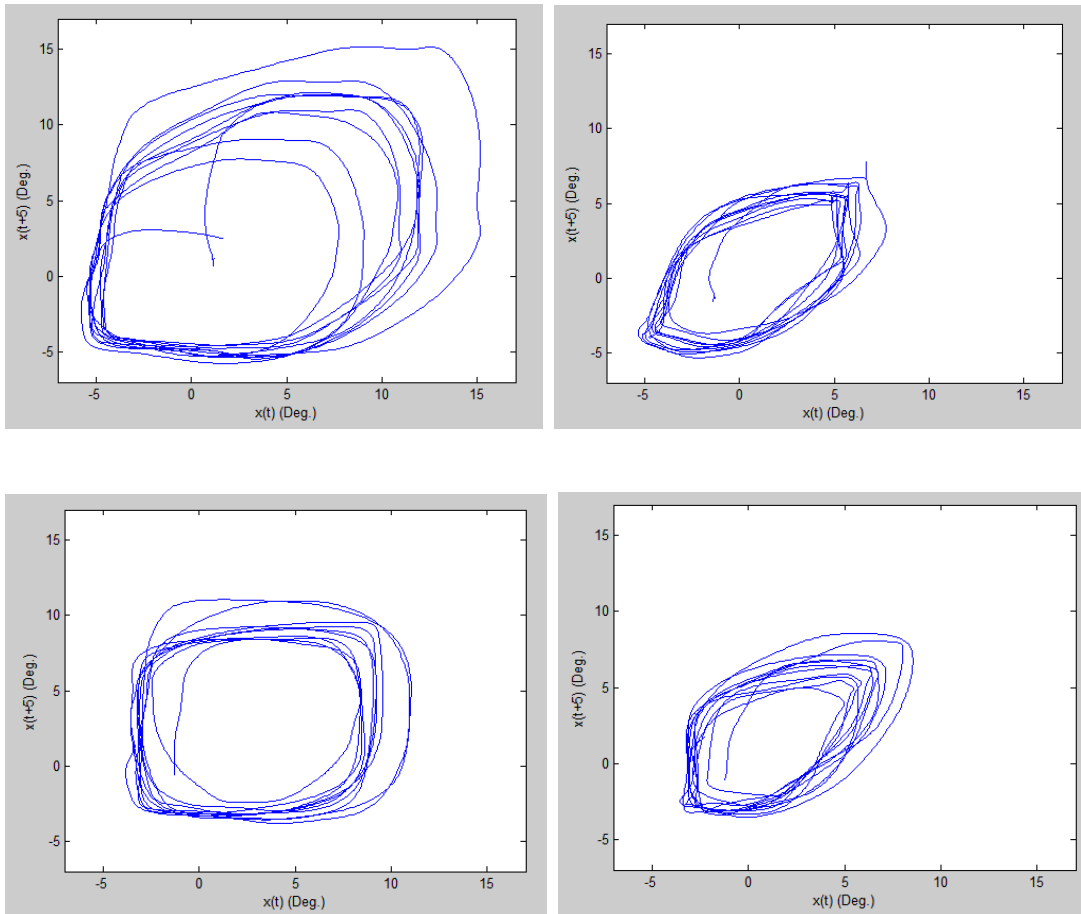


**Figure 21 Phase Plane plots for FE data against 0 lb, 5 lb, 10 lb and 15 lb respectively for participant 1 (left to right; top to bottom)**

From the above plots we can see that the trajectory follows a specific pattern with limited divergence. This indicates variability in the dynamic system. These plots can be compared to phase plane plots of perfectly periodic time series (sine wave).

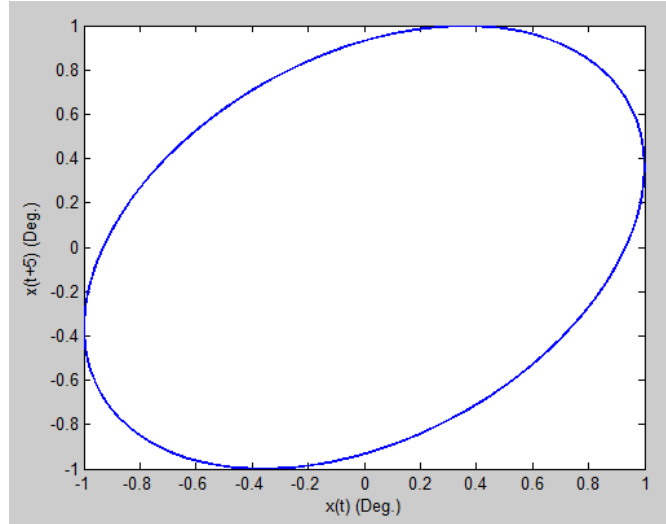


**Figure 22 Phase Plane plot of a perfectly periodic (sine wave) time series data**

Fig. 21 shows the Phase Plane plot of a sine wave. We can see that the trajectories overlap perfectly. The nature of the graph is ellipsoid because of the time delay value selected. This means that there is no variability in the data.

#### **4.3 Fast Fourier Transformation (FFT) –**

As mentioned in the previous chapter, one of the ways of detecting chaos in a dynamical system is to take FFT of the given data. FFT of a chaotic signal presents continuous spectra over a limited range and the energy is spread over a wider bandwidth. On the other hand, FFT of a periodic signal presents discrete spectra, where a finite number of frequencies contribute for the response (Mullin T. 1993, Moon F. C. 1992).

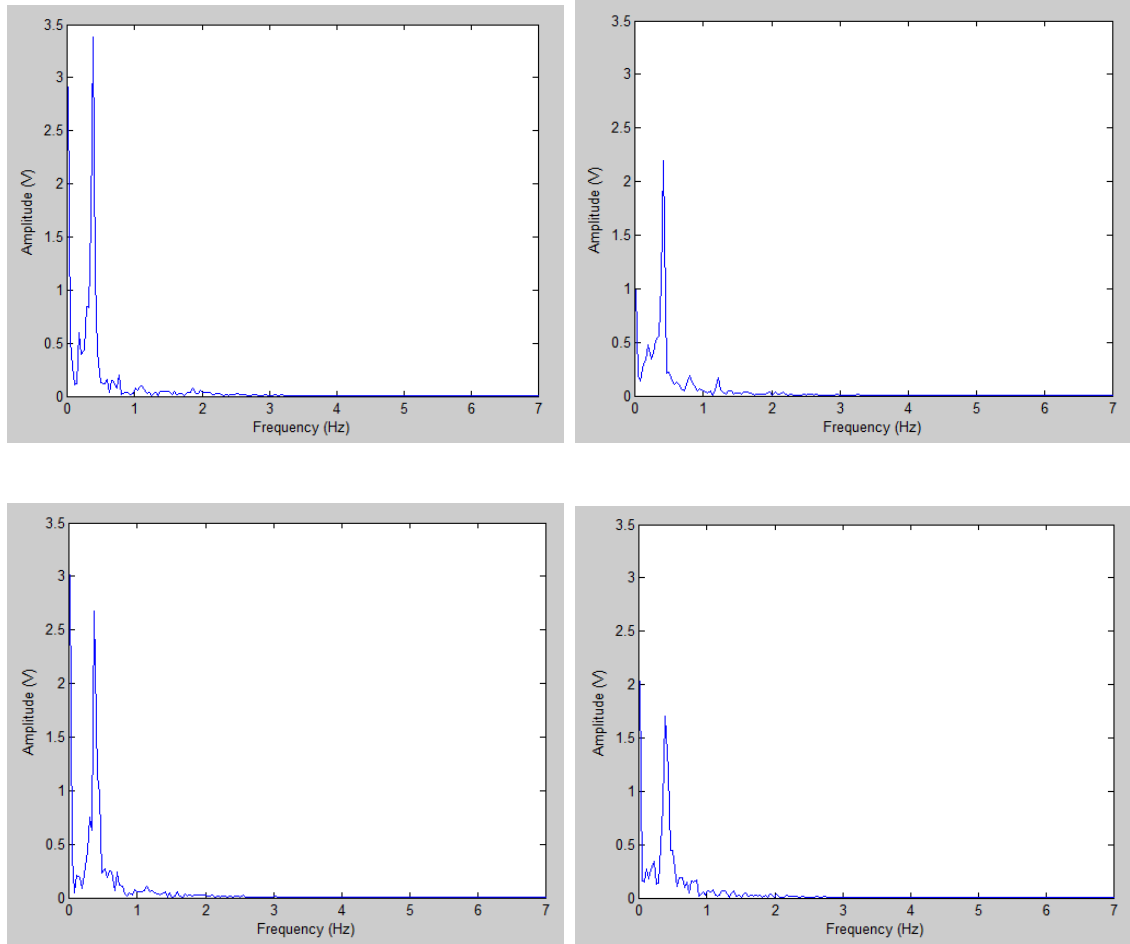


**Figure 23** FFT for FE data against 0 lb, 5 lb, 10 lb and 15 lb respectively for participant 1 (left to right; top to bottom)

We can see from above FFT plots that the experimental data recorded during FE for the participant consists of frequencies over a wide spectrum. This is an indication that the data that we have might be chaotic. We can compare this to a sine wave, which is an example of non chaotic data, which consists of a single frequency.

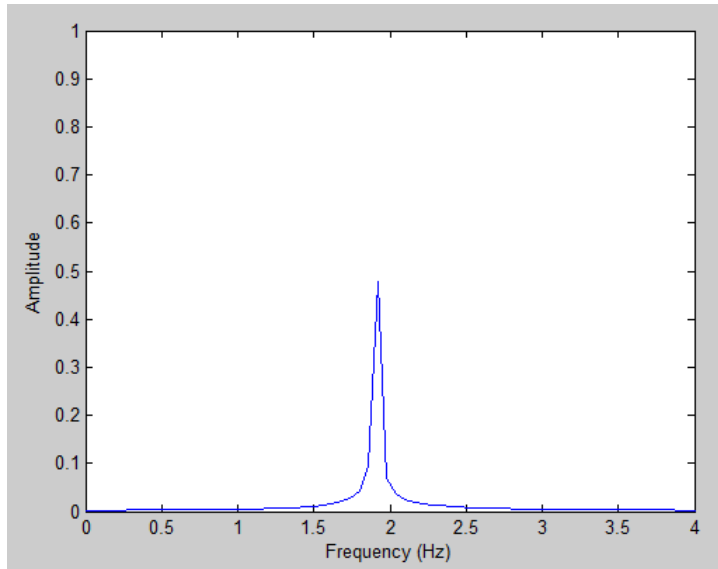


Figure 24 FFT of sine wave

#### 4.4 Approximate Entropy (ApEn) Results –

ApEn results were calculated using the algorithm developed by Pincus (Pincus, 1994). Below are the results for ApEn of experimental data recorded during FE, LB and ROT against 0 lb, 5 lb, 10 lb and 15 lb resistance.

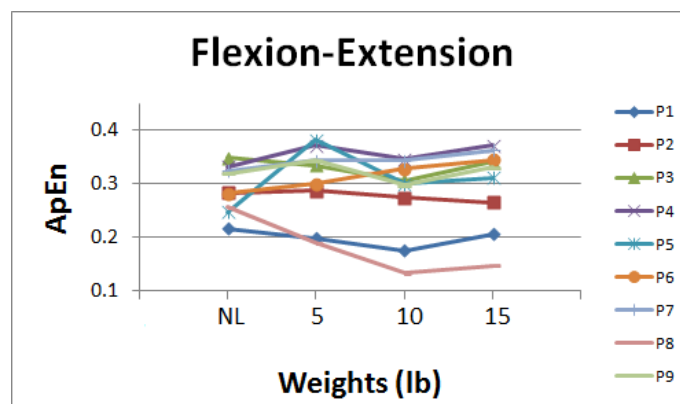


Figure 25 ApEn results for FE

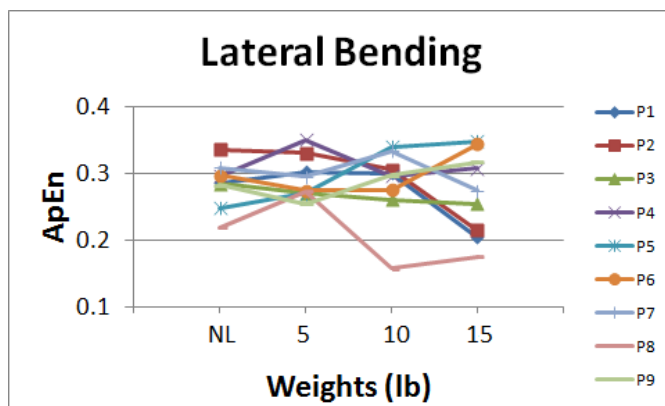


Figure 26 ApEn results for LB

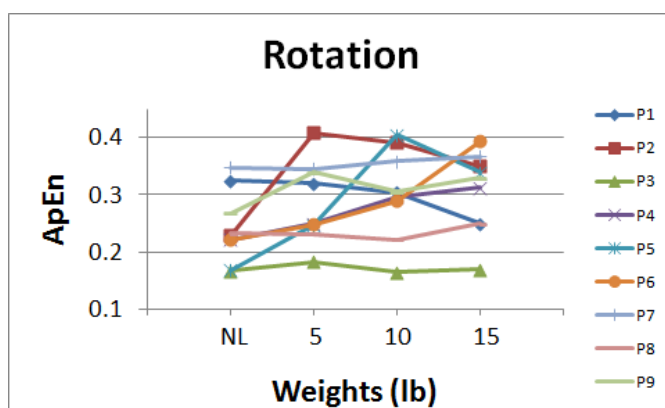


Figure 27 ApEn results for ROT

One factor ANOVA tests revealed that the ApEn values did not change significantly ( $p > 0.05$ ) as the resistance increased from zero to 15 lb during all the three types of exercises.

SUMMARY						
<i>Groups</i>	<i>Count</i>	<i>Sum</i>	<i>Average</i>	<i>Variance</i>		
Column 1	9	2.6096	0.289956	0.001987		
Column 2	9	2.7531	0.3059	0.004959		
Column 3	9	2.5042	0.278244	0.005593		
Column 4	9	2.6835	0.298167	0.005934		
ANOVA						
<i>Source of Variation</i>	<i>SS</i>	<i>df</i>	<i>MS</i>	<i>F</i>	<i>P-value</i>	<i>F crit</i>
Between Groups	0.003781	3	0.00126	0.272894	0.844479	2.90112
Within Groups	0.147779	32	0.004618			
Total	0.151559	35				

**Table 5 One factor ANOVA test on ApEn results for FE**

<b>Exercise</b>	<b>p-value</b>
Flexion – Extension	0.8444
Lateral Bending	0.8371
Rotation	0.2034

**Table 6 p-values for ApEn results**

#### **4.5 Correlation Dimension (CoD) Results –**

CoD for the motion data was calculated using an algorithm developed by Grassberger and Procaccia (1983). Below are the results for CoD of experimental data recorded during FE, LB and ROT against 0 lb, 5 lb, 10 lb and 15 lb resistance.



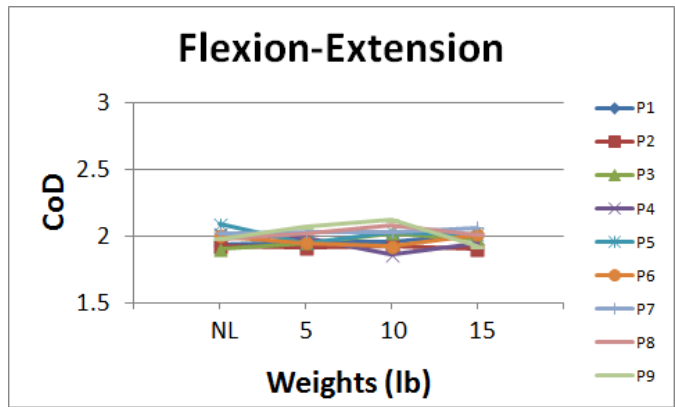


Figure 28 CoD results for FE

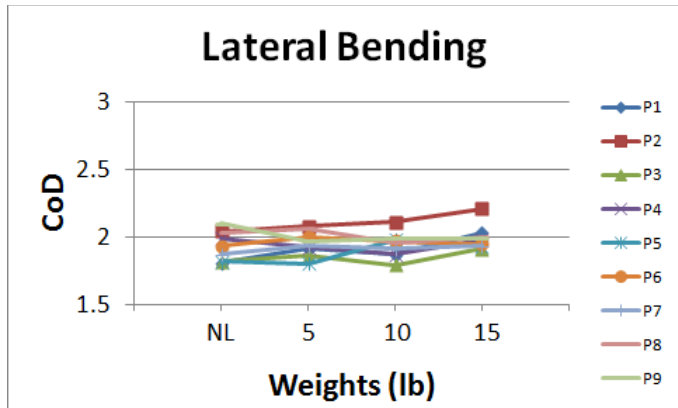


Figure 29 CoD results for LB

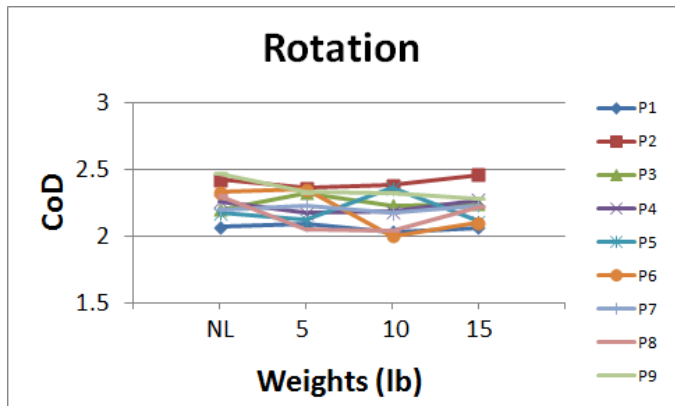


Figure 30 CoD results for ROT

The ANOVA tests revealed that the CoD did not change significantly ( $p > 0.05$ ) as the resistance increased from zero to 15 lb during all the three types of exercised. The p-values for FE, LB and ROT data sets came out to be 0.9734, 0.5668 and 0.6328 respectively.

SUMMARY						
<i>Groups</i>	<i>Count</i>	<i>Sum</i>	<i>Average</i>	<i>Variance</i>		
Column 1	9	17.83	1.981111	0.003436		
Column 2	9	17.83	1.981111	0.002536		
Column 3	9	17.94	1.993333	0.007075		
Column 4	9	17.86	1.984444	0.002678		
ANOVA						
<i>Source of Variation</i>	<i>SS</i>	<i>df</i>	<i>MS</i>	<i>F</i>	<i>P-value</i>	<i>F crit</i>
Between Groups	0.0009	3	0.0003	0.076312	0.972327	2.90112
Within Groups	0.1258	32	0.003931			
Total	0.1267	35				

**Table 7 One factor ANOVA test on CoD results for FE**

<b>Exercise</b>	<b>p-value</b>
Flexion - Extension	0.9723
Lateral Bending	0.5668
Rotation	0.6328

**Table 8 p-values for CoD results**

#### 4.6 EMG Frequency Analysis Results –

EMG signals were recorded from six muscle groups, namely Erector Spinae, Multifidus, Latissimus Dorsi, Internal Obliques, External Obliques and Rectus Abdominis. After the signals were recorded and processed, they were plotted to identify the muscles recruited by each participant for each type of low back exertion. It was interesting to note that not all the participants recruited the same muscles for the same type of low back exertion. The following table shows details about which muscle was recruited by how many participants for each type of low back exertion.

Muscle	No. of participants who used that muscle for that motion		
	Flexion-Extension	Lateral Bending	Rotation
ES Left	9	4	9
ES Right	9	9	9
EO Left	6	5	6
EO Right	6	9	6
IO Left	3	4	4
IO Right	3	4	3
RA Left	4	2	1
RA Right	4	2	1
LD Left	9	5	9
LD Right	9	9	9
MF Left	9	3	9
MF Right	9	9	9

**Table 9 Muscle recruitment during FE, LB and ROT by number of participants.**

Thus we can see that during FE, ES Left, ES Right, LD Left, LD Right, MF Left and MF Right were recruited by all the participants while the remaining muscles were not. Similarly, during LB, ES Right, EO Right, LD Right and MF Right were recruited by

all the participants. During ROT motion, ES Left, ES Right, LD Left, LD Right, MF Left and MF Right were recruited by all the participants.

For comparison purposes, the data from the muscles that were used by all the participants for that particular type of motion was used. Below are the results of mean and median frequency calculations for data obtained from muscles that were recruited by all the participants during FE, LB and ROT. After the mean and median frequency were calculated, One Factor ANOVA analysis with significance level of  $\alpha = 0.05$  was conducted to see if the mean and median frequency varied significantly with increase in resistance to motion.

#### 4.6.1 Mean and Median Frequency during Flexion – Extension motion –

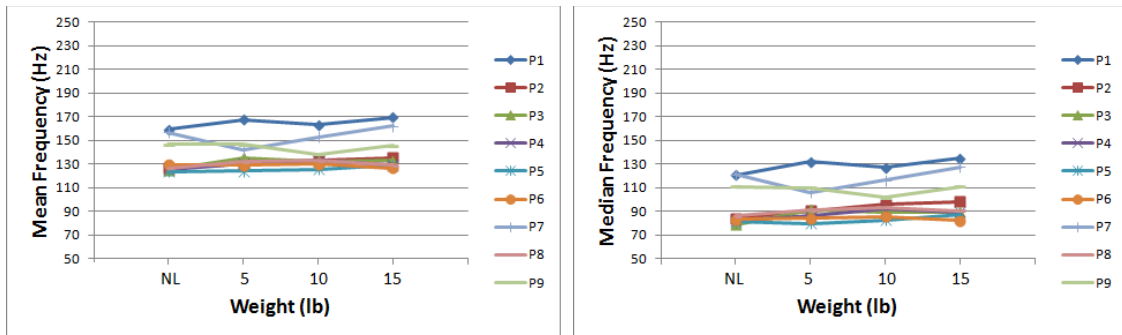


Figure 31 ES Left – Mean and Median Frequencies (Left and Right)

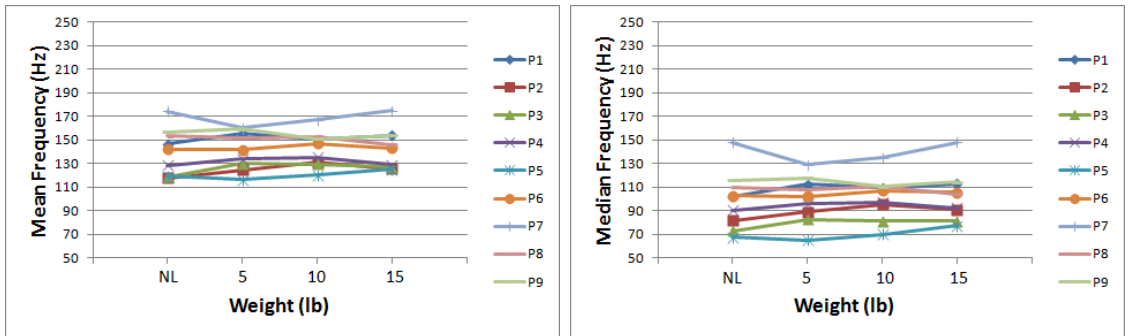


Figure 32 ES Right - Mean and Median Frequencies (Left and Right)

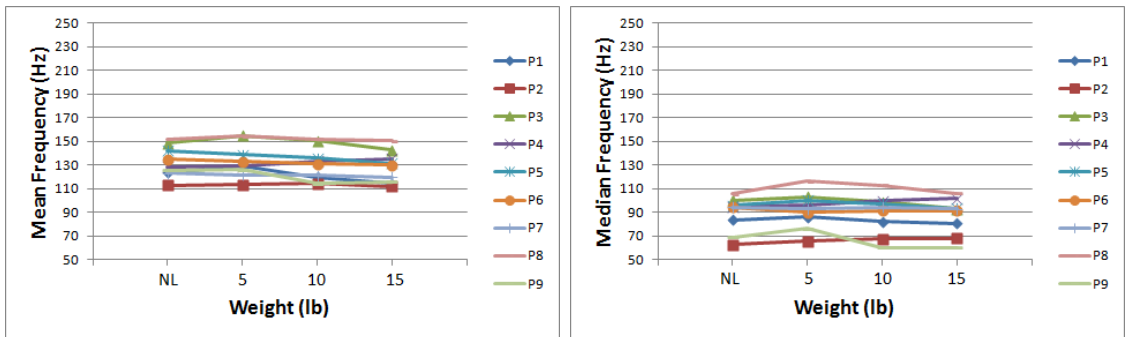


Figure 33 LD Left - Mean and Median Frequencies (Left and Right)

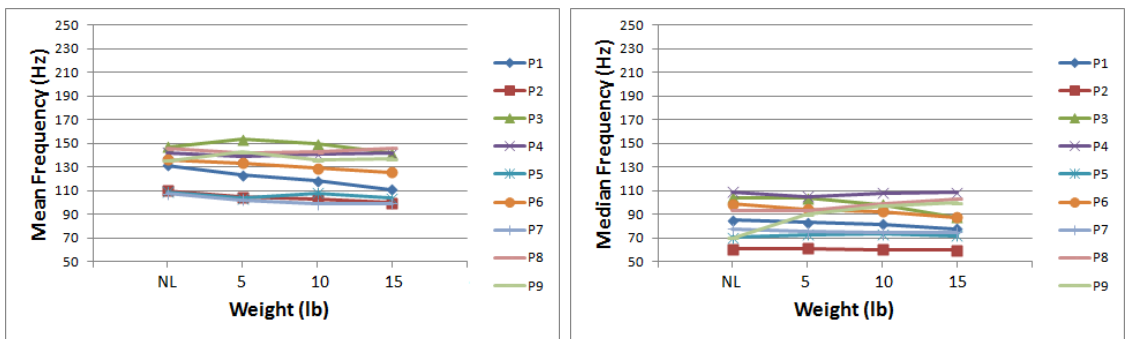


Figure 34 LD Right - Mean and Median Frequencies (Left and Right)

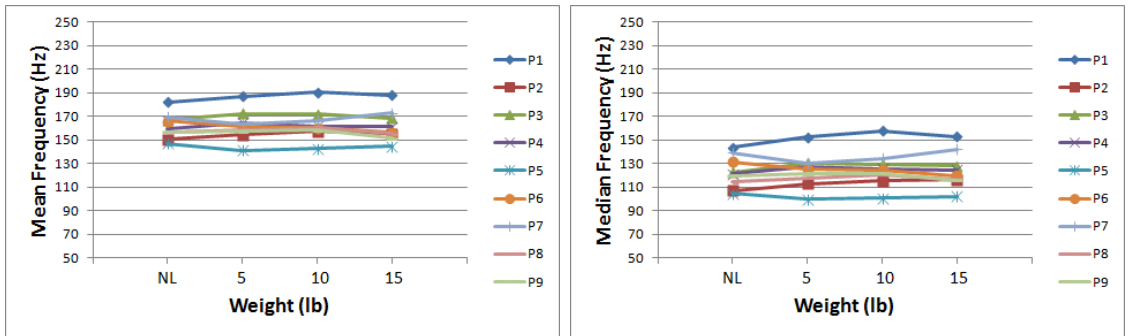


Figure 35 MF Left - Mean and Median Frequencies (Left and Right)

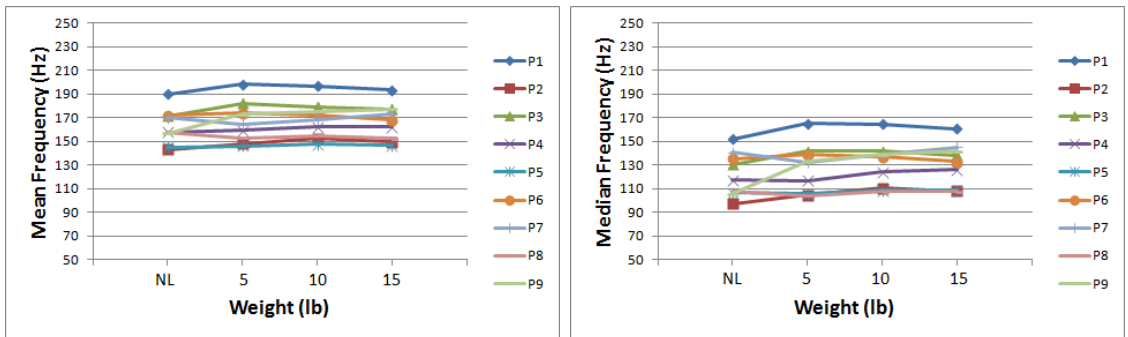


Figure 36 MF Right - Mean and Median Frequencies (Left and Right)

Muscle	Mean value of Mean Frequencies in Hz (S.D.)			
	NL	5 lb	10 lb	15 lb
ES Left	135.58 (4.85)	137.5 (4.4)	138.04 (4.01)	139.99 (5.29)
ES Right	139.85 (6.67)	141.50 (5.37)	142.83 (4.87)	142.21 (5.68)
LD Left	132.42 (4.30)	133.49 (4.64)	130.35 (4.74)	128.02 (4.51)
LD Right	129.44 (5.40)	127.22 (6.49)	125.21 (6.26)	122.9 (6.46)
MF Left	161.79 (3.60)	162.36 (4.20)	163.39 (4.28)	161.63 (4.35)
MF Right	162.75 (4.92)	166.49 (5.68)	167.73 (5.14)	166.71 (5.13)

**Table 10 Mean values of Mean Frequencies with increasing loads during FE**

Muscle	Mean value of Median Frequencies in Hz (S.D.)			
	NL	5 lb	10 lb	15 lb
ES Left	94.36 (5.97)	96.85 (5.47)	98.29 (4.91)	101.19 (6.31)
ES Right	99.06 (8.23)	100.38 (6.52)	101.85 (6.28)	103.02 (7.13)
LD Left	89.05 (4.79)	91.89 (4.98)	58.52 (5.54)	87.67 (5.05)
LD Right	85.57 (5.60)	86.65 (4.90)	87.29 (5.20)	85.75 (5.36)
MF Left	122.79 (4.48)	124.32 (4.80)	125.57 (5.10)	124.45 (5.04)
MF Right	121.54 (6.26)	126.96 (6.91)	130.22 (6.37)	129.95 (6.29)

**Table 11 Mean values of Median Frequencies with increasing loads during FE**

#### 4.6.2 Mean and Median Frequency during Lateral Bending motion –

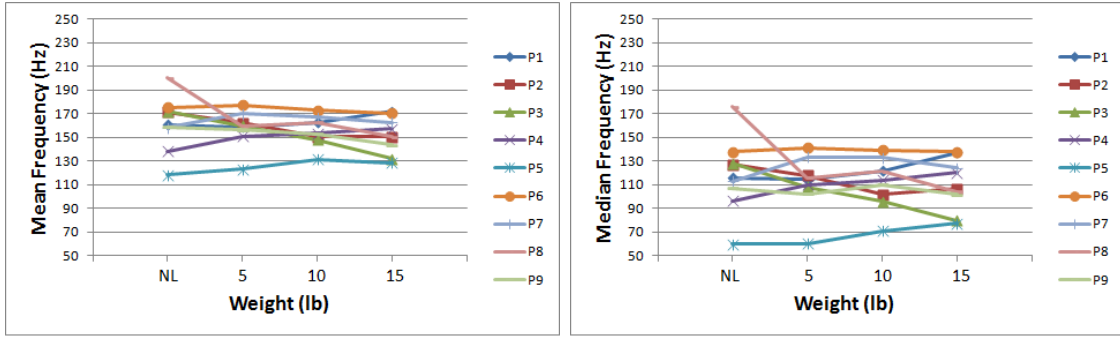


Figure 37 ES Right - Mean and Median Frequencies (Left and Right)

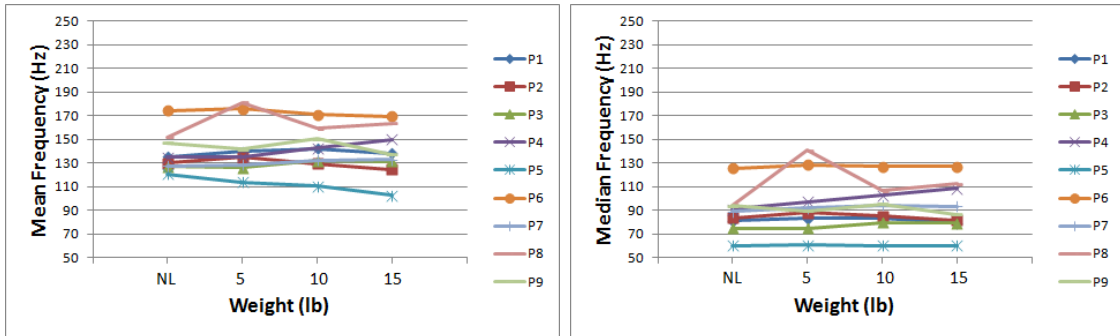


Figure 38 EO Right - Mean and Median Frequencies (Left and Right)

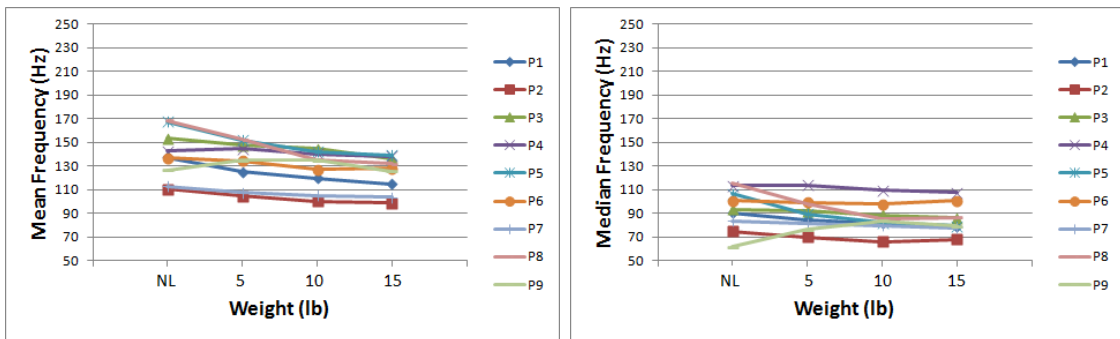
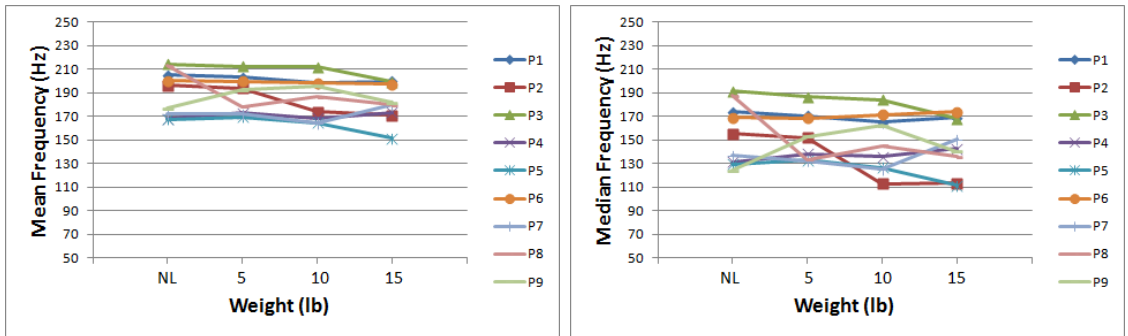


Figure 39 LD Right - Mean and Median Frequencies (Left and Right)





**Figure 40 MF Right - Mean and Median Frequencies (Left and Right)**

Muscle	Mean value of Mean Frequencies in Hz (S.D.)			
	NL	5 lb	10 lb	15 lb
ES Right	161.60 (7.73)	157.62 (5.00)	155.75 (4.09)	152.00 (5.15)
EO Right	138.85 (5.53)	142.00 (7.48)	141.21 (5.95)	139.01 (6.72)
LD Right	139.62 (7.05)	133.80 (6.02)	127.74 (5.37)	124.14 (4.99)
MF Right	190.37 (6.43)	188.28 (5.16)	184.77 (5.81)	181.60 (5.23)

**Table 12 Mean values for Mean Frequencies with increasing loads during LB**

Muscle	Mean value of Median Frequencies in Hz (S.D.)			
	NL	5 lb	10 lb	15 lb
ES Right	117.9 (10.4)	111.56 (7.57)	112.01 (6.87)	109.94 (7.39)
EO Right	88.38 (5.91)	95.07 (8.35)	92.78 (6.29)	92.13 (6.87)
LD Right	93.42 (6.01)	89.38 (4.42)	86.18 (4.03)	85.00 (4.10)
MF Right	155.53 (8.67)	152.10 (6.53)	147.71 (8.09)	145.10 (7.64)

**Table 13 Mean values for Median Frequencies with increasing loads during LB**

### 4.6.3 Mean and Median Frequency during Rotation motion –

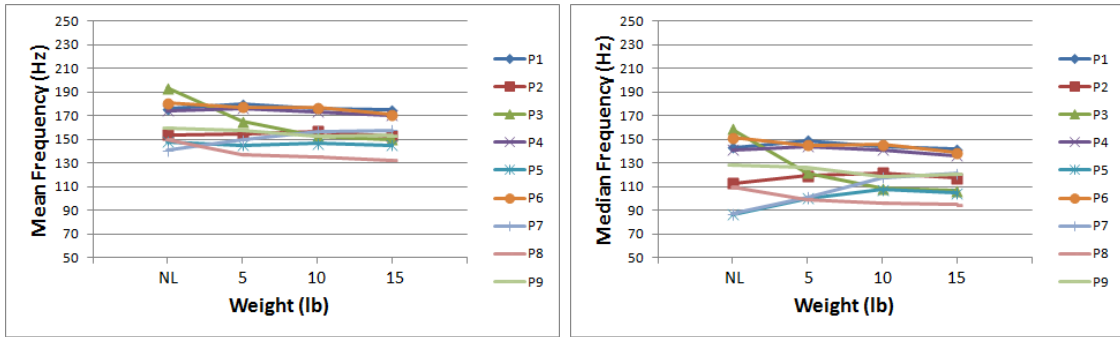


Figure 41 ES Left - Mean and Median Frequencies (Left and Right)

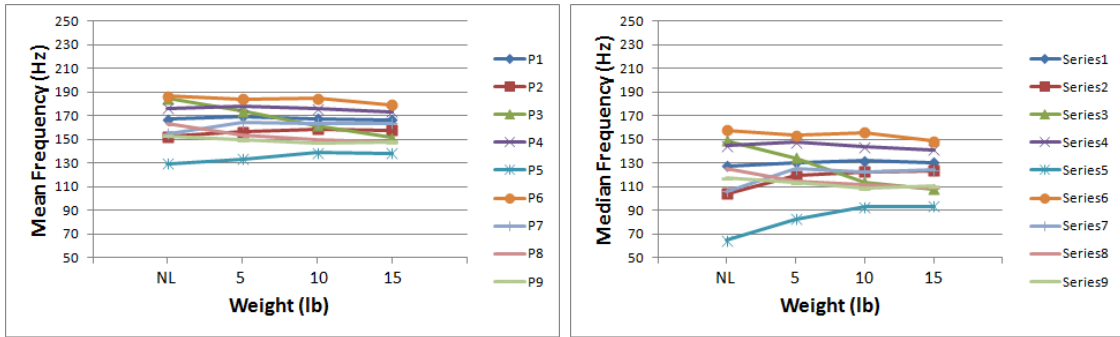


Figure 42 ES Right - Mean and Median Frequencies (Left and Right)

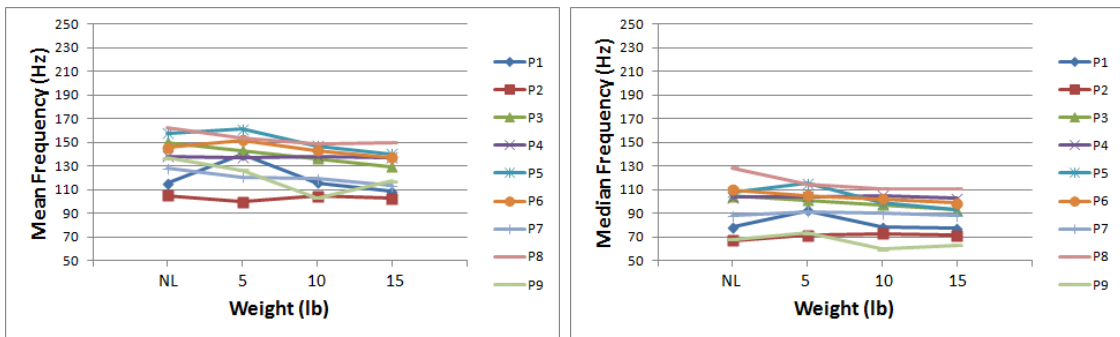


Figure 43 LD Left - Mean and Median Frequencies (Left and Right)

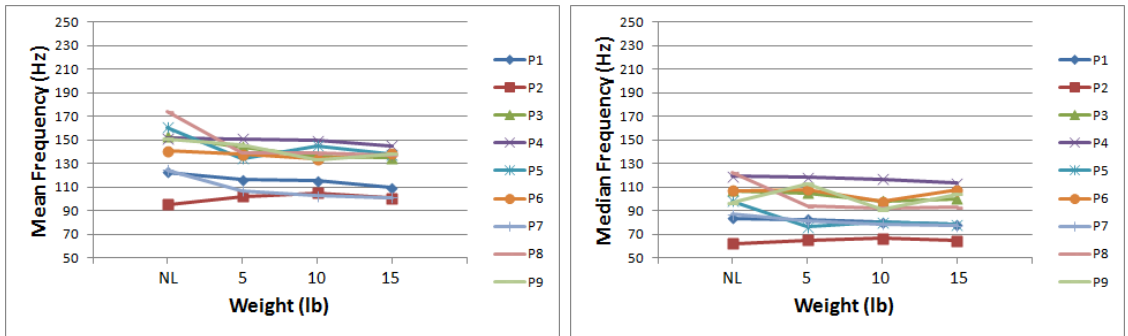


Figure 44 LD Right - Mean and Median Frequencies (Left and Right)

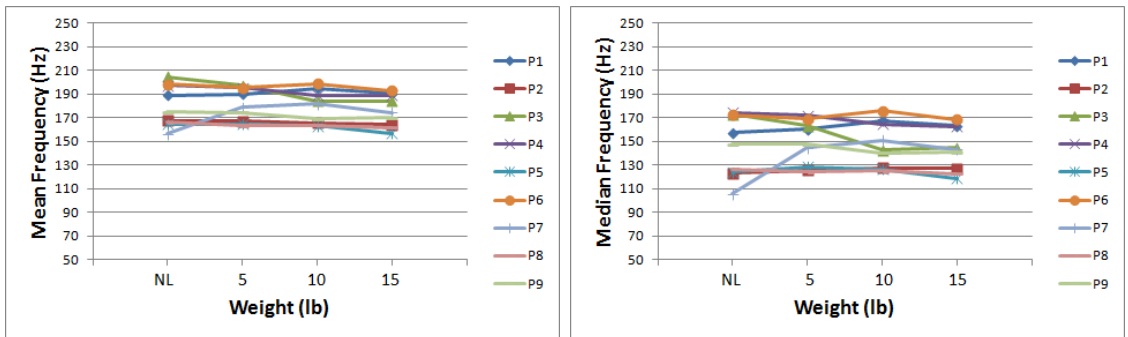


Figure 45 MF Left - Mean and Median Frequencies (Left and Right)

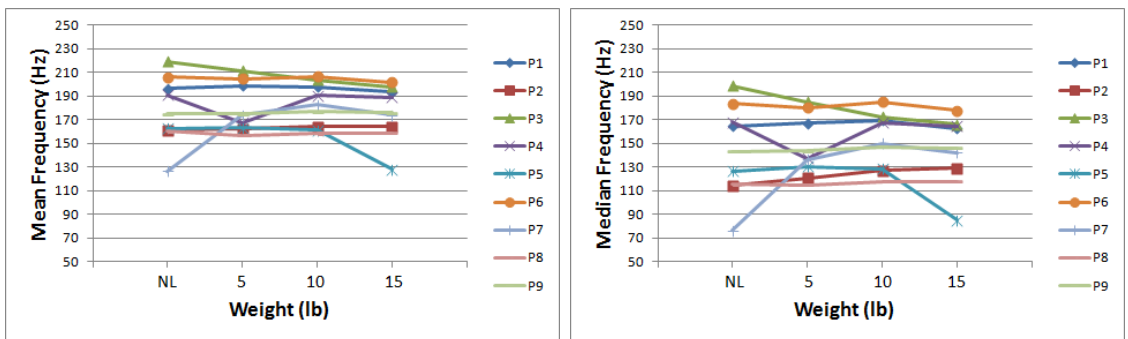


Figure 46 MF Right - Mean and Median Frequencies (Left and Right)

Muscle	Mean value of Mean Frequencies in Hz (S.D.)			
	NL	5 lb	10 lb	15 lb
ES Left	164.10 (5.89)	160.31 (5.12)	158.69 (4.71)	156.52 (4.59)
ES Right	163.16 (6.05)	162.58 (5.29)	160.89 (4.78)	158.64 (4.43)
LD Left	137.78 (6.30)	137.31 (6.34)	128.55 (6.00)	126.33 (5.44)
LD Right	141.58 (7.93)	130.95 (5.92)	128.95 (5.70)	127.04 (5.90)
MF Left	179.88 (5.87)	180.76 (4.71)	178.91 (4.62)	176.00 (4.53)
MF Right	177.65 (9.50)	179.28 (6.75)	182.40 (6.18)	175.94 (7.77)

**Table 14 Mean values of Mean Frequencies with increasing loads during ROT**

Muscle	Mean value of Median Frequencies in Hz (S.D.)			
	NL	5 lb	10 lb	15 lb
ES Left	124.44 (8.91)	122.91 (6.66)	122.41 (5.90)	120.21 (5.44)
ES Right	121.80 (9.43)	124.67 (6.95)	122.73 (6.35)	121.08 (5.83)
LD Left	95.23 (6.98)	96.62 (5.28)	90.66 (5.61)	88.75 (5.15)
LD Right	98.19 (6.25)	93.77 (6.15)	89.16 (4.86)	90.77 (5.56)
MF Left	144.96 (8.63)	148.41 (6.30)	146.91 (6.38)	143.60 (6.11)
MF Right	143.46 (12.95)	146.24 (8.46)	151.77 (7.84)	143.65 (9.70)

**Table 15 Mean values of Median Frequencies with increasing loads during ROT**

## CHAPTER 5

### DISCUSSION

The aim of this exercise was to develop test protocols for analysis of low back exertions in standing position. Traditional (ROM) and non-linear (ApEn and CoD) techniques were employed for analysis of low back motion while analysis of EMG data was done using mean and median frequency calculations.

The ROM, while giving accurate measures of motor variability within the system, is not explanatory of the underlying neural processes of human movement. The nonlinear measures helped us to understand the motor variability within a system, and not just to provide a measure of the amount of variability that is present. Furthermore, as stated previously, traditional linear tools can mask the true structure of motor variability, since a few strides are averaged to generate a “mean” picture of the subject’s gait. In this averaging procedure, the temporal variations of the gait pattern may be lost. On the contrary, nonlinear techniques focus on understanding how variations in the gait pattern change over time (Dingwell and Cusumano, 2000; Hausdorff et al., 1997). This is the reason for using both traditional and non-linear tools to analyze low back motion in our

case. The ROM does not describe the effect of increasing resistance on motion. It does not take into account the chaos in the dynamic motion of low back. Non-linear methods will help us better understand the dynamics of low back motion.

Motion and EMG data was recorded from nine healthy participants using the protocols approved by the IRB's of Auburn University, AL and Palmer College of Chiropractic, IA. One of the participants could not be used for data acquisition as the sensors could not be attached to the participant's lower back because of perspiration. Following data exporting and data reduction, motion data was analyzed using ROM, ApEn and CoD techniques. The values of ApEn and CoD results were similar to results obtained in some of the other studies conducted on healthy participants to study variability. Newell et. al. in their study of dimensional constraints on limb movement found out that the approximate entropy values increased from an average of 0.2 to 0.3 as participants went from gait with vision to gait without vision aid. Buzzi et. al. studied effect of aging on variability during gait and found out that CoD values for young people were 2.3 as compared to 2.7 for old people for variation in knee angle. Both traditional and non-linear methods were thus applied successfully to the human physiological data obtained.

Statistical analysis revealed that variability did not change significantly as the resistance to FE, LB and ROT increased from zero to 15 lb. It must be noted that the aim of this exercise was to develop test protocol to analyze low back exertion. The sample size used for this study was relatively small and statistical analysis results may not be enough to generalize the results for entire healthy population. The protocol needs to be fine tuned before it can be applied to a large scale study. Statistical analysis on results of

a much larger population will then give a correct estimate of effect of increasing loads on variability in motion of low back spine.

Though the overall results suggested that variability remained constant as the resistance to motion increased, there were some exceptions. One of them is discussed below.

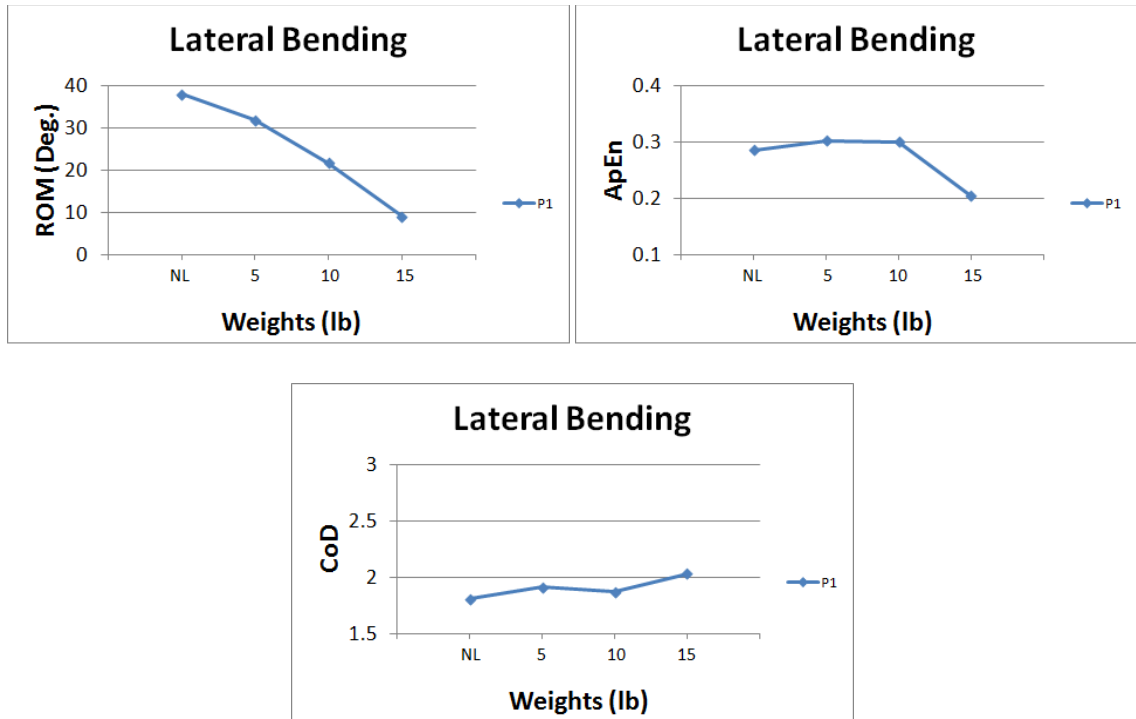
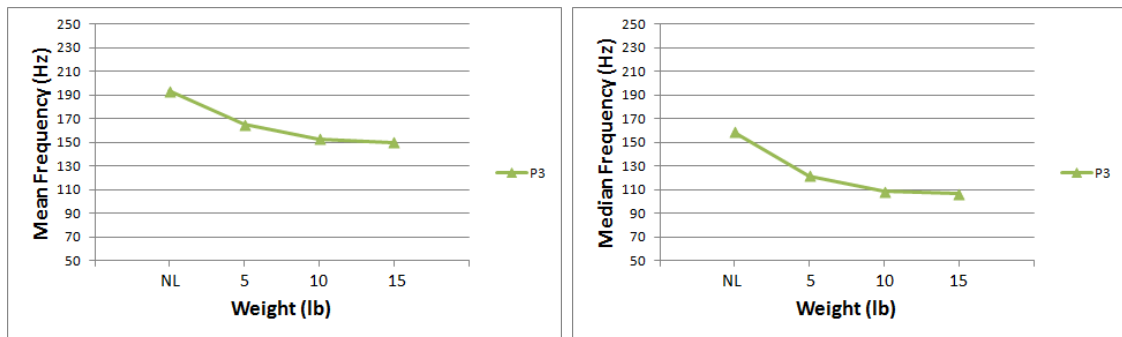


Figure 47 ROM, ApEn and CoD results for participant 1 during LB

In the graphs above, you can see the results for ROM, ApEn and CoD for participant 1 (Age – 59 yrs, Height – 164 cm, Weight – 66.2 kg). It can be noticed that as the resistance to lateral bending increases, the ROM falls sharply. This means that the participant found it difficult to cope with the increase in resistance. However, the values for ApEn and CoD do not change with increase in load. This means that even though the ROM decreased, the regularity of the repetition cycles did not change significantly. The age of the participant was significantly higher than the average age (43.2 yrs) of all the

participants. This may have been one of the reasons for decrease in ROM with increasing resistance. Thus you can see that to totally analyze motion, both traditional and non-linear tools are necessary.

Mean and median frequencies of recorded EMG signals were calculated to see the effect of increasing loads on muscle fatigue. As explained earlier, it was noticed that muscle fatigue typically results in decrease in the mean and median frequencies. Statistical analysis revealed that mean and median frequencies did not change significantly with increase in load. This means muscle fatigue was not induced in the participants due to increasing loads. This may be one of the reasons; variability in motion was not affected by increasing loads, as the muscles were able to provide the required neuro-muscular response to the increasing loads. However, as mentioned before, this is only the protocol development stage of the study and more testing will be needed before this conclusion can be generalized for the entire healthy population. As with the motion analysis results, there were some outliers in the EMG results also. A couple of them are discussed below.



**Figure 48 Mean and Median Frequency results for ES Left muscle for participant 3 during ROT**



It can be seen that the mean and median frequencies for participant 3 (Age – 24 yrs, Height – 181 cm, Weight – 80 kg) decrease as the resistance to motion increases. This means that fatigue is getting induced in the muscles of participant 3 as the load increases. This is not consistent with other results and hence may be considered an outlier. The reason might be less endurance when it comes to dealing with increasing resistance. This is a surprising result, as younger participants are expected to have higher muscle endurance.

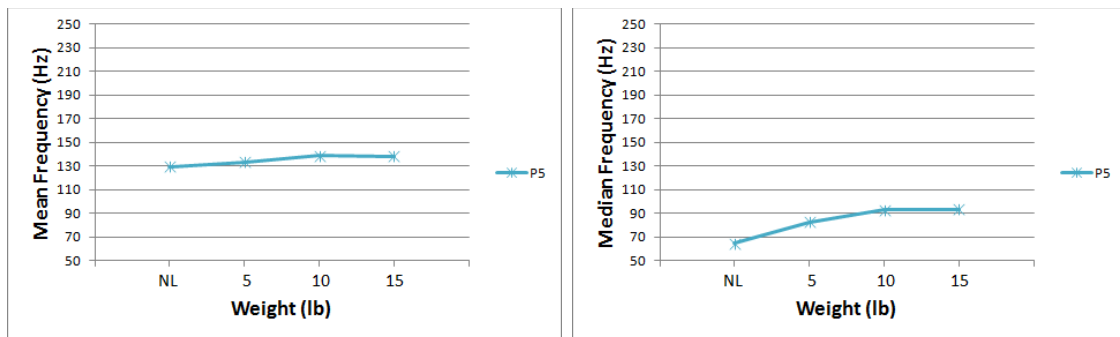


**Figure 49 Mean and Median Frequency results for ES Right muscle for participant 3 during ROT**

Fig. 49 shows us the mean and median frequency results for ES Right muscle of participant 5 (Age – 51 yrs, Height – 160 cm, Weight – 63 kg) during ROT. The overall results show that mean and median frequencies either remained constant or decreased slightly as the resistance to motion increased. However, in this case, the mean and median frequencies increased as the resistance to motion increases. This may happen if the participant uses the leg muscles to compensate for the increase in effort required to overcome the increase in resistance. The age of this participant is higher than the average age (43.2) of all the participants. Thus he might have needed his leg muscles to deal with the increasing resistance to motion. In this case the participant does not use only his back

muscle which may lead to them relaxing, resulting in increase in mean and median frequencies.

As mentioned before test methods need to be improved before using them in a larger study. Some of the recommendations to improve the protocol are listed below –

1. It was observed that the rotation data did not truly reflect the motion of participants because the skin was stretched during rotation. This can be minimized by applying a stiff plastic plate to the skin before the motion sensors are applied.

2. The participants were also asked to perform the exertions at their comfortable speeds. This may have allowed them to compensate for the increase in resistance to motion. It would be interesting to see the results if the participants are asked to perform these exertions under two different fixed speeds or under higher resistance. It has been previously reported that variability is less for slower trunk movements as compared to rapid ones. In this study healthy participants were asked to perform repetitive trunk flexion and extension movements at 20 and 40 cycles per second. Maximum Lyapunov exponents describing the expansion of the kinematic state-space were calculated from the measured trunk kinematics to estimate stability of the dynamic system. The values of the Maximum Lyapunov exponent were more for rapid movements than for slow movements (Granata et. al., 2006).

3. Another limitation of the study might be the fact that participants were able to use their leg muscle to compensate for the increase in load resistance. It was necessary to leave the legs unconstrained to simulate real world conditions. Before the data recording started, the participants were instructed to move only their upper body, from the waist up and perform the three types of exertions. However, it was observed that some of the

participants still used their leg muscle to compensate for increasing loads. To remedy this participants can be given a practice session to get better acquainted to the exercises.

Once the protocol had been developed, the next step would be to apply the protocol to larger sample sizes of healthy participants as well as patients with LBP. It has been shown previously that LBP affects trunk co-ordination and muscle activity during walking (Lamoth et. al., 2005). It will be interesting to see the effect of LBP on FE, LB and ROT exertions under increasing loads. If LBP affects variability significantly, then these exercises will be characterized by different values of ROM, ApEn and CoD.

When a patient under goes rehabilitation for LBP, then convergence of these values towards values for these parameters for healthy subjects may suggest that the treatment is working. Hence, this sort of variability analysis can be used as a diagnostic tool during rehabilitation. However, before this can be done, a solid database needs to be created by testing more healthy subjects, as nine subjects is not enough to generalize movement characteristics of entire healthy population. This should be followed by testing of patients with LBP to establish the difference in movement characteristics.

## CHAPTER 6

### CONCLUSION

Collectively, the results of kinematic analysis during FE, LB and ROT revealed that variability in motion does not change under gradual increase in resistance to motion. The findings of the traditional method (ROM) used were supported by non-linear analysis (ApEn and CoD) of motion. Thus, both traditional and non-linear methods were applied successfully to analyze motion. Also, the increasing resistance to motion did not induce enough fatigue in muscles of participants which might have helped the participants to provide required neuromuscular response to increasing loads. The measurements during rotation should be improved by attaching the sensors to prevent sliding over the skin. Future studies should be undertaken to increase the challenges by either increasing the load, or by asking the subjects to increase the speed. Studies recruiting larger number of subjects should be undertaken. These will ultimately lead to studies involving low back pain subjects and possible tools for diagnosing low back pain using motion measurements.

## REFERENCES

From the Centers for Disease Control and Prevention. Prevalence of disabilities and associated health conditions among adults—United States, 1999. *JAMA*. 2001; 285(12):1571-1572.

Stewart WF, Ricci JA, Chee E, Morganstein D, Lipton R. Lost productive time and cost due to common pain conditions in the US workforce. *JAMA*. 2003; 290(18):2443-2454.

Devereaux M. Low back pain. *Med Clin North Am*. 2009;93(2):477-501, x.

Katz JN. Lumbar disc disorders and low-back pain: socioeconomic factors and consequences. *J Bone Joint Surg Am*. 2006;88(suppl 2):21-24.

Rubin DI. Epidemiology and risk factors for spine pain. *Neurol Clin*. 2007;25(2): 353-371.

Carey TS, Garrett J, Jackman A, McLaughlin C, Fryer J, Smucker DR. The out-comes and costs of care for acute low back pain among patients seen by primary care practitioners, chiropractors, and orthopedic surgeons: the North Carolina Back Pain Project. *N Engl J Med*. 1995;333(14):913-917.

van Tulder M, Koes B, Bombardier C. Low back pain. *Best Pract Res Clin Rheumatol*. 2002;16(5):761-775.

Weiner DK, Kim YS, Bonino P, Wang T. Low back pain in older adults: are we utilizing healthcare resources wisely? *Pain Med*. 2006;7(2):143-150.

Deyo RA, Gray DT, Kreuter W, Mirza S, Martin BI. United States trends in lumbar fusion surgery for degenerative conditions. *Spine*. 2005;30(12):1441-1445.

Luo X, Pietrobon R, Hey L. Patterns and trends in opioid use among individuals with back pain in the United States. *Spine*. 2004;29(8):884-890.

Feuerstein M, Marcus SC, Huang GD. National trends in nonoperative care for nonspecific back pain. *Spine J*. 2004;4(1):56-63.

IJzelenberg W, Burdorf A. Patterns of care for low back pain in a working population. *Spine*. 2004;29(12):1362-1368.

Carey TS, Evans A, Hadler N, Kalsbeek W, McLaughlin C, Fryer J. Care-seeking among individuals with chronic low back pain. *Spine*. 1995;20(3):312-317.

Thorpe KE, Florence CS, Joski P. Which medical conditions account for the rise in health care spending? *Health Aff (Millwood)*. 2004;(suppl web exclusives): W4-437–W4-445.

Bergman, S. 2007. —Management of musculoskeletal pain. || *Best Practice & Research Clinical Rheumatology*, 21 (1): 153-166.

Papadakis, N.C., Christakis, D.G., Tzagarakis, G.N., Chlouverakis, G.I., Kampanis, N.A., Stergiopoulos, K.N., & Katonis, P.G. 2009. —Gait variability measurements in lumbar spinal stenosis patients: part A. Comparison with healthy subjects. || *Physiological Measurement*, 30: 1171–1186.

Panjabi M. M. ‘The stabilizing system of spine. Part I: Function, dysfunction, adaptation and enhancement’

Leon Glass and Michael C. Mackey ‘*From Clocks to Chaos: The Rhythms of Life*’

Gleick, J. 1987. *Chaos: Making a new Science*. New York: Viking Penguin.

Amato, I. 1992. Chaos breaks out at NIH, but order may come of it. *Science* 257:747

Fitzgerald, G.K., Wynveen, K.J., Rheault, W. & Rothchild, B. 1983. — Objective assessment with establishment of normal values for lumbar spinal range of motion. *Physical Therapy*, 63:1776-1781.

Chien-Jen Hsu, M.D., Yi-Wen Chang, PH.D., Wen-Ying Chou, M.D., M.S., Chou-Ping Chiou, PH.D., Wei-Ning Chang, M.D., M.S., and Chi-Yin Wong, M.D. 2008 ‘Measurement of spinal range of motion in healthy individuals using an electromagnetic tracking device’ *J Neurosurg Spine* 8:135–142

Shrawan Kumar 2010 ‘EMG in rotation–flexion of the torso’ *Journal of Electromyography and Kinesiology* 20; 1146–1154

Imtiaz Desai, Paul W.M. Marshall ‘Acute effect of labile surfaces during core stability exercises in people with and without low back pain’ *Journal of Electromyography and Kinesiology* 20 (2010) 1155–1162

Harbourne, R.T. & Stergiou, N. 2009. —Movement variability and use of nonlinear tools: Principles to Guide Physical Therapist Practice. *Physical Therapy*, 89(3): 267–282.

Stergiou, N. 2004. —Innovative Analysis of Human Movement. *Human Kinetics*.  
Kevin P. Granata, PhD and Scott A. England, MS ‘Stability of Dynamic Trunk Movement’ *Spine (Phila Pa 1976)*. 2006 May 1; 31(10): E271–E276

Ryan B.Graham, Erin M.Sadler, Joan M.Stevenson ‘Does the personal lift-assist device affect the local dynamic stability of the spine during lifting?’ *Journal of Biomechanics* 44 (2011) 461–466

Justin J. Kavanagh ‘Lower trunk motion and speed-dependence during walking’ *Journal of NeuroEngineering and Rehabilitation* 2009, 6:9

Ugo H. Buzzi, Nicholas Stergiou, Max J. Kurz, Patricia A. Hageman, Jack Heidel ‘Nonlinear dynamics indicates aging affects variability during gait’ *Clinical Biomechanics* 18 (2003) 435–443

HyunWook Lee, Kevin P. Granata, Michael L. Madigan ‘Effects of trunk exertion force and direction on postural control of the trunk during unstable sitting’ *Clinical Biomechanics* 23 (2008) 505–509

Claudine J. C. Lamoth, Onno G. Meijer, Andreas Daffertshofer, Paul I. J. M. Wuisman, Peter J. Beek ‘Effects of chronic low back pain on trunk coordination and back muscle activity during walking: changes in motor control’ *Eur Spine J* (2006) 15: 23–40

Available Online, <http://pilates.about.com/od/technique/ss/human-spine-anatomy.htm>

Available Online, [http://en.wikipedia.org/wiki/File:Gray\\_111\\_-\\_Vertebral\\_column-coloured.png](http://en.wikipedia.org/wiki/File:Gray_111_-_Vertebral_column-coloured.png)

Available Online, [http://en.wikipedia.org/wiki/Thoracic\\_vertebrae#cite\\_note-3](http://en.wikipedia.org/wiki/Thoracic_vertebrae#cite_note-3)

Available Online, [http://en.wikipedia.org/wiki/File:Thoracic\\_vertebrae.jpg](http://en.wikipedia.org/wiki/File:Thoracic_vertebrae.jpg)

Available Online, [http://en.wikipedia.org/wiki/File:Lumbar\\_vertebrae.jpg](http://en.wikipedia.org/wiki/File:Lumbar_vertebrae.jpg)

Available Online, [http://en.wikipedia.org/wiki/File:Lumbar\\_vertebrae.jpg](http://en.wikipedia.org/wiki/File:Lumbar_vertebrae.jpg)

Available Online, <http://www.britannica.com/EBchecked/topic/191213/erector-spinae>

Available Online, [http://en.wikipedia.org/wiki/Multifidus\\_muscle](http://en.wikipedia.org/wiki/Multifidus_muscle)

Available Online, [http://en.wikipedia.org/wiki/Latissimus\\_dorsi\\_muscle](http://en.wikipedia.org/wiki/Latissimus_dorsi_muscle)

Available Online, <http://training.seer.cancer.gov/anatomy/muscular/groups/trunk.html>

Gwanseob Shin, Clive D'Souza 'EMG activity of low back extensor muscles during cyclic flexion/extension' *Journal of Electromyography and Kinesiology* Volume 20, Issue 4, August 2010, Pages 742–749

P.A. Mathieu, M. Fortin 'EMG and kinematics of normal subjects performing trunk flexion/extensions freely in space' *Journal of Electromyography and Kinesiology* Volume 10, Issue 3, June 2000, Pages 197–209

Ruth Dickstein, Sara Shefi, Emanuel Marcovitz, Yael Villa 'Electromyographic activity of voluntarily activated trunk flexor and extensor muscles in post-stroke hemiparetic subjects' *Clinical Neurophysiology* 115 (2004) 790–796

W.S. Marras, K.P. Granata 'Spine loading during trunk lateral bending motion' *Journal of Biomechanics* Volume 30, Issue 7, July 1997, Pages 697–703

Joseph K.-F Ng, Carolyn A Richardson, Mohamad Parnianpour, Vaughan Kippers 'EMG activity of trunk muscles and torque output during isometric axial rotation exertion: a comparison between back pain patients and matched controls' *Journal of Orthopaedic Research* Volume 20, Issue 1, January 2002, Pages 112–121

Lenth, R.V. 2001. —Some practical guidelines for effective sample-size determination. *The American Statistician*, 55:187-193.

Patrick J. Lee, Kevin P. Granata and Kevin M. Moorhouse 'Active Trunk Stiffness During Voluntary Isometric Flexion and Extension Exertions' *Human Factors: The Journal of the Human Factors and Ergonomics Society* 2007 49: 100

Yu Okubo, Koji Kaneoka, Atsushi Imai, Itsuo Shiina, Masaki Tatsumura, Shigeki Izumi, Shumpei Miyakawa 'Electromyographic Analysis of Transversus Abdominis and Lumbar



Multifidus Using Wire Electrodes During Lumbar Stabilization Exercises' journal of orthopaedic & sports physical therapy Volume 40 Number 11 November 2010 743-750

M.B.I. Raez, M.S. Hussain, F. Mohd-Yasin 'Techniques of EMG signal analysis: detection, processing, classification and applications' Biol Proced Online. 2006; 8: 11–35

Sridhar Poosapadi Arjunan, Dinesh Kant Kumar, Wai Ming Poon, Heiko Rudolph, Yong Hu 'Variability in Surface Electromyogram During Gait Analysis of Low Back Pain Patients' *Journal of Medical and Biological Engineering* 2009, 30(3): 133-138

Rafael F Escamilla, Eric Babb, Ryan DeWitt, Patrick Jew, Peter Kelleher, Toni Burnham, Juliann Busch, Kristen D'Anna, Ryan Mowbray, Rodney T Imamura 'Electromyographic Analysis of Traditional and Nontraditional Abdominal Exercises: Implications for Rehabilitation and Training' *Physical Therapy* . Volume 86 . Number 5 . May 2006

Chatfield Chris 'The Analysis of Time Series: An Introduction'

McGregor A. H., Hughes SPF: The potential use of spinal motion as a measure of surgical outcome. *J Back Musculoskelet Rehabil* 17:77–82, 2004

Nissan M, Bar-Ilan K, Lugor EJ, Steinberg EL, Brown S, Dekel S: The normal, healthy low back: some functional parameters. *J Back Musculoskelet Rehabil* 12:1–5, 1999

Chou WY, Hsu CJ, Chang WN, Wong CY: Adjacent segment degeneration after lumbar spinal posterolateral fusion with instrumentation in elderly patients. *Arch Orthop Trauma Surg* 122:39–43, 2002

Lu WW, Luk KD, Ruan DK, Fei ZQ, Leong JC: Stability of the whole lumbar spine after multilevel fenestration and discectomy. *Spine* 24:1277–1282, 1999

L. F. P. FRANCA and M. A. SAVI 'Distinguishing Periodic and Chaotic Time Series Obtained from an Experimental Nonlinear Pendulum' *Nonlinear Dynamics* 26: 253–271, 2001

Mullin, T., *The Nature of Chaos*, Oxford Press, Oxford, 1993.

Moon, F. C., *Chaotic and Fractal Dynamics*, Wiley, New York, 1992.

Pincus, S. 1994 —Approximate entropy (ApEn) as a complexity measure. *Chaos*, 5(1):110-117.

Pincus, S. & Golberger, A.L. 1994. —Physiological time-series analysis: What does regularity quantify? *American Journal of Physiology*, 266(4):H1643-1656.

Pincus, S.M., Gladstone, I.M., Ehrenkranz, R.A. 1991. —A regularity statistic for medical data analysis. *Journal of Clinical Monitoring and Computing*, 7:335–345.

Abarbanel, H.D.I., 1996. *Analysis of Observed Chaotic Data*. Springer-Verlag, New York.

Baker, G.L., Gollub, J.P., 1996. *Chaotic Dynamics*. Cambridge University Press, New York.

Stergiou, N., Buzzi, U.H., Kurz, M.J., Heidel, J., 2004. Nonlinear tools in human movement. In: Stergiou, N. (Ed.), *Innovative Analyses of Human Movement*. Human Kinetics Publ., Champaign, IL, pp. 63–90.

Kennel MB, Brown R, Abarbanel HD. Determining embedding dimension for phase-space reconstruction using a geometrical construction. *Phys Rev A* 1992; 45: 3403-3411.

BIOPAC Systems Application notes; [http://www.biopac.com/Manuals/app\\_pdf/app118.pdf](http://www.biopac.com/Manuals/app_pdf/app118.pdf)

P. Grassberger and I. Procaccia, *Phys. Rev. Lett.* 50, 346 (1983)

M. Bilodeau, S. Schindler-Ivens, D.M. Williams, R. Chandran, S.S. Sharma ‘EMG frequency content changes with increasing force and during fatigue in the quadriceps femoris muscle of men and women’ *Journal of Electromyography and Kinesiology* 13 (2003) 83–92

Anne F. Mannion, Beth Connolly, Kherrin Wood, Patricia Dolan ‘The use of surface EMG power spectral analysis in the evaluation of back muscle function’ *Journal of Rehabilitation Research and Development* Vol . 34 No . 4, October 1997 Pages 427-439

Dingwell, J.B., Cusumano, J.P., 2000. Nonlinear time series analysis of normal and pathological human walking. *Chaos* 10, 848–863.

Hausdorff, J.M., Edelberg, H.K., Mitchell, S.L., et al., 1997. Increased gait unsteadiness in community dwelling elderly fallers. *Arch. Phys. Med. Rehab.* 78, 278–283.

Garnett P. Williams ‘Chaos Theory Tamed’ 1997.

## APPENDIX

### A. Auburn University IRB Approval Document –

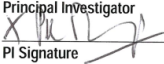

**AUBURN UNIVERSITY INSTITUTIONAL REVIEW BOARD for RESEARCH INVOLVING HUMAN SUBJECTS**  
**REQUEST for PROTOCOL MODIFICATION**  
 For information or help contact THE OFFICE OF HUMAN SUBJECTS RESEARCH, 307 Samford Hall, Auburn University  
 Phone: 334-844-5966 e-mail: hsubjec@auburn.edu Web Address: http://www.auburn.edu/research/vpr/ohs/index.htm

Complete this form using Adobe Acrobat **Writer** (versions 5.0 and greater). Hand written copies are not accepted.

1. Protocol Number: 09-344 MR 1001      2. IRB Approval Dates: From: 01/20/2011 To: 01/19/2012

3. Project Title: Development of Protocols for Biomechanical Tests and Measurement of Spinal Manipulative Procedures for Training of Research Personnel

4. P.K. Raju      Professor      Mech. Eng.      (334) 844-3301      rajupol@auburn.edu

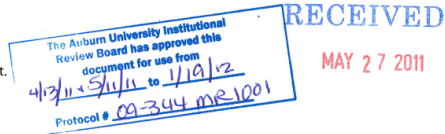
<b>Principal Investigator</b>	<b>Title</b>	<b>Department</b>	<b>Phone</b>	<b>AU E-Mail</b>
	270 Ross Hall, Auburn University, AL 36849			
<b>PI Signature</b>	<b>Mailing Address</b>			<b>Alternate E-Mail</b>
<b>Faculty Advisor</b>	<b>FA Signature</b>	<b>Department</b>	<b>Phone</b>	<b>AU E-Mail</b>
				
<b>Name of Current Department Head:</b> Jeffrey Suhling				<b>AU E-Mail:</b> suhling@auburn.edu

5. Current External Funding Agency: \_\_\_\_\_

6. List any contractors, sub-contractors, other entities or IRBs associated with this project: Palmer College of Chiropractic

7. Briefly list (numbered or bulleted) the activities that occurred up to this point, particularly those that involved participants.

No new activities since the last progress report.



8. Describe the requested changes to your research protocol, with an explanation and/or rationale for each. (Additional pages may be attached if needed to provide a complete response.)

We are adding another biomechanical test namely "Human Lumbar Spine Motion and Strength Test in Standing Position". During this test additional biomechanical measurements will be undertaken during movements from upright standing position. The participants will be recruited by the word of mouth. The participant will be screened for eligibility by a clinician using physical exam form developed earlier and by confirming that the participant meets the requirements of the inclusion criteria. The procedure for the biomechanical tests will be administered by a research assistant. Surface electrodes to measure muscle activity and position tracking sensors to record motion will be attached to the mid and lower back of the participant using double sided tape after the skin is prepared using alcohol prep pad and a skin abrasive. The spots where the electrodes are to be attached may be shaved using disposable razors if excessive hair is present at those spots which may affect the quality of the recorded data. Shaving will be done entirely with the participant's agreement and he may refuse to get shaved. The participant will be asked to wear a safety harness and a hand glove. The participant will then be asked to stand upright with comfortable feet position. This position of the feet will remain constant throughout the tests. The participant will have to pull a rope passing over a pulley to which a weight is attached. The participant will have to perform 3 types of motions against increasing load resistance –

- a) Lateral bending to the left/right by holding the rope with the left hand/right hand.
- b) Forward and backward bending by holding the rope close to the chest with both the hands.
- c) Twisting to the left /right by holding the rope with the left hand/right hand.

The participant will perform each of the above motion using loads of 10, 15 and 20 pounds. Data will be collected for 1 minute for each motion followed by a break of 30 seconds. The total duration of the biomechanical test will be approximately 45 minutes. Inclusion Criteria are included on the next page.

**Inclusion criteria** –

1. Participant must be an adult (over 18 years old) and capable of reading and understanding English language.
2. Participant should not have any musculoskeletal injury related to spine, hands or legs in the past 12 months.
3. Participant should not have a pacemaker or any non-removable metal object on them.
4. Participant should not experience any pain in the range of motion while performing the motions mentioned in the testing protocol.
5. The participants should not have any previously known neurological or dermatitis related symptoms.

The participant will be additionally screened for neurological or dermatitis related symptoms by certified clinicians before he performs the biomechanical tests. The screening will be based on questionnaire, physical tests and visual observation. If the participant exhibits these symptoms he will be excluded.

9. Are there any changes in the "key research personnel" that have access to participants or data?  NO  YES  
(If "YES", identify each individual and explain the reason(s) for each change.) Attach CITI proof of completion for all new key personnel.

Yuvraj Pawar, the previous graduate student associated with the study, is graduating. He is being replaced by Varun Soman, another graduate student.

**10. Identify any changes in the anticipated risks and / or benefits to the participants.**

The risks associated with this specific biomechanical test are mentioned here. Skin reaction to tape may be a rash or itching and is usually resolved within 48 hours. Some participants may have sore muscles after the testing procedures, which usually goes away within 48 hours. It is important to note that these side effects are extremely rare.

There is a possibility of participant falling down due to imbalance while performing the task. However, this possibility is minimized as the participant will be wearing a safety harness. Also to prevent rope burn to the participants hand in case he lets go the rope, he will be asked to wear a light weight hand glove.

It must be noted that these are the risks associated only with this specific biomechanical test. The other risks mentioned in the participant consent document are associated with some other biomechanical tests which are a part of ongoing research at Palmer College of Chiropractic and not related to the collaborative research between Palmer College of Chiropractic and Auburn University.

If the participants feel any kind of discomfort at any stage of testing, they may discontinue the test.

**11. Identify any changes in the safeguards or precautions that will be used to address anticipated risks.**

There is a possibility of participant falling down due to imbalance while performing the task. However, this possibility is minimized as the participant will be wearing a safety harness. Also to prevent rope burn to the participants hand in case he lets go the rope, he will be asked to wear a light weight hand glove.

If the participants feel any kind of discomfort at any stage of testing, they may discontinue the test.

12. Attach any additional supporting documentation to assist the IRB in evaluating your request for protocol modifications, including other agency or IRB approvals or renewals.
13. If research is being conducted at sites other than Auburn University or in cooperation with other entities, a letter from the site or program director must be included acknowledging their acceptance of the proposed changes.  
(See OHSR website for guidance: <http://www.auburn.edu/research/vpr/ohs/sample.htm> .)
14. Attach a copy of any and all "stamped" IRB-approved forms you are currently using (information letters, consents, etc.)
15. Attach a new copy of your consent document(s), including updated information regarding the requested changes.  
(Be sure to review the OHSR website for current consent document guidelines and updated contact information.)

When complete, submit hard copy with signatures to the Office of Human Subjects Research,  
307 Samford Hall, Auburn University, AL 36849

2 of 2

B. Palmer College of Chiropractic, IA IRB Approval Document –



April 27, 2011

M. Ram Gudavalli, PHD  
Palmer College of Chiropractic

IRB Assurance: 2008G116  
Development of protocols for bio-testing

Dear Dr. Gudavalli:

On April 20, 2011, the Palmer Chiropractic Research Institutional Review Board reviewed the progress report for continuation of the study:

Development of protocols for bio-testing

The IRB approved the continuation of this study, based on the information on the IRB Progress Report. This approval is valid for one year, after which time it will be required to complete an additional Progress Report.

The Board is fully aware of the regulations governing the institutional review board (Title 45 Code of Federal Regulations Part 46) and believed that its operations are in compliance with those regulations.

Sincerely,

A handwritten signature in blue ink, appearing to read "Ronnie L. Firth".

Ronnie L. Firth, DC  
IRB Chair

RLF/djl





**PALMER**  
College of Chiropractic

## Amendment Request Form

V2009.09.19

*This form is not for the addition of study personnel. To add study personnel, please complete a Personnel Roster (<http://w3.palmer.edu/irb/Forms.html>).*

*A separate form should be submitted for each requested amendment. Please type your responses in the boxes provided. Please answer each question — if a question is not applicable, put N/A in the box.*

<b>PCC Study Number (IRB Assurance Number):</b> 2008G116
<b>1. Research Study Title</b> Development of protocols for biomechanical tests and Measurements of Spinal Manipulative Procedures and for Training of Research Personnel.

<b>2. Principal Investigator and Contact Information</b>		
<b>a. Principal Investigator (including degrees)</b> Maruti Ram Gudavalli, PhD	<b>b. Academic Title</b> Associate Professor and Director of Biomechanics Core	<b>c. Affiliation</b> PCC-Davenport
<b>d. Phone number</b> (563)884-5260	<b>e. Fax number</b> (563)884-5227	<b>f. Email Address</b> ram.guadavalli@palmer.edu
<b>g. Project Manager Name</b> Ting Xia		<b>h. Mailing Address</b> 741 Brady Street Davenport, IA 52803
<b>i. Phone number</b> (563)884-5161	<b>k. Email Address</b> ting.xia@palmer.edu	
<b>j. Fax number</b> (563)884-5227		

<b>3. Type of Amendment</b>	
<b>a. Proposed amendment involves a change in:</b> Participation Procedures	<b>b. Type of Change (addition, deletion, modification, etc.)</b> Addition

<b>4. Amendment Description</b>  <b>a. Provide a full description of the amendment, a justification for the proposed change and indicate whether the change alters the overall study goals.</b>  We are adding certain amendments to the following biomechanical test previously approved – “Human Lumbar Spine Motion and Strength Test in Standing Position” <ol style="list-style-type: none"> <li>1. The participant will have to clear inclusion criteria before he can participate in the biomechanical test.              The following are the requirements of the inclusion criteria –             <ol style="list-style-type: none"> <li>a. Participant must be an adult (over 18 years old) and capable of reading and understanding English language.</li> <li>b. Participant should not have any musculoskeletal injury related to spine, hands or legs in the past 12 months.</li> <li>c. Participant should not have a pacemaker or any non-removable metal object on them.</li> <li>d. Participant should not experience any pain in the range of motion while performing the motions mentioned in the testing protocol.</li> <li>e. The participants should not have any previously known neurological or dermatitis related symptoms.</li> </ol> </li> </ol> <p>The participant will be additionally screened for neurological or dermatitis related symptoms by licensed clinicians before he performs the biomechanical tests. The screening will be based on questionnaire, physical tests and visual observation. If the participant exhibits these symptoms he will be excluded.</p>
--

PCC Institutional Review Board • 1000 Brady Street • Davenport, Iowa 52803 USA  
 voice: 563.884.5155 • fax: 563.884.5227 • email: [karen.grimm@palmer.edu](mailto:karen.grimm@palmer.edu)

Amendment Request Form: Page 1 of 3





Please note that all materials to be used with research participants must be reviewed and approved by the PCC Institutional Review Board before implementation.

*Merritt Ann Gundwall*

Principal Investigator Signature \_\_\_\_\_

6-13-2011  
Date

**This section for IRB use only**

*The amendment request is considered:*

- A minor change in previously approved research during the period (of one year or less) for which approval is authorized [46.110(b)(2)]. The amendment does not alter the risks/benefits of the study.

**Recommendation:**

- Approve as submitted  
 Conditional approval pending changes/clarifications (*Please attach comments*).  
 The amendment alters the risks/benefits of the study and requires completion of an IRB Application Form.

IRB Member Name: \_\_\_\_\_

Date: 6/14/11

### C. Motion Monitor Preference File Settings –

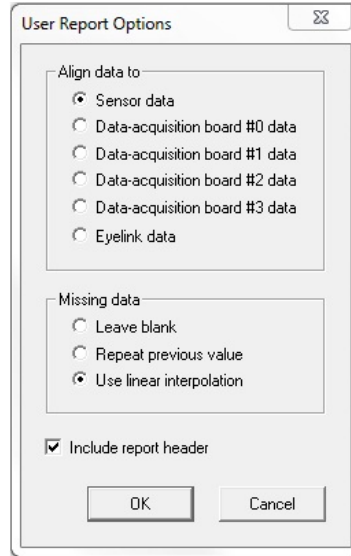


**Figure 50 User Report Options**

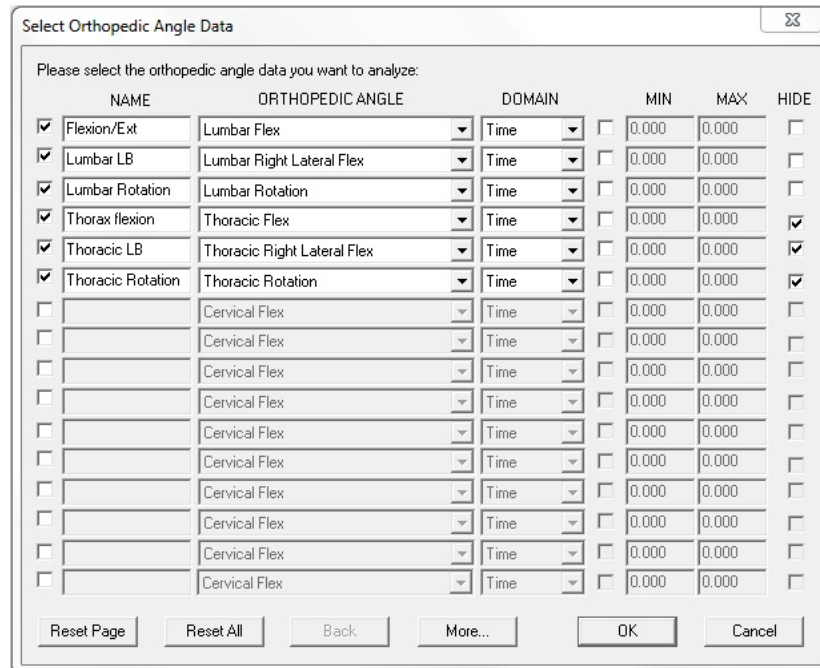


**Figure 51 Orthopedic Angle Selection**

Select Forceplate Data

Please select the forceplate data you want to analyze:

NAME	FORCEPLATE	REFERENCE FRAME			DATA TYPE	DATA ELEMENT	DDOMAIN	MIN	MAX	HIDE
		SEGMENT	SENSOR	POINT						
<input checked="" type="checkbox"/> GRF_Vertical	Forceplate #0	World			Force	Z	Time	600.000	1000.000	<input checked="" type="checkbox"/>
<input checked="" type="checkbox"/> COP X	Forceplate #0	World			Center Of Pressure	X	Time	0.000	0.000	<input checked="" type="checkbox"/>
<input checked="" type="checkbox"/> COP Y	Forceplate #0	World			Center Of Pressure	Y	Time	0.000	0.000	<input checked="" type="checkbox"/>
<input checked="" type="checkbox"/> COP XY	Forceplate #0	World			Center Of Pressure		Time	0.000	0.000	<input checked="" type="checkbox"/>
<input type="checkbox"/>	Forceplate #0	World			Force	X	Time	0.000	0.000	<input type="checkbox"/>
<input type="checkbox"/>	Forceplate #0	World			Force	X	Time	0.000	0.000	<input type="checkbox"/>
<input type="checkbox"/>	Forceplate #0	World			Force	X	Time	0.000	0.000	<input type="checkbox"/>
<input type="checkbox"/>	Forceplate #0	World			Force	X	Time	0.000	0.000	<input type="checkbox"/>
<input type="checkbox"/>	Forceplate #0	World			Force	X	Time	0.000	0.000	<input type="checkbox"/>
<input type="checkbox"/>	Forceplate #0	World			Force	X	Time	0.000	0.000	<input type="checkbox"/>
<input type="checkbox"/>	Forceplate #0	World			Force	X	Time	0.000	0.000	<input type="checkbox"/>
<input type="checkbox"/>	Forceplate #0	World			Force	X	Time	0.000	0.000	<input type="checkbox"/>
<input type="checkbox"/>	Forceplate #0	World			Force	X	Time	0.000	0.000	<input type="checkbox"/>
<input type="checkbox"/>	Forceplate #0	World			Force	X	Time	0.000	0.000	<input type="checkbox"/>
<input type="checkbox"/>	Forceplate #0	World			Force	X	Time	0.000	0.000	<input type="checkbox"/>
<input type="checkbox"/>	Forceplate #0	World			Force	X	Time	0.000	0.000	<input type="checkbox"/>
<input type="checkbox"/>	Forceplate #0	World			Force	X	Time	0.000	0.000	<input type="checkbox"/>
<input type="checkbox"/>	Forceplate #0	World			Force	X	Time	0.000	0.000	<input type="checkbox"/>
<input type="checkbox"/>	Forceplate #0	World			Force	X	Time	0.000	0.000	<input type="checkbox"/>

Reset Page    Reset All    Back    More...    OK    Cancel

Figure 52 Forceplate Data

Select EMG Data

Please specify the EMG data you want to analyze:

NAME	BOARD	CHANNEL	TRANSDUCER GAIN	LOWPASS FILTER (Hz)		NOTCH FILTERS (Hz)										SIGNAL TYPE	RMS PD. (ms)	EVA	MIN	MAX	HIDE		
				FILTER (Hz)	FILTER (Hz)	...	...	...	...	...	...	...	...	...	...							...	
<input checked="" type="checkbox"/> ES Left	0	6	1	<input checked="" type="checkbox"/> 500	<input checked="" type="checkbox"/> 20												Raw	100.000	EVA	<input type="checkbox"/>	0	0	<input type="checkbox"/>
<input checked="" type="checkbox"/> ES Right	0	7	1	<input checked="" type="checkbox"/> 500	<input checked="" type="checkbox"/> 20												Raw	50.00000	EVA	<input type="checkbox"/>	0	0	<input type="checkbox"/>
<input checked="" type="checkbox"/> RA Left	0	8	1	<input checked="" type="checkbox"/> 500	<input checked="" type="checkbox"/> 20												Raw	0	EVA	<input type="checkbox"/>	0	0	<input type="checkbox"/>
<input checked="" type="checkbox"/> RA Right	0	9	1	<input checked="" type="checkbox"/> 500	<input checked="" type="checkbox"/> 20												Raw	0	EVA	<input type="checkbox"/>	0	0	<input type="checkbox"/>
<input checked="" type="checkbox"/> Ext Obl Left	0	10	1	<input checked="" type="checkbox"/> 500	<input checked="" type="checkbox"/> 20												Raw	0	EVA	<input type="checkbox"/>	0	0	<input type="checkbox"/>
<input checked="" type="checkbox"/> Ext Obl Right	0	11	1	<input checked="" type="checkbox"/> 500	<input checked="" type="checkbox"/> 20	<input checked="" type="checkbox"/>											Raw	9.99999	EVA	<input type="checkbox"/>	0	0	<input type="checkbox"/>
<input checked="" type="checkbox"/> Int Obl Left	0	12	1	<input checked="" type="checkbox"/> 500	<input checked="" type="checkbox"/> 20	<input checked="" type="checkbox"/>											Raw	9.99999	EVA	<input type="checkbox"/>	-0.5	0.5	<input type="checkbox"/>
<input checked="" type="checkbox"/> Int Obl Right	0	13	1	<input checked="" type="checkbox"/> 500	<input checked="" type="checkbox"/> 20	<input checked="" type="checkbox"/>											Raw	200.000	EVA	<input type="checkbox"/>	0	0	<input type="checkbox"/>
<input checked="" type="checkbox"/> Lat Dorsi Left	0	14	1	<input checked="" type="checkbox"/> 500	<input checked="" type="checkbox"/> 20	<input checked="" type="checkbox"/>											Raw	200.000	EVA	<input type="checkbox"/>	0	0.2	<input type="checkbox"/>
<input checked="" type="checkbox"/> Lat Dorsi Right	0	15	1	<input checked="" type="checkbox"/> 500	<input checked="" type="checkbox"/> 20	<input checked="" type="checkbox"/>											Raw	0	EVA	<input type="checkbox"/>	0	0	<input type="checkbox"/>
<input checked="" type="checkbox"/> ES Left	0	6	1	<input checked="" type="checkbox"/> 500	<input checked="" type="checkbox"/> 20												RMS	250	EVA	<input type="checkbox"/>	0	0	<input checked="" type="checkbox"/>
<input checked="" type="checkbox"/> ES Right	0	7	1	<input checked="" type="checkbox"/> 500	<input checked="" type="checkbox"/> 20												RMS	250	EVA	<input type="checkbox"/>	0	0	<input checked="" type="checkbox"/>
<input checked="" type="checkbox"/> RA Left	0	8	1	<input checked="" type="checkbox"/> 500	<input checked="" type="checkbox"/> 20												RMS	250	EVA	<input type="checkbox"/>	0	0	<input checked="" type="checkbox"/>
<input checked="" type="checkbox"/> RA Right	0	9	1	<input checked="" type="checkbox"/> 500	<input checked="" type="checkbox"/> 20												RMS	250	EVA	<input type="checkbox"/>	0	0	<input checked="" type="checkbox"/>
<input checked="" type="checkbox"/> Ext Obl Left	0	10	1	<input checked="" type="checkbox"/> 500	<input checked="" type="checkbox"/> 20												RMS	250	EVA	<input type="checkbox"/>	0	0	<input checked="" type="checkbox"/>
<input checked="" type="checkbox"/> Ext Obl Right	0	11	1	<input checked="" type="checkbox"/> 500	<input checked="" type="checkbox"/> 20												RMS	250	EVA	<input type="checkbox"/>	0	0	<input checked="" type="checkbox"/>

Reset Page    Reset All    Notch Settings...    Back    More    OK    Cancel

Figure 53 EMG Data 1

Select EMG Data

Please specify the EMG data you want to analyze:

NAME	BOARD	CHANNEL	TRANSDUCER GAIN	LOWPASS FILTER (Hz)	HIGHPASS FILTER (Hz)	NOTCH FILTERS (Hz)										SIGNAL TYPE	RMS PD. (ms)	EVA	MIN	MAX	HIDE	
<input checked="" type="checkbox"/> Int Obl Left	0	12	1	<input checked="" type="checkbox"/> 500	<input checked="" type="checkbox"/> 20	<input type="checkbox"/>	<input type="checkbox"/>	<input type="checkbox"/>	<input type="checkbox"/>	<input type="checkbox"/>	<input type="checkbox"/>	<input type="checkbox"/>	<input type="checkbox"/>	<input type="checkbox"/>	<input type="checkbox"/>	<input type="checkbox"/>	RMS	250	<input type="checkbox"/>	0	0	<input checked="" type="checkbox"/>
<input checked="" type="checkbox"/> Int Obl Right	0	13	1	<input checked="" type="checkbox"/> 500	<input checked="" type="checkbox"/> 20	<input type="checkbox"/>	<input type="checkbox"/>	<input type="checkbox"/>	<input type="checkbox"/>	<input type="checkbox"/>	<input type="checkbox"/>	<input type="checkbox"/>	<input type="checkbox"/>	<input type="checkbox"/>	<input type="checkbox"/>	<input type="checkbox"/>	RMS	250	<input type="checkbox"/>	0	0	<input checked="" type="checkbox"/>
<input checked="" type="checkbox"/> Lat Dorsi Left	0	14	1	<input checked="" type="checkbox"/> 500	<input checked="" type="checkbox"/> 20	<input type="checkbox"/>	<input type="checkbox"/>	<input type="checkbox"/>	<input type="checkbox"/>	<input type="checkbox"/>	<input type="checkbox"/>	<input type="checkbox"/>	<input type="checkbox"/>	<input type="checkbox"/>	<input type="checkbox"/>	<input type="checkbox"/>	RMS	250	<input type="checkbox"/>	0	0	<input checked="" type="checkbox"/>
<input checked="" type="checkbox"/> Lat Dorsi Right	0	15	1	<input checked="" type="checkbox"/> 500	<input checked="" type="checkbox"/> 20	<input type="checkbox"/>	<input type="checkbox"/>	<input type="checkbox"/>	<input type="checkbox"/>	<input type="checkbox"/>	<input type="checkbox"/>	<input type="checkbox"/>	<input type="checkbox"/>	<input type="checkbox"/>	<input type="checkbox"/>	<input type="checkbox"/>	RMS	250	<input type="checkbox"/>	0	0	<input checked="" type="checkbox"/>
<input checked="" type="checkbox"/> ES Left	0	6	1	<input checked="" type="checkbox"/> 500	<input checked="" type="checkbox"/> 20	<input type="checkbox"/>	<input type="checkbox"/>	<input type="checkbox"/>	<input type="checkbox"/>	<input type="checkbox"/>	<input type="checkbox"/>	<input type="checkbox"/>	<input type="checkbox"/>	<input type="checkbox"/>	<input type="checkbox"/>	<input type="checkbox"/>	PSD	0	<input type="checkbox"/>	0	0	<input checked="" type="checkbox"/>
<input checked="" type="checkbox"/> ES Right	0	7	1	<input checked="" type="checkbox"/> 500	<input checked="" type="checkbox"/> 20	<input type="checkbox"/>	<input type="checkbox"/>	<input type="checkbox"/>	<input type="checkbox"/>	<input type="checkbox"/>	<input type="checkbox"/>	<input type="checkbox"/>	<input type="checkbox"/>	<input type="checkbox"/>	<input type="checkbox"/>	<input type="checkbox"/>	PSD	0	<input type="checkbox"/>	0	0	<input checked="" type="checkbox"/>
<input checked="" type="checkbox"/> RA Left	0	8	1	<input checked="" type="checkbox"/> 500	<input checked="" type="checkbox"/> 20	<input type="checkbox"/>	<input type="checkbox"/>	<input type="checkbox"/>	<input type="checkbox"/>	<input type="checkbox"/>	<input type="checkbox"/>	<input type="checkbox"/>	<input type="checkbox"/>	<input type="checkbox"/>	<input type="checkbox"/>	<input type="checkbox"/>	PSD	0	<input type="checkbox"/>	0	0	<input checked="" type="checkbox"/>
<input checked="" type="checkbox"/> RA Right	0	9	1	<input checked="" type="checkbox"/> 500	<input checked="" type="checkbox"/> 20	<input type="checkbox"/>	<input type="checkbox"/>	<input type="checkbox"/>	<input type="checkbox"/>	<input type="checkbox"/>	<input type="checkbox"/>	<input type="checkbox"/>	<input type="checkbox"/>	<input type="checkbox"/>	<input type="checkbox"/>	<input type="checkbox"/>	PSD	0	<input type="checkbox"/>	0	0	<input checked="" type="checkbox"/>
<input checked="" type="checkbox"/> Ext Obl Left	0	10	1	<input checked="" type="checkbox"/> 500	<input checked="" type="checkbox"/> 20	<input type="checkbox"/>	<input type="checkbox"/>	<input type="checkbox"/>	<input type="checkbox"/>	<input type="checkbox"/>	<input type="checkbox"/>	<input type="checkbox"/>	<input type="checkbox"/>	<input type="checkbox"/>	<input type="checkbox"/>	<input type="checkbox"/>	PSD	0	<input type="checkbox"/>	0	0	<input checked="" type="checkbox"/>
<input checked="" type="checkbox"/> Ext Obl Right	0	11	1	<input checked="" type="checkbox"/> 500	<input checked="" type="checkbox"/> 20	<input type="checkbox"/>	<input type="checkbox"/>	<input type="checkbox"/>	<input type="checkbox"/>	<input type="checkbox"/>	<input type="checkbox"/>	<input type="checkbox"/>	<input type="checkbox"/>	<input type="checkbox"/>	<input type="checkbox"/>	<input type="checkbox"/>	PSD	0	<input type="checkbox"/>	0	0	<input checked="" type="checkbox"/>
<input checked="" type="checkbox"/> Int Obl Left	0	12	1	<input checked="" type="checkbox"/> 500	<input checked="" type="checkbox"/> 20	<input type="checkbox"/>	<input type="checkbox"/>	<input type="checkbox"/>	<input type="checkbox"/>	<input type="checkbox"/>	<input type="checkbox"/>	<input type="checkbox"/>	<input type="checkbox"/>	<input type="checkbox"/>	<input type="checkbox"/>	<input type="checkbox"/>	PSD	0	<input type="checkbox"/>	0	0	<input checked="" type="checkbox"/>
<input checked="" type="checkbox"/> Int Obl Right	0	13	1	<input checked="" type="checkbox"/> 500	<input checked="" type="checkbox"/> 20	<input type="checkbox"/>	<input type="checkbox"/>	<input type="checkbox"/>	<input type="checkbox"/>	<input type="checkbox"/>	<input type="checkbox"/>	<input type="checkbox"/>	<input type="checkbox"/>	<input type="checkbox"/>	<input type="checkbox"/>	<input type="checkbox"/>	PSD	0	<input type="checkbox"/>	0	0	<input checked="" type="checkbox"/>
<input checked="" type="checkbox"/> Lat Dorsi Left	0	14	1	<input checked="" type="checkbox"/> 500	<input checked="" type="checkbox"/> 20	<input type="checkbox"/>	<input type="checkbox"/>	<input type="checkbox"/>	<input type="checkbox"/>	<input type="checkbox"/>	<input type="checkbox"/>	<input type="checkbox"/>	<input type="checkbox"/>	<input type="checkbox"/>	<input type="checkbox"/>	<input type="checkbox"/>	PSD	0	<input type="checkbox"/>	0	0	<input checked="" type="checkbox"/>
<input checked="" type="checkbox"/> Lat Dorsi Right	0	15	1	<input checked="" type="checkbox"/> 500	<input checked="" type="checkbox"/> 20	<input type="checkbox"/>	<input type="checkbox"/>	<input type="checkbox"/>	<input type="checkbox"/>	<input type="checkbox"/>	<input type="checkbox"/>	<input type="checkbox"/>	<input type="checkbox"/>	<input type="checkbox"/>	<input type="checkbox"/>	<input type="checkbox"/>	PSD	0	<input type="checkbox"/>	0	0	<input checked="" type="checkbox"/>
<input checked="" type="checkbox"/> Multi. Left	1	0	1	<input checked="" type="checkbox"/> 500	<input checked="" type="checkbox"/> 20	<input type="checkbox"/>	<input type="checkbox"/>	<input type="checkbox"/>	<input type="checkbox"/>	<input type="checkbox"/>	<input type="checkbox"/>	<input type="checkbox"/>	<input type="checkbox"/>	<input type="checkbox"/>	<input type="checkbox"/>	<input type="checkbox"/>	Raw	0	<input type="checkbox"/>	0	0	<input checked="" type="checkbox"/>
<input checked="" type="checkbox"/> Multi. Right	1	1	1	<input checked="" type="checkbox"/> 500	<input checked="" type="checkbox"/> 20	<input type="checkbox"/>	<input type="checkbox"/>	<input type="checkbox"/>	<input type="checkbox"/>	<input type="checkbox"/>	<input type="checkbox"/>	<input type="checkbox"/>	<input type="checkbox"/>	<input type="checkbox"/>	<input type="checkbox"/>	<input type="checkbox"/>	Raw	0	<input type="checkbox"/>	0	0	<input checked="" type="checkbox"/>

Reset Page    Reset All    Notch Settings...    Back    More    OK    Cancel

Figure 54 EMG Data 2

Select EMG Data

Please specify the EMG data you want to analyze:

NAME	BOARD	CHANNEL	TRANSDUCER GAIN	LOWPASS FILTER (Hz)	HIGHPASS FILTER (Hz)	NOTCH FILTERS (Hz)										SIGNAL TYPE	RMS PD. (ms)	EVA	MIN	MAX	HIDE	
<input checked="" type="checkbox"/> Multi. Left	1	0	1	<input checked="" type="checkbox"/> 500	<input checked="" type="checkbox"/> 20	<input type="checkbox"/>	<input type="checkbox"/>	<input type="checkbox"/>	<input type="checkbox"/>	<input type="checkbox"/>	<input type="checkbox"/>	<input type="checkbox"/>	<input type="checkbox"/>	<input type="checkbox"/>	<input type="checkbox"/>	<input type="checkbox"/>	RMS	250	<input type="checkbox"/>	0	0	<input checked="" type="checkbox"/>
<input checked="" type="checkbox"/> Multi. Right	1	1	1	<input checked="" type="checkbox"/> 500	<input checked="" type="checkbox"/> 20	<input type="checkbox"/>	<input type="checkbox"/>	<input type="checkbox"/>	<input type="checkbox"/>	<input type="checkbox"/>	<input type="checkbox"/>	<input type="checkbox"/>	<input type="checkbox"/>	<input type="checkbox"/>	<input type="checkbox"/>	<input type="checkbox"/>	RMS	250	<input type="checkbox"/>	0	0	<input checked="" type="checkbox"/>
<input checked="" type="checkbox"/> Multi. Left	1	0	1	<input checked="" type="checkbox"/> 500	<input checked="" type="checkbox"/> 20	<input type="checkbox"/>	<input type="checkbox"/>	<input type="checkbox"/>	<input type="checkbox"/>	<input type="checkbox"/>	<input type="checkbox"/>	<input type="checkbox"/>	<input type="checkbox"/>	<input type="checkbox"/>	<input type="checkbox"/>	<input type="checkbox"/>	PSD	0	<input type="checkbox"/>	0	0	<input checked="" type="checkbox"/>
<input checked="" type="checkbox"/> Multi. Right	1	1	1	<input checked="" type="checkbox"/> 500	<input checked="" type="checkbox"/> 20	<input type="checkbox"/>	<input type="checkbox"/>	<input type="checkbox"/>	<input type="checkbox"/>	<input type="checkbox"/>	<input type="checkbox"/>	<input type="checkbox"/>	<input type="checkbox"/>	<input type="checkbox"/>	<input type="checkbox"/>	<input type="checkbox"/>	PSD	0	<input type="checkbox"/>	0	0	<input checked="" type="checkbox"/>
<input type="checkbox"/>	0	0	1	<input type="checkbox"/> 0	<input type="checkbox"/> 0	<input type="checkbox"/>	<input type="checkbox"/>	<input type="checkbox"/>	<input type="checkbox"/>	<input type="checkbox"/>	<input type="checkbox"/>	<input type="checkbox"/>	<input type="checkbox"/>	<input type="checkbox"/>	<input type="checkbox"/>	<input type="checkbox"/>	Raw	0	<input type="checkbox"/>	0	0	<input type="checkbox"/>
<input type="checkbox"/>	0	0	1	<input type="checkbox"/> 0	<input type="checkbox"/> 0	<input type="checkbox"/>	<input type="checkbox"/>	<input type="checkbox"/>	<input type="checkbox"/>	<input type="checkbox"/>	<input type="checkbox"/>	<input type="checkbox"/>	<input type="checkbox"/>	<input type="checkbox"/>	<input type="checkbox"/>	<input type="checkbox"/>	Raw	0	<input type="checkbox"/>	0	0	<input type="checkbox"/>
<input type="checkbox"/>	0	0	1	<input type="checkbox"/> 0	<input type="checkbox"/> 0	<input type="checkbox"/>	<input type="checkbox"/>	<input type="checkbox"/>	<input type="checkbox"/>	<input type="checkbox"/>	<input type="checkbox"/>	<input type="checkbox"/>	<input type="checkbox"/>	<input type="checkbox"/>	<input type="checkbox"/>	<input type="checkbox"/>	Raw	0	<input type="checkbox"/>	0	0	<input type="checkbox"/>
<input type="checkbox"/>	0	0	1	<input type="checkbox"/> 0	<input type="checkbox"/> 0	<input type="checkbox"/>	<input type="checkbox"/>	<input type="checkbox"/>	<input type="checkbox"/>	<input type="checkbox"/>	<input type="checkbox"/>	<input type="checkbox"/>	<input type="checkbox"/>	<input type="checkbox"/>	<input type="checkbox"/>	<input type="checkbox"/>	Raw	0	<input type="checkbox"/>	0	0	<input type="checkbox"/>
<input type="checkbox"/>	0	0	1	<input type="checkbox"/> 0	<input type="checkbox"/> 0	<input type="checkbox"/>	<input type="checkbox"/>	<input type="checkbox"/>	<input type="checkbox"/>	<input type="checkbox"/>	<input type="checkbox"/>	<input type="checkbox"/>	<input type="checkbox"/>	<input type="checkbox"/>	<input type="checkbox"/>	<input type="checkbox"/>	Raw	0	<input type="checkbox"/>	0	0	<input type="checkbox"/>
<input type="checkbox"/>	0	0	1	<input type="checkbox"/> 0	<input type="checkbox"/> 0	<input type="checkbox"/>	<input type="checkbox"/>	<input type="checkbox"/>	<input type="checkbox"/>	<input type="checkbox"/>	<input type="checkbox"/>	<input type="checkbox"/>	<input type="checkbox"/>	<input type="checkbox"/>	<input type="checkbox"/>	<input type="checkbox"/>	Raw	0	<input type="checkbox"/>	0	0	<input type="checkbox"/>
<input type="checkbox"/>	0	0	1	<input type="checkbox"/> 0	<input type="checkbox"/> 0	<input type="checkbox"/>	<input type="checkbox"/>	<input type="checkbox"/>	<input type="checkbox"/>	<input type="checkbox"/>	<input type="checkbox"/>	<input type="checkbox"/>	<input type="checkbox"/>	<input type="checkbox"/>	<input type="checkbox"/>	<input type="checkbox"/>	Raw	0	<input type="checkbox"/>	0	0	<input type="checkbox"/>
<input type="checkbox"/>	0	0	1	<input type="checkbox"/> 0	<input type="checkbox"/> 0	<input type="checkbox"/>	<input type="checkbox"/>	<input type="checkbox"/>	<input type="checkbox"/>	<input type="checkbox"/>	<input type="checkbox"/>	<input type="checkbox"/>	<input type="checkbox"/>	<input type="checkbox"/>	<input type="checkbox"/>	<input type="checkbox"/>	Raw	0	<input type="checkbox"/>	0	0	<input type="checkbox"/>
<input type="checkbox"/>	0	0	1	<input type="checkbox"/> 0	<input type="checkbox"/> 0	<input type="checkbox"/>	<input type="checkbox"/>	<input type="checkbox"/>	<input type="checkbox"/>	<input type="checkbox"/>	<input type="checkbox"/>	<input type="checkbox"/>	<input type="checkbox"/>	<input type="checkbox"/>	<input type="checkbox"/>	<input type="checkbox"/>	Raw	0	<input type="checkbox"/>	0	0	<input type="checkbox"/>
<input type="checkbox"/>	0	0	1	<input type="checkbox"/> 0	<input type="checkbox"/> 0	<input type="checkbox"/>	<input type="checkbox"/>	<input type="checkbox"/>	<input type="checkbox"/>	<input type="checkbox"/>	<input type="checkbox"/>	<input type="checkbox"/>	<input type="checkbox"/>	<input type="checkbox"/>	<input type="checkbox"/>	<input type="checkbox"/>	Raw	0	<input type="checkbox"/>	0	0	<input type="checkbox"/>
<input type="checkbox"/>	0	0	1	<input type="checkbox"/> 0	<input type="checkbox"/> 0	<input type="checkbox"/>	<input type="checkbox"/>	<input type="checkbox"/>	<input type="checkbox"/>	<input type="checkbox"/>	<input type="checkbox"/>	<input type="checkbox"/>	<input type="checkbox"/>	<input type="checkbox"/>	<input type="checkbox"/>	<input type="checkbox"/>	Raw	0	<input type="checkbox"/>	0	0	<input type="checkbox"/>
<input type="checkbox"/>	0	0	1	<input type="checkbox"/> 0	<input type="checkbox"/> 0	<input type="checkbox"/>	<input type="checkbox"/>	<input type="checkbox"/>	<input type="checkbox"/>	<input type="checkbox"/>	<input type="checkbox"/>	<input type="checkbox"/>	<input type="checkbox"/>	<input type="checkbox"/>	<input type="checkbox"/>	<input type="checkbox"/>	Raw	0	<input type="checkbox"/>	0	0	<input type="checkbox"/>

Reset Page    Reset All    Notch Settings...    Back    More    OK    Cancel

Figure 55 EMG Data 3

D. Literature Review Summary Sheets –

Study	Title	Health Status and number of participants	Gender		Age in years (SD)	Weight in kg (SD)	Height in cm (SD)
			Males	Females			
Cavanagh et. al. 2007	Approximate entropy detects the effect of a secondary cognitive task on postural control in healthy young adults: a methodological report	Healthy - 30	15	15	21.7 (2.3)	71 (13.3)	173 (11)
Kavanagh et. al 2006	Lumbar and cervical erector spinae fatigue elicit compensatory postural responses to assist in maintaining head stability during walking	Healthy - 8	8	0	23 (4)	77 (12)	181 (9)
Kavanagh et. al 2009	Lower trunk motion and speed-dependence during walking	13	7	6	23 (3)	71 (11)	171 (11)
Fell et. al. 2000	Nonlinear analysis of continuous ECG during sleep II. Dynamical measures	Healthy - 12	12	0	27.3 (4.2)	Not Clear	Not Clear
Lee et. al. 2010	Non-linear Analysis of Single Electroencephalography (EEG) for Sleep-Related Healthcare Applications	Healthy - 4	4	0	27.5	Not Clear	Not Clear
Newell et. al. 2000	Dimensional constraints on limb movements	Healthy - 8	8	0	Not Clear	Not Clear	Not Clear
Buzzi et. al. 2003	Nonlinear dynamics indicates aging affects variability during gait	Healthy young - 10 Healthy older - 10	0	20	25.1 (5.3) 74.6 (2.55)	63.93 (6.53) 64.07 (9.69)	170 (4.9) 159 (5.3)

**Demographics Summary**

Study	Title	Rate of data collection	Duration	r, m	ApEn
Cavanaugh et. al. 2007	Approximate entropy detects the effect of a secondary cognitive task on postural control in healthy young adults: a methodological report	100 Hz	Not Clear	r = 0.2 m = 2	No significant interaction was found between cognitive task and sensory condition for ApEn-AP and ApEn-ML
Kavanagh et. al 2006	Lumbar and cervical erector spinae fatigue elicit compensatory postural responses to assist in maintaining head stability during walking	Motion - 250 Hz EMG - 1000 Hz	Time required to walk 30 m level walkway at comfortable speed.	r = 0.2 m = 1	ApEn values did not show significant change when data obtained after fatigue induced in neck and trunk region were compared.
Kavanagh et. al 2009	Lower trunk motion and speed-dependence during walking	512 Hz	Time required to walk 30 m level walkway at comfortable speed.	r = 0.2 m = 1	ApEn values increased as the walking speed increased. The increase in value ranged from 0.15 to 0.24 depending on axis of inclinometer.
Newell et. al. 2000	Dimensional constraints on limb movements	100 Hz	2 minutes	r = 0.25 m = 2	ApEn values increased as the subjects went from preferred with vision to random and no vision type of motion. The increase was in the range of 0.2 to 0.3.

### Approximate Entropy Studies Summary